Studies towards a Solution Structure of the Peptidoglycan Glycosyltransferases

Professor Daniel Kahne Yihui Wu

Harvard University May 2012

Studies towards a Solution Structure of the Peptidoglycan Glycosyltransferases

Abstract

Peptidoglycan glycosyltransferases (PGTs) are highly conserved bacterial enzymes that catalyze the polymerization of the lipidic disaccharide, Lipid II, to form individual peptidoglycan (PG) strands which are subsequently cross-linked to form mature PG, the major skeletal component of the bacterial cell wall. Recent advances in the preparation of well-defined PGT substrates have enabled the biochemical characterization of Lipid II polymerization by the PGTs. In the course of these studies, we have observed that a distinctive lag phase in the initial rate of PG synthesis by the PGTs can be abrogated if the enzyme is preincubated with Lipid IV, the shortest PG fragment.

The origins of this lag phase are intriguing because the chemical transformation involved in coupling Lipid II to yield Lipid IV is identical to the transformation involved in the synthesis of longer PG fragments from Lipid II. Crystallographic structures of the PGTs with Moenomycin A, an inhibitor that is believed to bind to the same site as Lipid IV, suggest that the PGTs possess flexible regions near the putative active site that can undergo substrate-induced conformational changes to accelerate PG synthesis. However, there is currently no structural evidence on how the PGTs interact with its substrates.

The work in this thesis lays the foundation for pursuing a solution structure of a Lipid IV bound PGT complex by Nuclear Magnetic Resonance (NMR) spectroscopy, enabling the study of important enzyme conformational states and structural dynamics involved in PG

synthesis. Specifically, Chapter 2 of this thesis presents the biochemical evidence that the preincubation of the PGTs with a Lipid IV derivative, Gal-Lipid IV abrogates the lag phase and accelerates the initial rate of PG synthesis. Chapter 3 presents a robust methodology for obtaining multimilligram quantities of isotope labeled, monodisperse and monomeric SgtB, a PGT from a clinically relevant pathogen, *Staphylococcus aureus* for solution structural studies. Chapter 4 describes the systematic development of a methodology for producing a well-behaved, stable sample of Moenomycin A bound SgtB for NMR spectroscopy. Chapter 5 delineates the adaptation of the methodology described in Chapter 4 for pursuing the solution structure of Lipid IV bound SgtB.

Table of Contents

List of Figures

Glossary of Abbreviations

Abs	Absorbance
Ala	Alanine
Amp	Ampicillin
CHES	2-(cyclohexylamino)ethansulfonic acid
CHAPS	3-[(3-Cholamidopropyl)dimethylammonio]-1-propanesulfonate
CV	Column volume
DMSO	Dimethyl sulfoxide
EDTA	Ethylenediaminetetraacetic acid
ESI-MS	Electrospray ionization mass spectrometry
fHSQC	Fast heteronuclear single quantum coherence spectroscopy
FPLC	Fast protein liquid chromatography
GalT	β-1,4-galactosyltransferase
GB1	Streptococcal protein G domain B1
GB1A	Streptococcal protein G domain B1 acidic variant
GB1B	Streptococcal protein G domain B1 basic variant
GlcNAc	N-acetylglucosamine
GST	Glutathione S-transferase
Glu	Glutamic acid
Gly	Glycine
HEPES	4-(2-hydroxyethyl)piperazine-1-ethansulfonic acid

His	Histadine
His_6	Six histadine repeat sequence Nickel-affinity purification tag
HTS	High throughput screening
HSQC	Heteronuclear single quantum coherence spectroscopy
IC_{50}	Half maximal inhibitory concentration
IMAC	Immobilized metal affinity chromatography
Imid	Imidazole
IPTG	Isopropyl β-D-1-thiogalactopyranoside
LB	Luria-Bertani
Lys	Lysine
MBP	Maltose binding protein
MmA	Moenomycin A
MES	2-(N-morpholino)ethansulfonic acid
MurNAc	N-acetylmuramic acid
MWCO	Molecular weight cutoff
NaCl	Sodium chloride
NaPi	Sodium phosphate
Ni-NTA	Nickel-nitriloacetic acid
NMR	Nuclear magnetic resonance
PBP	Penicillin binding protein
PG	Peptidoglycan
PGT	Peptidoglycan glycosyltransferase
SDS-PAGE	Sodium dodecyl sulfate polyacrylamide gel electrophoresis

SEC	Size-exclusion chromatography
TCP	Total cell protein extract
TEV	Tobacco etch virus
TEV_{pc}	Tobacco etch virus protease cleavage amino acid sequence (ENLYFQG)
TM	Transmembrane
TP	Transpeptidase
TRACT	TROSY for rotational correlation times
Tris	2-Amino-2-hydroxymethyl-propane-1,3-diol
TROSY	Transverse relaxation optimized spectroscopy
Trx	Thioredoxin
UDP	Uridine diphosphate
UDP-Gal	Uridine diphosphate galactose
UDP-GlcNAc	Uridine diphosphate N-acetylglucosamine
UDP-MurNAc-pentapeptide	Uridine diphosphate N-acetylmuramic acid peptapeptide
UMP	Uridine monophosphate

Acknowledgements

Writing these acknowledgements has been harder than I had imagined it to be. During my time in graduate school, I've zigzagged through two campuses, transversed several groups and met countless individuals that have influenced me and added a fresh perspective in one way or another. Looking back, it all seems to become a kaleidoscopic whirl and I don't know how I should begin that would do justice to this rich experience. I have way too many people to thank, to all the individuals that I have failed to mention by name, let me say upfront that I owe a debt of gratitude to you all. Anyhow, here's an attempt to get this out in a coherent fashion.

It was a stroke of luck and a great privilege to be a student of Professor Dan Kahne. There were moments when tough choices had to be made. However, Dan has always found a way to put things in perspective and steady the ship. During my time in his lab, as much as I've learned to think rigorously about science, he has made me grow plenty as a person. I've always enjoyed listening Dan's renderings on life that often punctuate our scientific discussions. I know I'm going to miss that a lot.

When I made the transition to the biochemical side of the cell wall project, Professor Suzanne Walker generously opened her lab to me. The Walker lab (with its associated spacious cold room in Armenise) has been my home base for a substantial portion of my time in graduate school. I have learned a great deal from her about the nuances in PGT protein biochemistry during our cell wall subgroup meetings, some of which inspired the experimental approaches detailed in this manuscript. It has been great fun working and hanging out as an adopted member of the Walker lab.

Much of this thesis would not be possible without the guidance of Professor Gerhard Wagner and members of his group, namely Dr. Ricard Rodriguez-Mias, Dr. Haribabu Arthanari, and Dr. Tsyr-Yan (Dharma) Yu. Spectroscopy is usually made out to be a complex and technical endeavor but Ricard, Hari and Dharma have shown me that it isn't always the case. Thank you guys, I really appreciate all your help.

To Professor Alan Saghatelian, many thanks for being on my committee all these years and witnessing this project unfold. Helen Correiro and Mike Quinn have always made it easy to zip through administrative matters.

When I joined Dan's group as a first year, Micha Fridman took me under his wing and taught me many "tricks" in sugar synthesis and how to get that mass spec to work when things got cranky. We shared “unpressed” burgers at O'Sullivan's and many jokes about stuff that shall remain forever buried. I found a fellow Bill Evans fan in the ever meticulous Shinichiro Fuse, who along with Hirokazu Tsukamoto honed my technical skills at chemical synthesis. Tetsuya Tanikawa taught me the deft art of maintaining solvent stills and how to really work a wrench. I recall reminiscing with Shu Sin Chng about the days at Sungei Gedong, conversations which inevitably lead to the street food that we both miss at home. Having had little previous exposure to the world of enzymology and kinetics, Andrew and Tania quickly brought me up to speed on the art of the isobutyric acid perfumed paper strip oragami (with tweezers!). Yanqiu Yuan helped me get started on PGT protein biochemistry on very short notice. Yuriy Rebets and I shared many caffeination trips, late nights in Armenise and certainly a good laugh at my first failed attempt to clone. Many thanks to Christian Gampe and Janine May for giving me comments on my thesis on such short notice.

Finally, I would like to thank my parents who have cheered me on for 31 years of my life. It has been quite a ride and both of you have been there with me every step of the way.

Chapter One: Introduction to the Biosynthesis of Peptidoglycan

1.1 Overview on the biosynthesis of peptidoglycan

Peptidoglycan (PG) is the major skeletal component of the bacterial cell wall that is essential for the survival of bacteria under environmental conditions which induce high internal osmotic pressure.[1,2] It is a unique and highly conserved organelle among most bacteria and its biosynthetic pathway has been targeted by some of the world's most successful antibiotics, namely Penicillin G and Vancomycin.[3,4,5] PG derives its strength and rigidity from the formation of a complex web of glycan chain polymers that are linked together by their peptide side chains.[6,7] Presumably, this enables the PG to function as an exo-skeleton that ensures the integrity of the fluid cytoplasmic membrane, preventing lysis.[8]

Structurally, these glycan chain polymers are composed of repeating disaccharide units of N-acetylglucosamine (GlcNAc) and N-acetylmuramic acid (MurNAc) residues. Short peptides attached as appendages on the lactic acid moiety of the N-acetylmuramic acid enable adjacent glycan strands to be cross-linked through an amide bond.[9]

The biosynthesis of PG can be delineated into three distinct stages (**Figure 1.1**).[10,11,12] Briefly, the first stage involves the conversion of UDP-GlcNAc into UDP-MurNAc-pentapeptide through a series of enzymatic transformations performed in the cytoplasm.[13] In the second stage of the biosynthesis, the UDP-MurNAc-pentapeptide is brought to the inner face of the cytoplasmic membrane by the attachment of a C_{55}-Lipid, undecaprenyl pyrophosphate by MraY to generate Lipid I.[14] MurG then glycosylates Lipid I with GlcNAc to form a β(1,4)-linked disaccharide

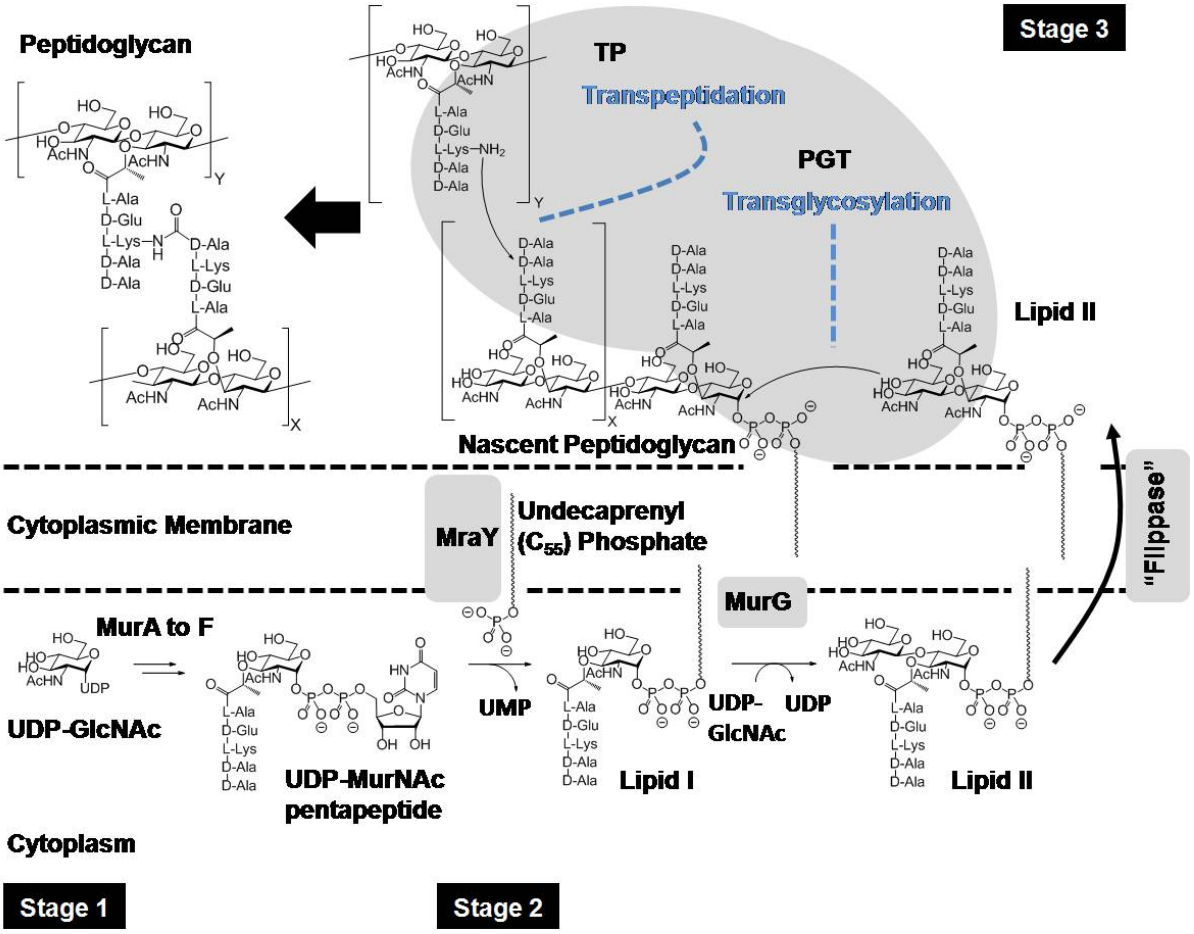

Figure 1.1 Biosynthesis of Peptidoglycan

called Lipid II.[15,16,17] Lipid II is then brought to the outer leaflet of the cytoplasmic membrane by a putative flippase for the final stage of PG synthesis.[18,19,20] The final assembly of peptidoglycan from Lipid II is performed by two classes of enzymes: the peptidoglycan glycosyltransferases (PGT) and the transpeptidases (TP).[21] PGTs and TPs can exist as independent, monofunctional proteins or alternately, as separate domains that are combined into a single bifunctional protein (e.g. *Staphylococcus aureus* Penicillin-binding Protein 2) (**Figure 1.2**).

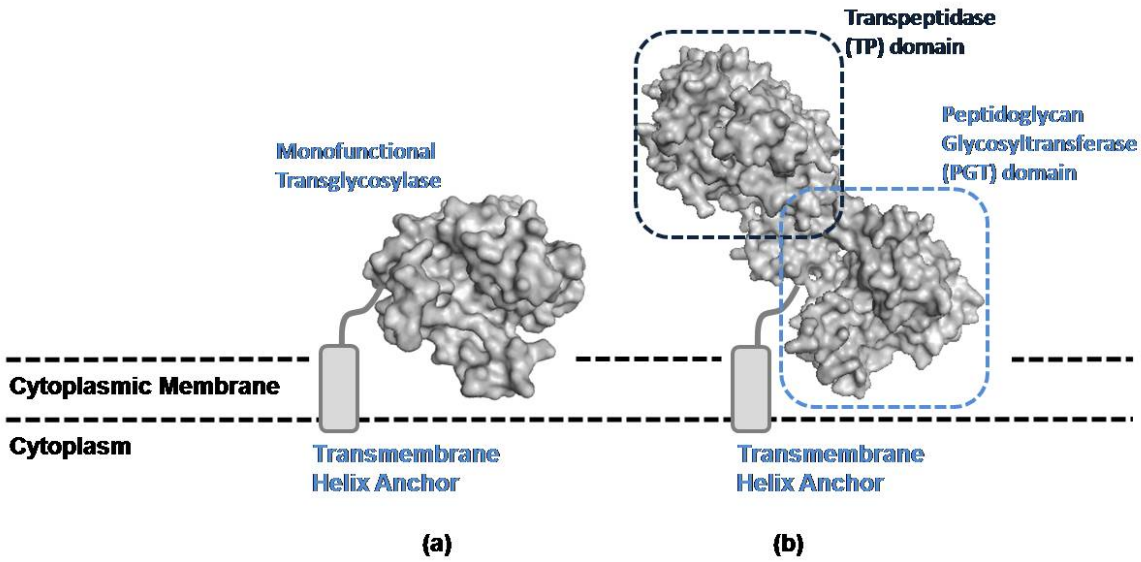

Figure 1.2 Topology of the PGTs. PGT enzyme can exist either as (a) a monofunctional protein that is anchored to the cytoplasmic membrane via a transmembrane helix, or (b) as a distinct domain within a bifunctional enzyme.

PGTs initiate the process by joining two identical units of Lipid II via a β(1,4) glycosidic bond between the C4-hydroxyl group of GlcNAc from the acceptor and the C1-anomeric end of MurNAc from the donor to give a tetrasaccharide product, Lipid IV. The undecaprenyl pyrophosphate lipid moiety from the donor is released, presumably providing the driving force for the reaction. Lipid IV is elongated by the addition of another Lipid II unit. This process is repeated multiple times to form nascent glycan strands bearing the desired polymer length properties. Finally, these nascent glycan strands are cross-linked together via their peptide appendages by the TPs to yield peptidoglycan.

1.2 Progress towards understanding the mechanistic details of the PGTs

The polymerase activity of the PGT is a key component of the cell wall biosynthetic machinery, yet the mechanistic details underlying the transglycosylation reaction performed by the PGTs have only recently emerged. Historically, the lack of pure Lipid II substrate as

well as chemically defined substrate fragments of PG presented a major impediment to PGT research.[22]

In 2001, the development of a chemoenzymatic synthesis of the Lipid II substrate opened the door to the efficient preparation of radio-labeled Lipid II substrates. This circumvented the crude and low yielding preparation of radiolabeled Lipid II from bacterial membrane extracts.[23,24,25] As a result, PG synthesis from Lipid II could be monitored in a quantitative fashion by radiological assays that in turn enabled the preliminary characterization of PGT reaction kinetics (**Figure 1.3**).[26,27] Synthetic access to Lipid IV provided a roadmap for preparing various PG fragments that were crucial for probing the enzymatic process of synthesizing PG.[28] For instance, the ability to prepare Gal-Lipid IV, a PG fragment that cannot be glycosylated in a β(1,4) fashion on the nonreducing end showed that the nascent glycan strand is elongated on the reducing end.[29,30] The ability to prepare PG fragments with varying lipid lengths revealed that the donor binding site of the PGT requires a substrate bearing a lipid chain longer than 20 carbon atoms for polymerization.[31] This suggests that the lipidic moiety of the donor substrate forms an important interaction with the enzyme that is required for transglycosylation.

The availability of well-defined substrates also spurred the development new chromatographic means of analyzing the PG polymer products of the reaction. Specifically, the development of a high-resolution SDS-PAGE chromatographic assay that separates glycan polymers based on length revealed that the PGTs function as processive polymerases: the resultant nascent PG is not released into

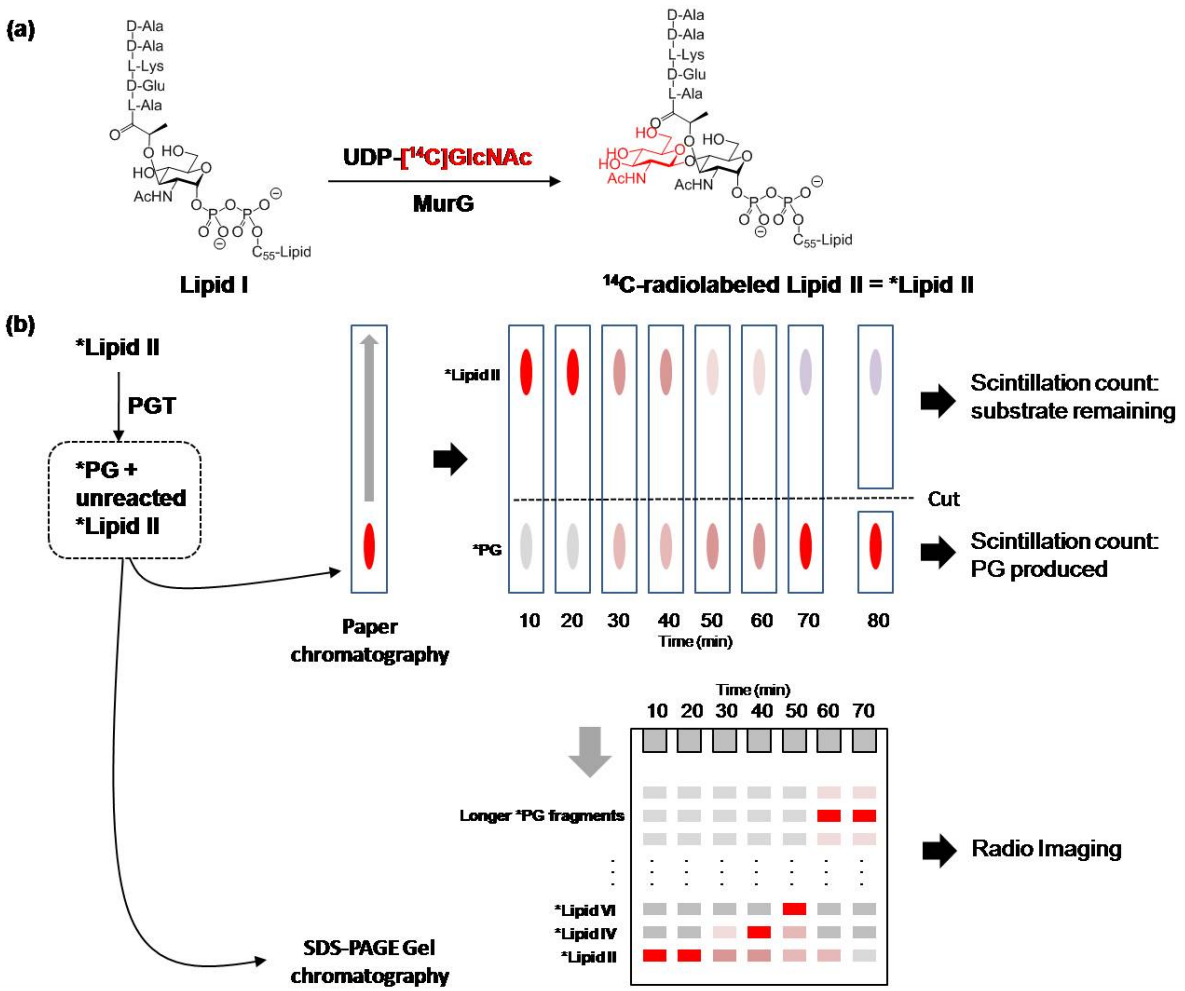

Figure 1.3 Biochemical tools for studying the PGTs. (a) ^{14}C-radiolabeled Lipid II can be prepared by using MurG to glycosylate Lipid I with UDP-[^{14}C]GlcNAc. Lipid I is chemically synthesized. (b) Paper chromatography can be used to separate PG from unreacted Lipid II substrate. This format is often used for analyzing PGT kinetics by monitoring the rates of substrate conversion to PG over time. SDS-PAGE gel chromatography of PG fragments was developed to analyze the distribution of PG fragment size.

bulk solution after each transglycosylation but rather, is utilized as the donor for a subsequent round of transglycosylation.[32]

Taken together, these results enabled a working model of PGT polymerization to be proposed. Briefly, the process is initiated by the uptake of two molecules of Lipid II by the PGTs to synthesize a nascent PG fragment, Lipid IV. In order for the PGT to elongate Lipid

IV on its reducing end in a processive manner, the same Lipid IV molecule has to be translocated to the donor binding site so that another Lipid II molecule can bind as an acceptor (**Figure 1.4**). By performing multiple cycles of transglycosylation and translocation, the nascent PG is elongated to yield a glycan polymer of desired length before it is released.

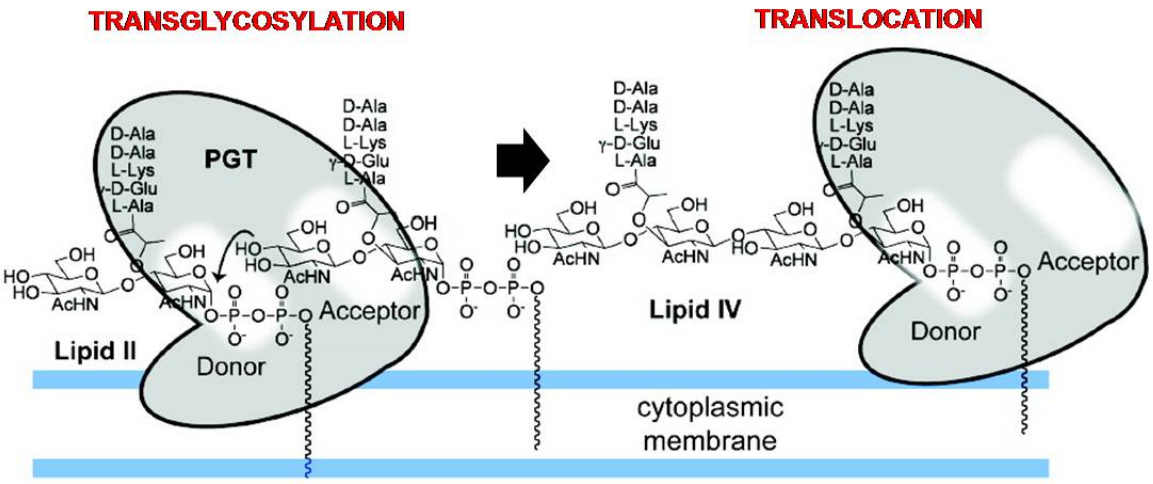

Figure 1.4 Transglycosylation and translocation of substrates by PGTs. The donor site and acceptor site both bind a Lipid II molecule. The PGT transglycosylates the Lipid II substrates to yield Lipid IV. Lipid IV is then translocated to the donor site so that the acceptor site can take up Lipid II to perform another transglycosylation. Figure adapted from Wang, T.S., Lupoli, T.J., Sumida Y., Tsukamoto H., Wu, Y., Rebets, Y., Kahne, D.E., Walker, S. (2011) *J. Am. Chem. Soc. 133*, 8528-8530.

Apparent from this model and the biochemical evidence thus far, PG synthesis is a complex operation for the PGT enzyme. A molecular picture of how the PGTs physically interact with its substrates, manage this process of shuffling substrates between binding sites, and perform transglycosylations would greatly enhance our understanding of PG synthesis. Structural studies of the PGTs have been hampered by the challenges of producing and handling these membrane-associated proteins, which aggregate rapidly. Early attempts to overexpress PGTs that did not possess an aggregation prone segment of the protein – a transmembrane α-helical anchor - resulted in protein that had low enzymatic activity or

degraded rapidly.[33,34,35,36] Fortunately, constructs that produced stable protein that can be purified to homogeneity were eventually identified, leading to four PGT X-ray crystal structures derived from *Staphylococcus aureus* PBP2, *Aquifex aeolicus* PBP1A, *Escherichia coli* PBP1B and *Staphylococcus aureus* SgtB.[37,38,39,40] These studies revealed that the PGTs are highly α-helical proteins that comprise of two lobes whose boundaries are demarcated by an extensive cleft. Remarkably, the structures bear a strong resemblance to a well-characterized PG hydrolase, the bacteriophage λ-lysozyme that catalyzes the cleavage of the β(1,4)-glycosidic bond between MurNAc and GlcNAc – the reverse reaction of PG synthesis.[38,41] As a result, it is postulated that the residues within this cleft are responsible for binding the nascent PG and Lipid II and performing the transglycosylation reaction. Sequence alignments of the PGTs with λ-lysozyme along with mutagenesis studies on the PGTs suggest a conserved glutamic acid residue present within the cleft may function as a catalytic base that deprotonates the C4-hydroxyl of GlcNAc moiety of Lipid II to attack the C1 MurNAc from the nascent PG.[42] Unfortunately, the molecular details of how the substrates interact with the PGTs remain unknown because these crystal structures did not incorporate any PG fragment or substrate. As a result, one cannot ascertain whether the observed PGT structural conformation is functionally relevant in PG synthesis.

The structures of *Staphylococcus aureus* PBP2 and *Aquifex aeolicus* PBP1A were solved in the presence and absence of Moenomycin A, the only known natural inhibitor of the PGTs, revealing changes in conformation in the lower lobe region between the apo-

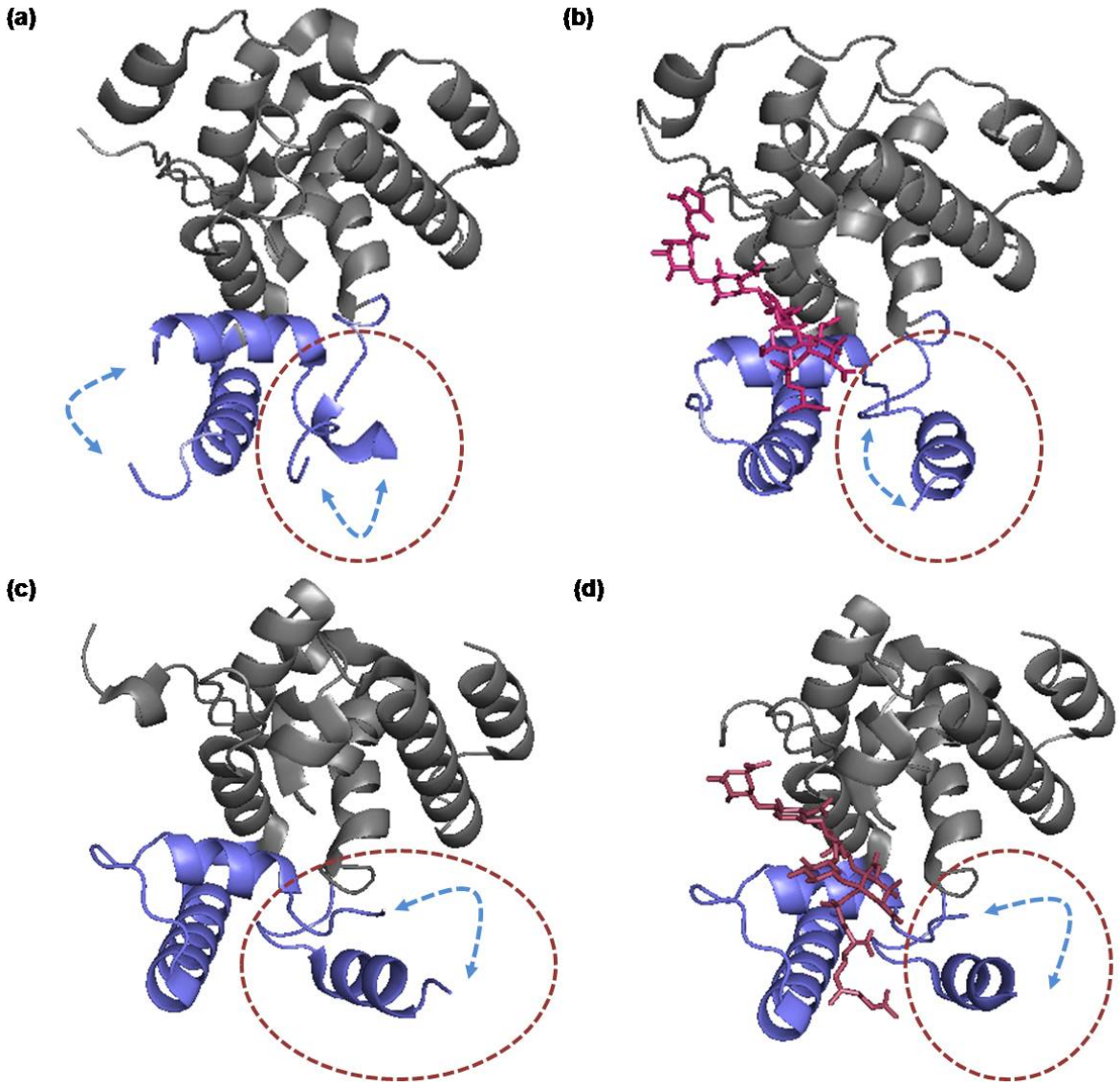

Figure 1.5 Structure of PGTs from *S. aureus* PBP2 and *A. aeolicus* PBP1A. Lower lobe region is denoted in blue, blue arrows indicate segments with missing electron density. (a) apo *S. aureus* PBP2 PGT domain. (b) Moenomycin A bound S. aureus PBP2 PGT domain. (c) apo A. aeolicus PBP1A PGT domain. (d) C_{10}-Neryl-Moenomycin A bound A. aeolicus PBP1A PGT domain. C_{10}-Neryl-Moenomycin A is a derivative of Moenomycin A that has a C_{10}-Neryl lipid chain in place of a C_{25}-moenocinol lipid chain.

enzyme and the Moenomycin A bound form.[37,43] Moreover, poor electron density in loop segments that bridge the α-helices of the lower lobe also suggests that the lower lobe is floppy and some of these conformational dynamics may be important in performing its catalytic function (**Figure 1.5**).[44,45,46]

1.3 Probing the conformational dynamics of the PGTs by NMR

PGT structures from X-ray crystallography have presented molecular detail into the structural form of the enzymes. However, the very nature of crystallographic technique often reveals only the "ground-state" conformation that may not be crucial for enzymatic function, leading to an incomplete structural interpretation of how a biochemical transformation physically occurs.[47,48,49,50] In Chapter 2, we show that the PGT's characteristic initial lag-phase kinetics can be abrogated by precubating the enzyme with Gal-Lipid IV.[51] This observation suggests that the association of Gal-Lipid IV with the PGT enable the enzyme to access a "rate-enhanced" state. There is no structural evidence that explains why the transglycosylation of two Lipid II molecules is slower than that between Gal-Lipid IV and Lipid II. We postulate that the PGTs can undergo a conformational change to accelerate the initiation of PG synthesis. To begin, a structure of a Gal-Lipid IV bound PGT will be required to compare and contrast the differences in conformation, as well as changes in structural mobility between the apo and substrate-bound enzyme.

Nuclear Magnetic Resonance (NMR) Spectroscopy is the only structural technique that enables one to obtain a three-dimensional structure of a protein and quantitatively probe the conformational dynamics of the protein at an atomic-level without introducing additional structural perturbations.[52,53] The time scale available to NMR techniques ranges over 15

orders of magnitude (10^{-12} to 10^{3} s), covering all of the relevant dynamic motions in proteins.[54] However, there are two major limitations in implementing this technique, both of which stem from the protein sample itself. First of all, the protein complex of interest (including the ligands and any associated detergent micelle) has to be small – under 35 kDa for the practical purposes of obtaining a solution structure.[53] Secondly, one needs to be able to produce multi-milligram quantities of the protein in a form that incorporates NMR-active nuclei (e.g. ^{13}C, ^{15}N), is homogeneous and stable at a pH below 7.0, and most importantly, does not form aggregates over time upon extensive exposure to room temperature (on the order of weeks).[55,56,57]

Staphylococcus aureus SgtB is a 26.2 kDa monomeric and monofunctional PGT that was successfully crystallized by Pfizer Research and Development in a form that was bound to Moenomycin A.[40] Although the protein requirements for crystallographic studies are less demanding (the protein is not isotopically-labeled, does not require extended stability at room temperature), it nonetheless requires the ability to produce multi-milligram quantities of pure protein that is properly folded and monodisperse. The existence of an efficient preparation method as well as small mass make the SgtB construct utilized by Pfizer an ideal starting ground for the development of a PGT NMR sample aimed at elucidating the solution structure of Gal-Lipid IV bound PGT complex and its associated conformational dynamics.

1.4 Research Statement

The polymerase activity of the PGTs is a key component of the cell wall biosynthetic machinery. Thus far, there are no structural data that can give us insight into how the complex polymerase activity of the PGTs is physically performed. The research in this thesis examines how the observation of a rate-enhancement effect on the PGTs by Gal-Lipid IV inspires the systematic development of an SgtB NMR sample that can potentially yield insights into the structural configuration of Gal-Lipid IV bound SgtB, enabling the use of NMR spectroscopic techniques for the study of PGT conformational dynamics.

Chapter 2 of this thesis details the observation of a rate-enhancement effect on the PGTs by Gal-Lipid IV. Chapter 3 describes the development of a high-yielding, rapid and robust preparation of *S. aureus* SgtB protein that is monomeric and monodisperse in a format suited for the production of an SgtB NMR sample. Chapter 4 details the development of a method for preparing a Moenomycin A bound SgtB protein sample that is stable at room temperature for more than three weeks that yields high quality [^{1}H,^{15}N]-HSQC spectra, indicating the feasibility for conducting solution structure studies on this sample. Because the modular format of this sample preparation method allows for the incorporation of various SgtB ligands, Chapter 5 outlines the path towards obtaining a Lipid IV bound SgtB solution structure. In closing, we show how the ability to generate multimilligram quantities of monomeric, monodisperse SgtB in a highly efficient and scalable manner enables the practical implementation of a high-throughput screen for new inhibitors of SgtB that may be the basis for new antibacterials.

1.5 References

1. Holtje, J. V. (1998) Growth of the stress-bearing and shape-maintaining murein sacculus of Escherichia coli, *Microbiol. Mol. BIol. Rev. 62*, 181-203.
2. Vollmer, W., and Bertsche, U. (2008) Murein (peptidoglycan) structure, architecture and biosynthesis in Escherichia coli, *Biochim. Biophys. Acta 1778*, 1714-1734.
3. Koch, A. L. (2003) Bacterial wall as target for attack: Past, present, and future research, *Clin. Microbiol. Rev 16*, 673-687.
4. Kahne, D., Leimkuhler, C., Lu, W., and Walsh, C. (2005) Glycopeptide and lipoglycopeptide antibiotics, *Chem. Rev. 105*, 425-448.
5. Fisher, J. F., Merouch, S. O., and Mobashery, S. (2009) Bacterial resistance to beta-lactam antibiotics: compelling opportunism, compelling opportunity, *Chem. Rev. 105*, 395-424.
6. Vollmer, W. and Seligman, S. J. (2010) Architecture of peptidoglycan: more data and more models, Trends Microbiol. 18, 59-66.
7. Meroueh, S. O., Bencze, K. Z., Hesek D., Lee, M., Fisher, J. F., Stemmler, T. L., and Mobashery, S. (2006) Three-dimensional structure of the bacterial cell peptidoglycan, *Proc. Natl. Acad. Sci. U. S. A. 103*, 4404-4409.
8. Dmitriev, B. A., Toukach, F., and Ehlers, S. (2005) Towards a comprehensive view of the bacterial cell wall, *Trends Microbiol. 13*, 569-574.
9. Vollmer, W. Blanot, D., and de Pedro, M. A. (2008) Peptidoglycan structure and architecture, *FEMS MIcrobiol. Rev. 32*, 149-167.
10. Van Heijenoort, J. (2007) Lipid Intermediates in the biosynthesis of bacterial peptidoglycan, *Microbiol. Mol. Biol. Rev. 71*, 620-635

11. Bugg, T. D. and Walsh, C. T. (1992) Intracellular steps of bacterial cell wall peptidoglycan biosynthesis: enzymology, antibiotics, and antibiotic resistance, *Nat. Prod. Rep. 9*, 199-215.

12. Van Heijenoort, J. (2001) Recent advances in the formation of the bacterial peptidoglycan monomer unit, *Nat. Prod. Rep. 18*, 503-519.

13. Barreteau, H. Kovac., A., Boniface, A., Sova, M., Gobec, S., and Blanot, D. (2008) Cytoplasmic steps of peptidoglycan biosynthesis, *FEMS Microbiol. Rev. 32*, 168-207.

14. Bouhss, A., Trunkfield, A. E., Bugg, T. D., and Mengin-Lecruelx, D. (2008) The biosynthesis of peptidoglycan lipid-linked intermediates, *FEMS MIcrobiol. Rev. 32*, 208-233

15. Ha, S., Walker, D., Shi, Y., and Walker, S. (2000) The 1.9A crystal structure of Escherichia coli MurG, a membrane-associated glycosyltransferase involved in peptidoglycan biosynthesis. *Protein Sci. 9*, 1045-1052.

16. Chen, L., Men, H., Ha, S., Ye, X. Y., Brunner, L., Hu, Y., and Walker, S. (2002) Intrinsic lipid preferences and kinetic mechanism of Escherichia coli MurG, *Biochemistry 41*, 6824-6833.

17. Men, H., Park, P., Ge, M., and Walker, S., (1998) Substrate synthesis and activity assay for MurG, J. Am. Chem. Soc. 120, 2484-2485

18. Ruiz, N. (2008) Bioinformatics identification of MurJ (MviN) as the peptidoglycan Lipid II flippase in Escherichia coli, *Proc. Natl. Acad. Sci. U. S. A. 105*, 15553-15557.

19. Inoue, A. Murata, Y. Takahashi, H., Tsuji, N. Fujisaki, S., and Kato, J. (2008) Involvement of an essential gene, mviN, in murein synthesis in Escherichia coli, *J. Bacteriol. 190*, 7298-7301.

20. Mohammadi, T., van Dam, V., Sijbrandi, R., Vernet, T., Zapun, A., Bouhss, A., Diepeveen-de Bruin, M., Nguyen-Disteche, M., de Kruijff, B., and Breukink, E., (2011) Identification of FtsW as a transporter of lipid-linked cell wall precursors across the membrane, *EMBO J. 30*, 1425-1432.

21. Sauvage, E., Kerff, F., Terrak, M., Ayala, J. A., and Charlier, P. (2008) The penicillin-binding proteins: structure and role in peptidoglycan biosynthesis, FEMS Microbiol. Rev. 32, 234-258.

22. Welzel, P. (2005) Syntheses around the transglycosylation step in peptidoglycan biosynthesis, Chem. Rev. 105, 4610-4660.

23. Schwartz, B., Markwalder, J. A., and Wang, Y. (2001) Lipid II: total synthesis of the bacterial cell wall precursor and utilization as a substrate for glycosyltransfer and transpeptidation by penicillin-binding protein PBP1b of Escherichia coli, *J. Am. Chem. Soc. 123*, 11638-11643.

24. Ye, X. Y., Lo, M. C., Brunner, L., Walker, D., Kahne, D., and Walker, S. (2001) Better substrates for bacterial transglycosylases, *J. Am. Chem. Soc. 123*, 3155-3156.

25. VanNieuwenhze, M.S., Mauldin, S. C., Zia-Ebrahimi, M., Winger, B. E., Hornback, W. J., Saha, S. J., Aikins, J. A., and Blaszczak, L. C., (2002) The first total synthesis of Lipid II: the final monoeric intermediate in bacterial cell wall biosynthesis, *J. Am. Chem. Soc. 124*, 3656-3660.

26. Chen, L. Walker, D., Sun, B., Hu, Y., Walker, S., and Kahne, D. (2003) Vancomycin analogues active against vanA-resistant strains inhibit bacterial transglycosylase without binding substrate, *Proc. Natl. Acad. Sci. U. S. A. 100*, 5658-5663.

27. Barrett, D., Leimkuhler, C., Chen., L., Walker, D., Kahne, D., and Walker S., (2005) Kinetic characterization of the glycosyltransferase module of Staphylococcus aureus PBP2, *J. Bacteriol. 187*, 2215-2217.

28. Zhang, Y., Fechter, E. J., Wang, T. S., Barrett, D., Walker, S., and Kahne, D. E. (2007) Synthesis of heptaprenyl-lipid IV to analyze peptidoglycan glycosyltransferases, *J. Am. Chem. Soc. 129*, 3080-3081.

29. Perlstein, D. L., Zhang, Y., Wang, T. S., Kahne, D. E., an d Walker, S. (2007) The direction of glycan chain elongation by peptidoglycan glycosyltransferases, *J. Am. Chem. Soc. 129*, 12674-12675.

30. Ward, J. B., and Perkins, H. R. (1973) The direction of glycan synthesis in a bacterial peptidoglycan, *Biochem. J. 135*, 721-728.

31. Perlstein, D. L., Wang, T. S., Doud, E. H., Kahne, D., and Walker, S. (2010) The role of substrate lipid in processive glycan polymerization by the peptidoglycan glycosyltransferases, *J. Am. Chem. Soc. 132*, 48-49.

32. Barrett, D., Wang, T. S., Yuan, Y., Zhang, Y., Kahne, D., and Walker, S. (2007) Analysis of glycan polymers produced by peptidoglycan glycosyltransferases, *J. Biol. Chem. 282*, 31964-31971.

33. Wang, C.C., Schultz, D> E., and Nicholas, R. A., (1996) Localization of a putative second membrane association site in penicillin-binding protein 1b of Escherichia coli, *Biochem. J. 316*, 149-156

34. Di Guilmi, A. M., Mouz, N., Andrieu, J. P., Hoskins, J., Jaskunas, S. R., Gagnon, J., Dideberg, O., and Vernet, T. (1998) Identification, purification, and characterization of transpeptidase and glycosyltransferase domains of Streptococcus pneumonia penicillin-binding protein 1a, *J. Bacteriol. 180*, 5652-5659

35. Di Guilmi, A. M., Mouz, N., Martin, L., Hoskins, J., Jaskunas, S. R., Dideberg, O., and Vernet, T. (1999) Glycosyltransferase domain of penicillin-binding protein 2a from Streptococcus pneumonia is membrane associated, *J. Bacteriol. 181*, 2773-2781

36. Lovering, A. L., de Castro, L. H., Lim, D., and Strynadka, N. C., (2006) Structural analysis of an "open" form of PBP1b from Streptococcus pneumonia, *Protein Sci. 15*, 1701-1709

37. Lovering, A. L., de Castro, L. H., Lim, D., and Strynadka, N. C. J. (2007) Structural insight into the transglycosylation step of bacterial cell-wall biosynthesis, *Science 315*, 1402-1405.

38. Yuan, Y., Barrett, D., Zhang, Y., Kahne, D., Sliz, P., and Walker, S. (2007), Crystal structure of a peptidoglycan glycosyltransferase suggests a model for processive glycan chain synthesis, *Proc. Natl. Acad. Sci. U. S. A. 104*, 5348-5353.

39. Sung, M. T., Lai, Y. T., Huang, C. Y., Chou, L. Y., Shih, H. W., Cheng, W. C., Wong, C. H., and Ma, C. (2009) Crystal structure of the membrane-bound bifunctional transglycosylase PBP1b from Escherichia coli, *Proc. Natl. Acad. Sci. U. S. A. 106*, 8824-8829.

40. Heaslet, H., Shaw, B., Mistry, A., and Miller, A. A. (2009) Characterization of the active site of S. aureus monofunctional glycosyltransferase (Mtg) by site-directed

mutation and structural analysis of the protein complexed with moenomycin, *J. Struct. Biol. 167*, 129-135.

41. Leung, A. K. W., Duewel, H. S., Honek, J. F., and Berghuis, A. M. (2001) Crystal structure of the lytic transglycosylase from bacteriophage lambda in complex with hexa-N-acetylchitohexose, Biochemistry 40, 5665-5673.

42. Terrak, M., Ghosh, T. K., van Heijenoort, J., Van Beeumen, J., Lampilas, M., Aszodi, J., Ayala, J. A., Ghuysen, J. M., and Nguyen-Disteche, M. (1999) The catalytic, glycosyltransferase and acyl transferase modules of the cell wall peptidoglycan-polymerizing penicillin-binding protein 1b of Escherichia coli, *Mol. Microbiol. 34*, 350-364.

43. Yuan, Y., Fuse, S., Ostash, B., Sliz, P., Kahne, D., and Walker, S. (2008) Structural analysis of the contacts anchoring moenomycin to peptidoglycan glycosyltransferases and implications for antibiotic design, *ACS Chem. Biol. 3*, 429-436.

44. Lovering, A.L, Gretes, M., and Stynadka, N. C. (2008) Structural details of the glycosyltransferase step of peptidoglycan assembly, *Curr. Opin. Struct. Biol. 18*, 534-543.

45. Lovering, A. L., de Castro, L., and Strynadka, N. C. (2008) Identification of dynamic structural motifs involved in peptidoglycan glycosyltransfer, *J. Mol. Biol. 383*, 167-177.

46. Breyer, W. A., and Matthews, B. W. (2001) A structural basis for processivity, *Protein Sci. 10*, 1699-1711.

47. Wagner, G. (1995) The importance of being floppy, Nat. Struct. Biol. 2, 255-257.

48. Kay, L. E., (1998) Protein dynamics from NMR, Nat. Struct. Biol. 5 Suppl., 513-517.

49. Ishima, R., and Torchia, D. A. (2000) Protein dynamics from NMR, Nat. Struct. Biol. 7, 740-745.

50. Baldwin, A. J., and Kay, L. E. (2009) NMR spectroscopy brings invisible protein states into focus, Nat. Chem. Biol. 5, 808-814.

51. Wang, T.S., Lupoli, T.J., Sumida Y., Tsukamoto H., Wu, Y., Rebets, Y., Kahne, D.E., and Walker, S. (2011) Primer preactivation of peptidoglycan polymerases, *J. Am. Chem. Soc. 133*, 8528-8530.

52. Boehr, D. D., Dyson, J., and Wright, P. E. (2006) An NMR perspective on enzyme dynamics, Chem. Rev. 106, 3055-3079.

53. Marintchev, A., Frueh, D., and Wagner, G. (2007) NMR methods for studying protein-protein interactions involved in translation initiation, *Method Enzymol. 430*, 283-331.

54. Kleckner, I. R., and Foster, M. P. (2011) An introduction to NMR-based approaches for measuring protein dynamics, *Biochim. Biophys. Acta 1814*, 942-968.

55. Billeter, M., Wagner, G., and Wüthrich, K. (2008) Solution NMR structure determination of proteins revisited, J. Biomol. NMR 42, 155-158.

56. Bagby, S., Tong, K. Il, and Ikura, M. (2001) Optimization of protein solubility and stability for protein nuclear magnetic resonance, Method Enzymol. 339, 20-41.

57. Lepre, C. A., and Moore, J. M. (1998) Microdrop screening: a rapid method to optimize solvent conditions for NMR spectroscopy of proteins, *J. Biomol. NMR 4*, 493-499.

Chapter Two: PGT Rate Enhancement by Peptidoglycan Fragment Analog Gal-Lipid IV

Work in this chapter is adapted with permission from:

Wang, T.S.; Lupoli, T. J., Sumida, Y., Tsukamoto, H., Wu, Y., Rebets, Y., Kahne, D.E., and Walker S. (2011) Primer preactivation of peptidoglycan polymerases, *J. Am. Chem. Soc.* 133, 8528-8530. Copyright 2011 American Chemical Society.

Individual contributions are laid out in Section 2.3 of this chapter.

2.1 Introduction

Peptidoglycan glycosyltransferases (PGTs) are highly conserved bacterial enzymes that catalyze Lipid II polymerization to form peptidoglycan (PG) polymers that constitute the bulk of the bacterial cell wall.[1] These PGT enzymes can exists either as independent, monofunctional proteins or alternately, as separate domains that are combined into a single bifunctional protein (e.g. *Staphylococcus aureus* Penicillin-binding Protein 2). Because the bacterial cell wall integrity has to be maintained during growth and cell division to prevent lysis, it has been proposed that the PGTs function within a tightly coordinated multi-protein complex that can speed up or shut down cell wall synthesis in concert with growth and division signals.[2,3,4]

The emergence of antibacterial resistance in our current drug arsenal has been a major driving force for discovering new druggable enzymatic targets for developing new antibacterials.[5] The PGTs have emerged as a promising therapeutic target because of their essential role in PG synthesis.[6,7] In order to design multiple drugs that can disrupt the function of the PGTs in different ways, a detailed understanding of their mechanism of action is required.[8] Well-defined substrates and inhibitors of the peptidoglycan biosynthetic process have enabled researchers to piece together a view of how peptidoglycan (PG) is synthesized (**Figure 2.1**). In particular, we now know that Lipid II is the only substrate that is required for the PGTs to synthesize glycan polymers and that the PGTs utilize a processive mechanism to produce long glycan polymers.[9] It has also been shown recently that polymer extension proceeds via the reducing end of the glycan chain.[10]

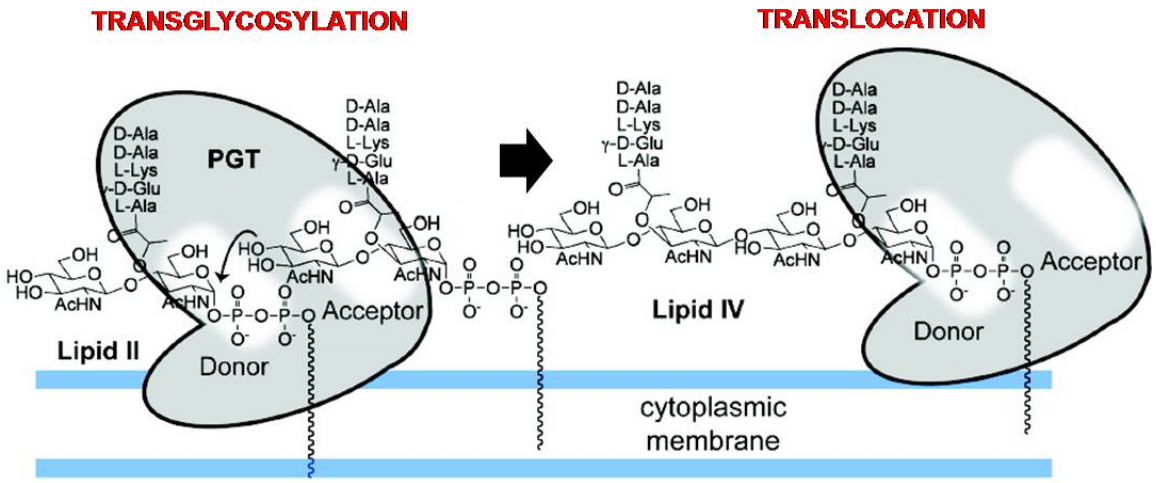

Figure 2.1 Biosynthesis of peptidoglycan.

In the course of these studies, researchers have observed that the reaction time courses of different PGTs exhibit a prolonged lag phase that could be due to a slow conformational rearrangement of the enzyme to an active form and/or a slow first coupling step.[9,11,12] We reasoned that if the formation of Lipid IV, the product of the first coupling of two Lipid II molecules, is rate-limiting, then the addition of Lipid IV should prime the enzyme and accelerate the polymerization of Lipid II.

In this chapter, we show that Gal-Lipid IV, a PG fragment that is able to act as a glycosylation donor to Lipid II, enhances the PGT's initial rate of polymerization. Additionally, we demonstrate how the availability of monodisperse and monomeric SgtB - the only well-behaved PGT in the group studied - is pivotal in demonstrating that the lag-phase phenomenon is an intrinsic feature of the enzyme. This result, along with previous observations of various PGT structures, suggest that a conformational change is induced by the binding of Gal-Lipid IV by the PGTs, resulting in an "activated" elongation-competent state.

2.2 Results and Discussion

2.2.1. Pre-incubation of PGTs with Gal-Lipid IV increases the rate of PG synthesis from Lipid II

In order to test the hypothesis that Lipid IV can accelerate the initial rate of PG synthesis, we needed a Lipid IV substrate that is incapable of reacting with itself but is reactive with Lipid II to form peptidoglycan. We cannot use the natural Lipid IV substrate because it can be utilized as a monomeric building block by the PGT to give peptidoglycan.[13,14] Perlstein and coworkers developed a Gal-Lipid IV substrate that cannot be glycosylated on the non-reducing end of Lipid IV by blocking it with Galactose.[10] This blocked substrate can be easily prepared by incubating Lipid IV with UDP-Galactose in the presence of GalT enzyme, a β1-4 galactosetransferase that transfers Galactose to C4-hydroxyl of terminal *N*-acetylglucosamine (GlcNAc) residues on a wide variety of molecules.[15,16,17,18] By capping off the non-reducing end of Lipid IV, Gal-Lipid IV is incapable of reacting with itself but can be extended by sequential addition of Lipid II on the non-reducing end to form peptidoglycan (**Figure 2.2**).

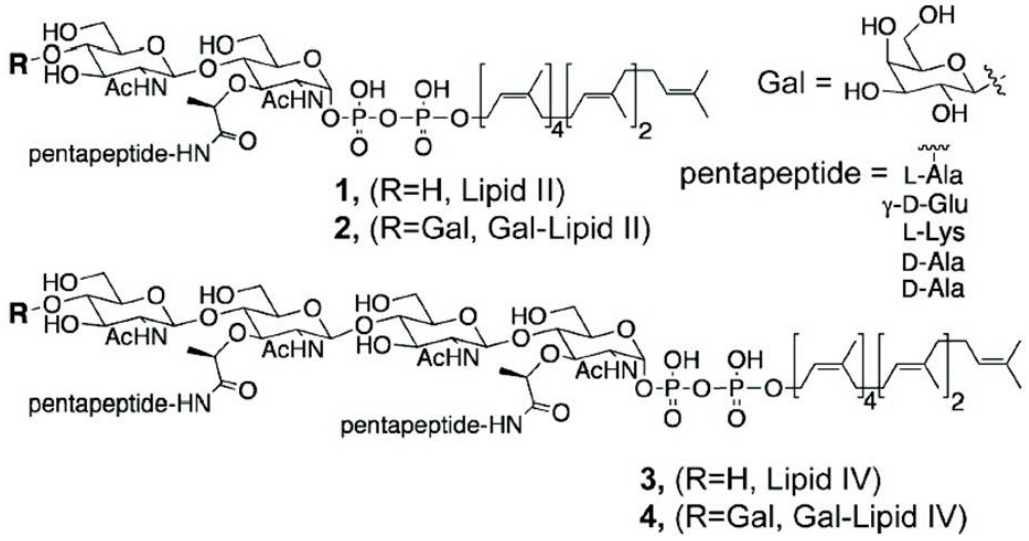

Figure 2.2 Synthesized substrates used in analyzing PGT reactions. Compound 1: Lipid II, featuring a C_{35}-lipid tail that balances solubility and reactivity. Naturally occurring Lipid II possesses a C_{55}-undecaprenyl lipid tail that confers poor solubility and cannot be used in in-vitro assays. Compound 2: Gal-Lipid II featuring a C_{35}-lipid tail. Compound 3: Lipid IV, featuring a C_{35}-lipid tail. Compound 4: Gal-Lipid IV, featuring a C_{35}-lipid tail.

Since Gal-Lipid IV functions as a "donor-only" substrate that mimics the product of the first coupling step of the PGT, we tested its effect on the reaction rate of *Escherichia coli* PBP1A, which contains an N-terminal PGT domain and a C-terminal transpeptidase domain. We incubated the enzyme for 20 minutes with Gal-Lipid IV to prime/activate the enzyme. Radiolabeled Lipid II was then added. The reaction mixtures were incubated for varying periods of time and then analyzed by paper chromatography, which separates the long peptidoglycan product from the shorter oligomeric starting materials Lipid II and Gal-Lipid IV. As a control, we prepared a separate reaction where we incubated the enzyme with a buffer aliquot that did not contain Gal-Lipid IV for 20 minutes before the addition of Lipid

II. Unlike the control reaction, there was no lag phase in the presence of Gal-Lipid IV, and the reaction rate was approximately 4-fold higher (**Figure 2.3**).

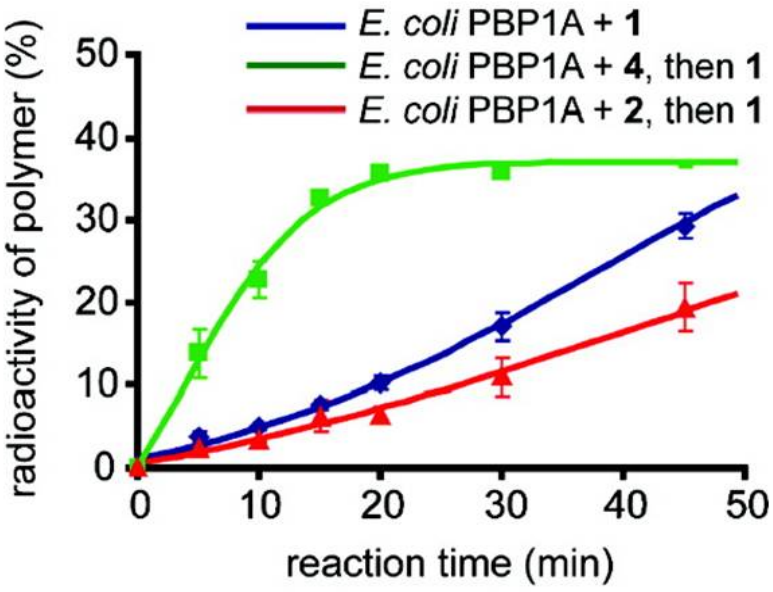

Figure 2.3. Peptidoglycan synthesis by the PGT from E. coli PBP1A under the priming influence of various substrates. Blue: No priming substrate is added. Green: Gal-Lipid IV (compound 4) primed E. coli PBP1A. Red: Gal-Lipid II (compound 2) primed E. coli PBP1A.

We repeated this series of experiments with another PGT, *Escherichia coli* PBP1B, and observed that Gal-Lipid IV had a similar rate-enhancement effect on the enzyme (**Figure 2.4a**). Because the *E. coli* PBP1A and PBP1B are bifunctional enzymes with a distinct transpeptidase domain that is in close proximity to the PGT domain, we were curious as to whether the transpeptidase domain was involved with this rate-enhancement effect. TP-truncated variants of the *E. coli* PBP1A and PBP1B displayed a characteristic lag-phase in the time course of peptidoglycan synthesis that is abrogated by the addition of Gal-Lipid IV, resulting in 5- and 2-fold rate enhancement respectively (**Figure 2.4b and 2.4c**). This allows us to conclude that this activation phenomenon is localized to the PGT domain of the enzyme. Because the PGTs tested thus far originated from Gram-negative bacteria, we

repeated the same set of experiments with the *Staphylococcus aureus* PBP2 and observed a 2-fold rate enhancement (**Figure 2.4d**). This suggests that this activation phenomenon by Gal-Lipid IV may be general for the PGTs, although the magnitude of the rate enhancement varied depending on the enzyme.

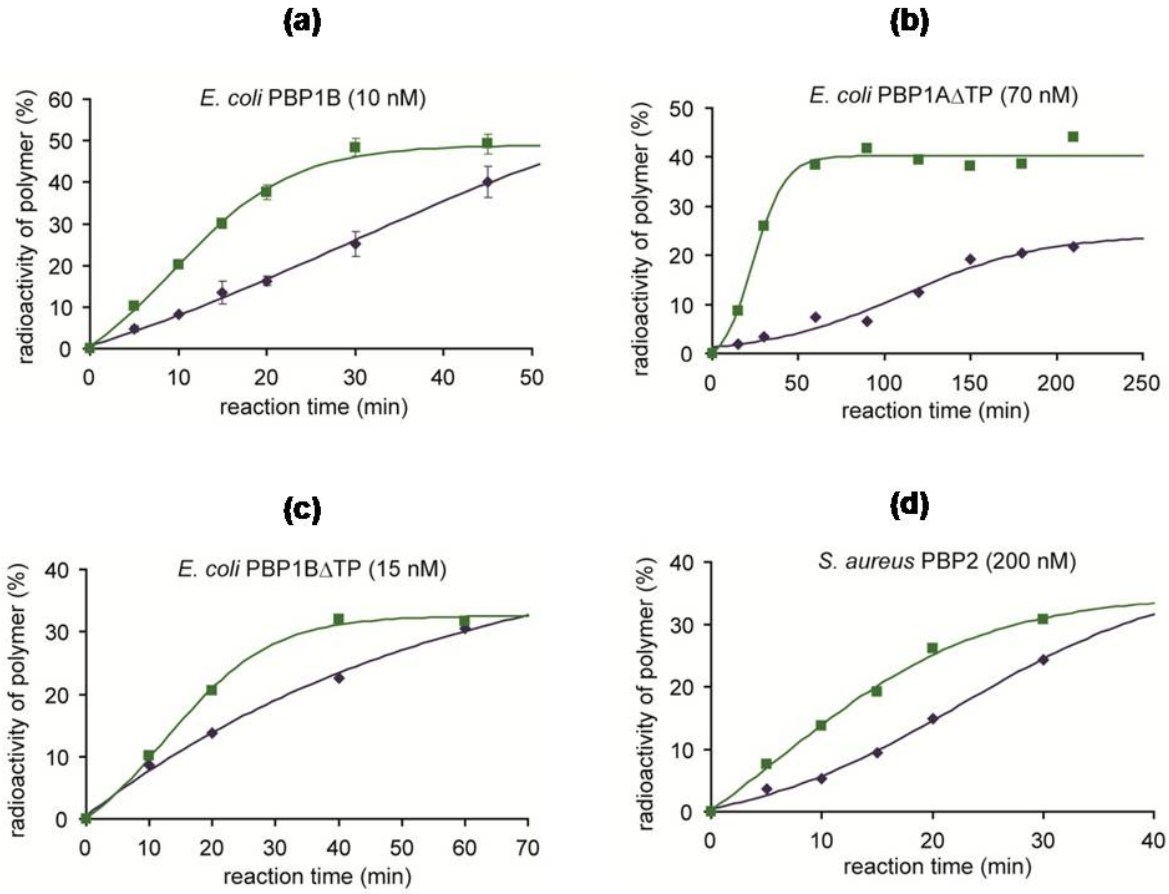

Figure 2.4 Summary of rate-enhancement effect by Gal-Lipid IV on various PGTs. (a) E. coli PBP1B primed by Gal-Lipid IV (green) vs. unprimed (purple). (b) E. coli PBP1B ΔTM primed by Gal-Lipid IV (green) vs. unprimed (purple). (c) E. coli PBP1B ΔTM primed by Gal-Lipid IV (green) vs. unprimed (purple). (d) S. aureus PBP2 primed by Gal-Lipid IV (green) vs. unprimed (purple).

2.2.2. The product distribution of Gal-Lipid IV activated PGTs suggests that Lipid IV increases the concentration of "elongation-competent" PGTs

The Kahne and Walker labs have previously reported that PGTs produce long glycan polymers even at a 1:1 enzyme: substrate ratio.[19] This remarkable insensitivity of PGT product lengths to the enzyme:substrate ratio can be explained if initiation is so much slower than elongation that only a small fraction of the available enzyme makes polymer before the substrate runs out.[20,21,22] If Gal-Lipid IV does indeed increase the fraction of rate-enhanced "activated" enzyme, then its addition would be expected to decrease the glycan chain lengths produced at a given enzyme:substrate ratio, since more enzyme molecules would be competing for substrate.[23,24] To test this prediction, we incubated *Escherichia coli* PBP1A in the presence or absence of Gal-Lipid IV and then added 7-fold excess of Lipid II. The product distribution was evaluated using an SDS-PAGE gel chromatographic method that separates products with single-disaccharide resolution.[9] Consistent with this prediction, the addition of Gal-Lipid IV resulted in a decrease in product length. This suggests that Gal-Lipid IV preincubation generates a higher concentration of "activated" PGT enzymes (**Figure 2.5**).

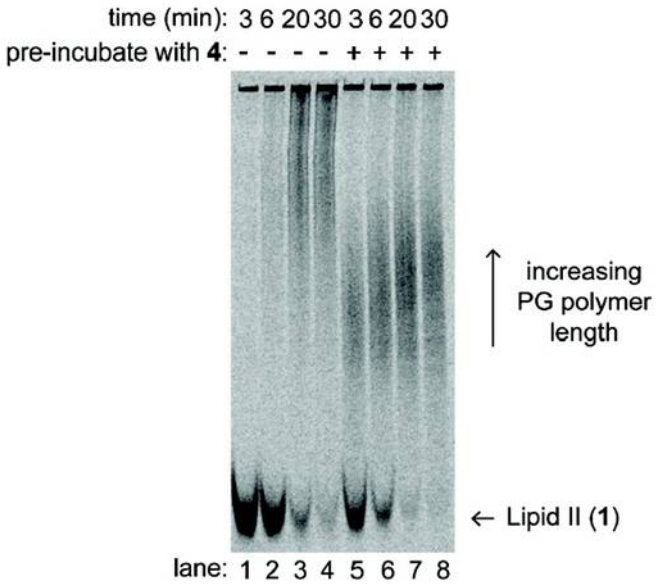

Figure 2.5 SDS-PAGE of PG polymers produced by *E. coli* PBP1A. Lanes (1–4): Control, no Gal-Lipid IV primer is added, resulting in longer peptidoglycan polymers. Lanes (5-8): Preincubation of Gal-Lipid IV**,** resulting in shorter peptidoglycan polymers, and notably faster consumption of substrate Lipid II.

2.2.3 Initial rate-enhancement by Gal-Lipid IV does not depend on the aggregation state of the PGTs.

Our experiments thus far have utilized preparations of PGTs that are soluble monodisperse aggregates. It is unclear whether these aggregates are a native state of the PGTs. It is possible that the observed lag phase may be an artifact of the enzyme having to function in a suboptimal, nonnative aggregated state.[25,26] Nonnative protein aggregates are poorly folded and may not be able to efficiently access important conformational states that are required for enzymatic function. It is possible that the binding of Gal-Lipid IV may assist poorly folded PGT aggregates to access the "activated" state.

SgtB is the only PGT that we were able to prepare in a pure, monodisperse and monomeric form (**Figure 2.6**).[27] By incubating SgtB in the presence and absence of Gal-

Lipid IV, we were able to observe 7-fold rate enhancement (**Figure 2.7**). We were able to infer that the ability to undergo rate acceleration by Gal-Lipid IV is not an artifact of the aggregation state of the PGTs.

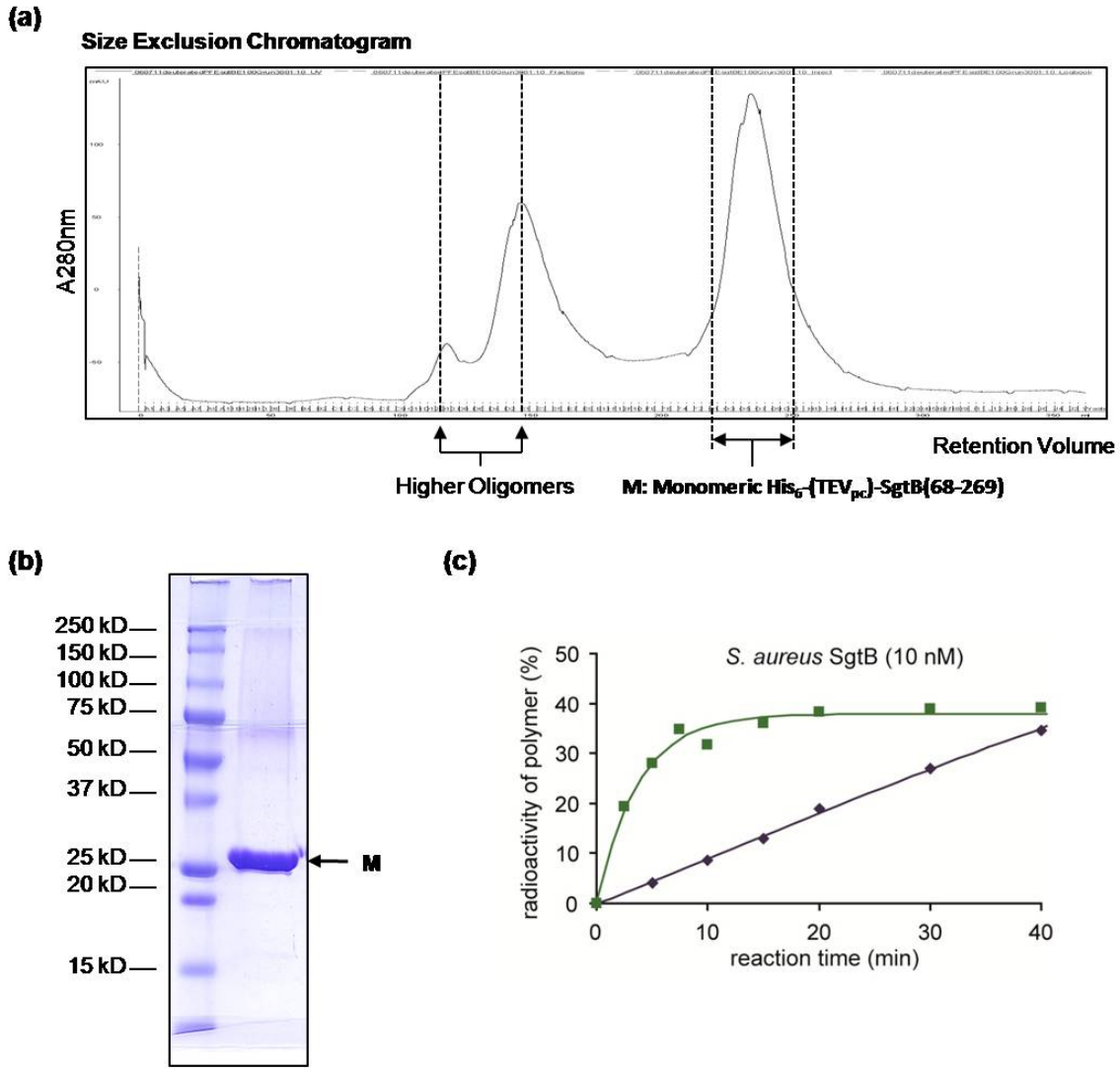

Figure 2.6 Isolating monomeric and monodisperse SgtB. (a) Size-exclusion profile of Ni-NTA purified SgtB. The monomeric fraction M is isolated for enzymological studies. (b) SDS-PAGE gel of fraction M. (c) Rate-enhancement effect by Gal-Lipid IV on SgtB.

2.2.4. The synthesis of Lipid IV is rate-limiting in PG synthesis

Our observation that the preincubation of PGTs with Gal-Lipid IV accelerates the initial rate of PG synthesis suggests that the formation of Lipid IV may be rate-limiting. In order to test this hypothesis, we prepared Gal-Lipid II, whose non-reducing end is blocked in the same manner as in Gal-Lipid IV. Gal-Lipid II was preincubated with *E. coli* PBP1A prior to initiating the reaction with Lipid II, but its presence did not accelerate the reaction. Because Gal-Lipid II, like Gal-Lipid IV, was incorporated into the newly synthesized PG, it can bind to the donor site of the PGT like Gal-Lipid IV but yet cannot influence it in the same manner (**Figure 2.3**). This experiment showed that initial rate-acceleration does not depend simply on having a functional "donor-only" substrate. Instead, the donor substrate must contain a tetrasaccharide or longer fragment of the elongating chain. Taken together, this data suggest that the slow step of PG synthesis involves the formation of Lipid IV.

Thus far, we do not have any insight as to why the formation of Lipid IV is rate-limiting on a molecular level. This is especially intriguing since the chemical transformation involved in coupling Lipid II to yield Lipid IV is identical in the elongation of higher PG fragments using Lipid II. A multitude of possibilities exist: Lipid IV may induce a conformational change in PGT such that (1) transglycosylation is more efficient, (2) the uptake of Lipid II substrate in the acceptor site is more efficient, or, Lipid IV simply binds more efficiently to the donor site than Lipid II (**Figure 2.7**). Previous studies by Dr. Andrew Wang from the Kahne lab estimated the affinity of Gal-Lipid IV towards PGT to be 7 fold of Lipid II.[28]

Recent biochemical evidence support the notion that conformational changes in the enzyme bring about rate-enhancement: *E. coli* PBP1B can undergo a similar rate

enhancement effect in the presence of an accessory protein, LpoB. This result shows that stronger affinity of Gal-Lipid IV for the PGT does not fully explain the observed rate-enhancement, instead, the PGTs might possess a distinct "activated" conformation that can be similarly achieved through the binding of Lipid IV.[29]

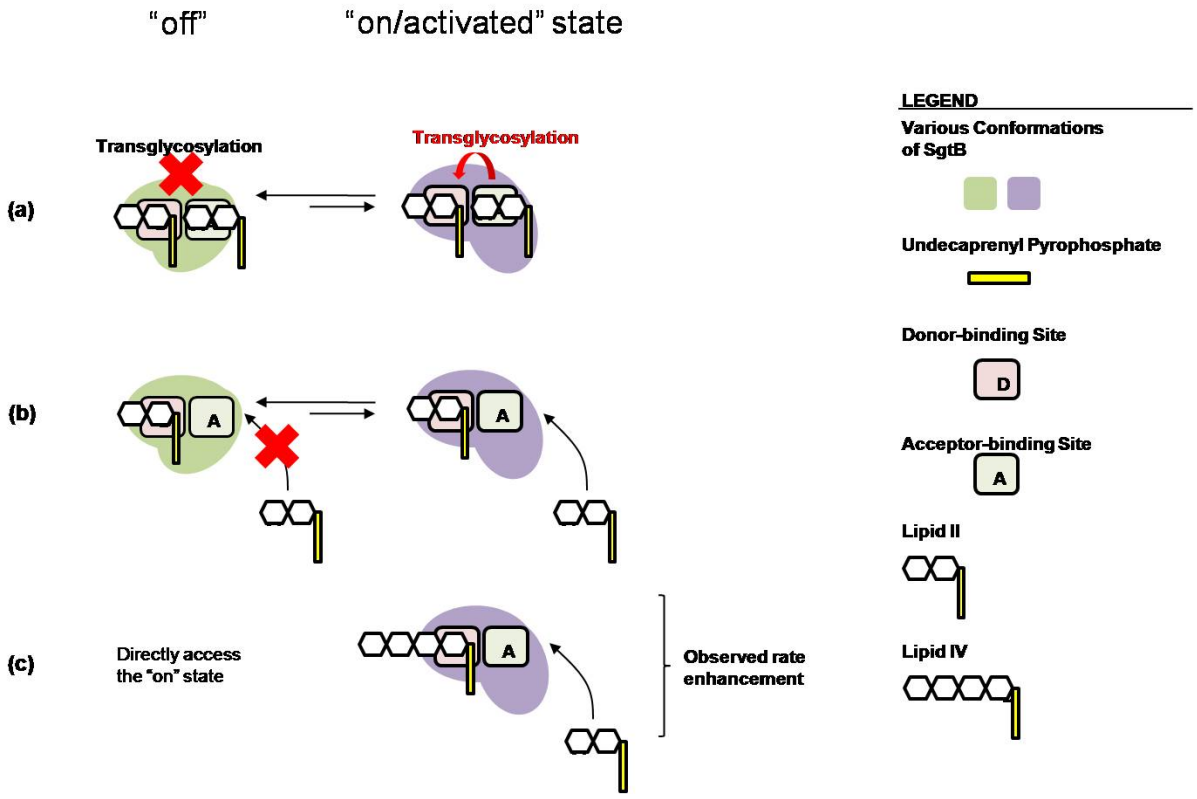

Figure 2.7 Possible causes of the observed initial lag phase kinetics in PGTs. (a) A conformational change into an "on/activated" form that makes transglycosylation is more efficient. (b) A conformational change into an "on/activated" form that makes uptake of Lipid II more efficient. (c) Binding of Lipid IV or interaction with LpoB may induce conformational changes to access the "on/activated" form.

Studies by Dr. Andrew Wang suggest that in the case of an *E. coli* PBP1A, Gal-Lipid IV may bind to the PGT in a similar fashion as Moenomycin A because preincubating the PGT with Gal-Lipid IV increases the IC_{50} of Moenomycin A by 5-fold over that of the untreated enzyme.[30] This raises the question of whether the Moenomycin A bound PGT structure in any way reflects the Gal-Lipid IV bound/"activated" state of the PGT. Moreover, there may be other points of flexibility that are not revealed in the crystallized form of the protein that are essential for its catalytic function.

This view portends the perceived conformational flexibility of the protein and how it may be crucial for its function in a physiological context. Previous structural work on the PGTs has revealed points of flexibility that are proximal to the putative active site of the enzyme. The lack of electron density on a series of PGT structures in the lower lobe region of the enzyme suggests that this region of the protein is highly disordered (**Figure 2.8**).[31,32,33,34,35] We need more information on the conformational changes that take place as the PGT interacts with its ligands. This sets up our motivation for pursuing the solution structure and studying the conformational dynamics of the PGTs using SgtB as a model system in Chapters 3 and 4.

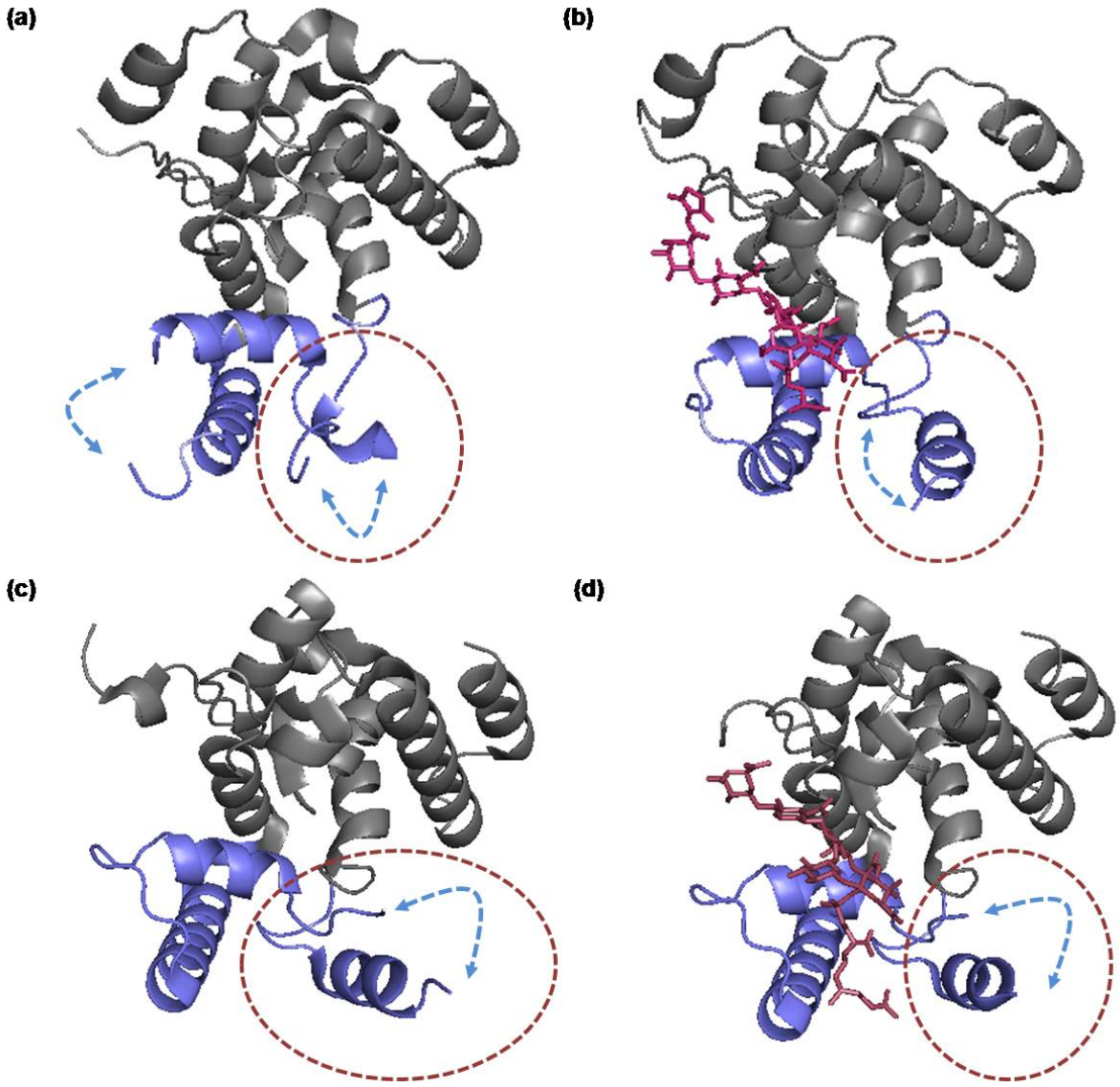

Figure 2.8 Structure of PGTs from *S. aureus* PBP2 and *A. aeolicus* PBP1A. Lower lobe region is denoted in blue, blue arrows indicate segments with missing electron density. (a) apo *S. aureus* PBP2 PGT domain. (b) Moenomycin A bound *S. aureus* PBP2 PGT domain. (c) apo *A. aeolicus* PBP1A PGT domain. (d) C_{10}-Neryl-Moenomycin A bound *A. aeolicus* PBP1A PGT domain. C_{10}-Neryl-Moenomycin A is a derivative of Moenomycin A that has a C_{10}-Neryl lipid chain in place of a C_{25}-moenocinol lipid chain.

2.3 Selected Materials and Methods

2.3.1 Materials

C_{35}-Lipid II was synthesized and radiolabeled by Dr. Yuto Sumida as described previously.[36] C_{35}-Lipid IV was synthesized and radiolabeled by Dr. Yi Zhang as previously reported.[13] Gal-Lipid II and Gal-Lipid IV were converted from C_{35}-Lipid II and C_{35}-Lipid IV, respectively, by Dr. Andrew Wang as described previously.[10] Full-length *E. coli* PBP1A was purified by Dr. Andrew Wang and *S. aureus* PBP2 was purified by Dr. Yuriy Rebets following procedures described previously.[9,19] TP truncated *E. coli* PBP1A(M1-N251) was purified by Dr. Andrew Wang as previously reported.[19] Full length *E. coli* PBP1B plasmid was obtained from the Bernhardt lab (Harvard Medical School) and purified by Dr. Tania Lupoli as described. TP truncated mutant PBP1B (M1-S409) was cloned and purified by Dr. Tania Lupoli. *S. aureus* SgtB (D68-R269), overexpression plasmid was obtained from Dr. Alita Miller (Pfizer Global Research and Development, MTA:A12545) and purified by Yihui Wu as described in detail in Chapter 3 of this thesis. Moenomycin A was isolated from Flavomycin-80 feedstock (provided by Merck Research Laboratories) by Dr. Hirokazu Tsukamoto and Yihui Wu as previously described.[37] All other chemicals were purchased from Sigma-Aldrich, unless otherwise indicated.

2.3.2 Peptidoglycan glycosyltransferase (PGT) initial rate assays: (performed by Dr. Andrew Wang, Dr. Tania Lupoli, and Yihui Wu)

In a typical PGT assay, PGT was incubated in reaction buffer (indicated below), and then [^{14}C]- or [^{3}H]-Lipid II was added to initiate polymerization. For preincubation experiments, Gal-Lipid II (1.2 μM) or Gal-Lipid IV (1.2 μM) was preincubated with reaction buffer and PGT for 20 minutes, and then [^{14}C]- or [^{3}H]-Lipid II was added to initiate polymerization. Reaction buffers were optimized for each PGT enzyme. For full length and TP truncated *E.*

coli PBP1A and PBP1B: 50 mM HEPES (4-(2-hydroxyethyl)-1-piperazineethanesulfonic acid (pH = 7.5), 10 mM $CaCl_2$, 1000 units mL-1 penicillin G and 20% DMSO (v/v). For *S. aureus* PBP2: 50 mM CHES (*N*-Cyclohexyl-2-aminoethanesulfonic acid), 50 mM HEPES, 50 mM acetic acid, 50 mM MES (2-(*N*-morpholino)ethanesulfonic acid) (pH =5), 10 mM $CaCl_2$ and 20% (v/v) DMSO. For *S. aureus* SgtB: 12.5 mM HEPES (pH = 7.5), 2 mM $MnCl_2$, 0.25 mM Tween-80, and 20% (v/v) DMSO. The reaction mixtures were incubated at room temperature for the time points specified. For the paper chromatography assay, reaction mixtures were quenched by mixing with an equal volume of 1 μM Moenomycin A in 10% Triton X-100 solution on ice. The mixtures were then spotted on 1 × 20 cm 3MM CHR chromatography paper strips (Whatman) before eluting with isobutyric acid/1M NH_4OH (5:3, v/v). Starting material migrates on the strip, while polymer product remains at the origin. The paper strips were cut, immersed into EcoLite(+) liquid scintillation cocktail (MP Biomedical), and analyzed by a LS 6500 scintillation counter (Beckman Coulter). The percent radioactivity of the polymer product was calculated by comparing the amount of radioactivity that remains at the origin (peptidoglycan) to the total amount of radioactivity on the strip. The reaction rate was estimated from the initial linear range of each time course. The rate enhancement of Gal-Lipid IV preincubation was calculated by comparison with the normal Lipid II reaction (without Gal-Lipid IV).

2.3.3 SDS-PAGE Assay:
(performed by Dr. Andrew Wang)

E. coli PBP1A (600 nM) was incubated with and without Gal-Lipid IV (1.2 μM) for twenty minutes before the reaction was initiated with [^{14}C]-Lipid II in the reaction mixture described above. Time points were quenched by heating samples for 5 minutes at 90°C at the various time points indicated. Gel electrophoresis analysis was carried out as described in Barrett *et al*. Briefly, samples were dried and resuspended in sample buffer (125 mM Tris-HCl (pH = 6.8), 40% glycerol, 15% SDS (sodium dodecyl sulfate), 0.004% bromophenol blue) before being loaded onto a 20 × 20 cm gel (1 mm thick) and separated at 30 mA until the dye front was 1 cm from the bottom. Gels were dried overnight, and then exposed to a phosphorimage screen (GE Healthcare) for 1 week before being scanned using a Typhoon 9400 scanner (GE Healthcare). Radioactive bands were detected using the ImageQuant TL software package (GE Healthcare).

2.4 References

1. Sauvage, E., Kerff, F., Terrak, M., Ayala, J. A., and Charlier, P. (2008) The penicillin-binding proteins: structure and role in peptidoglycan biosynthesis, FEMS Microbiol. Rev. 32, 234-258.
2. Goehring, N. W., and Beckwith, J. (2005) Diverse paths to midcell: assembly of the bacterial cell division machinery, *Curr. Biol. 15*, R514-R526.
3. Den Blaauwen, T., de Pedro, M. A., Nguyen-Disteche, M., and Ayala, J. A. (2008) Morphogenesis of rod-shaped sacculi, *FEMS Microbiol. Rev. 32*, 321-344.
4. Margolin, W. (2009) Sculpting the bacterial cell, *Curr. Biol. 19*, R812-R822.
5. Walsh, C. T., (2003) Where will new antibiotics come from?, *Nat. Rev. Microbiol. 1*, 65-70.
6. Ostash, B., and Walker, S. (2005) Bacterial transglycosylase inhibitors, *Curr. Opin. Chem. Biol. 9*, 459-466.
7. Halliday, J., McKeveney, D., Muldoon, C., Rajaratnam, P., and Meutermans, W. (2006) Targeting the forgotten transglycosylases, *Biochem. Pharmacol. 71*, 957-967.
8. Ostash, B., and Walker, S. (2010) Moenomycin family antibiotics: chemical synthesis, biosynthesis, and biological activity, Nat. Prod. Rep. 27, 1594-1617.
9. Barrett, D., Wang, T. S., Yuan, Y., Zhang, Y., Kahne, D., and Walker, S. (2007) Analysis of glycan polymers produced by peptidoglycan glycosyltransferases, *J. Biol. Chem. 282*, 31964-31971.
10. Perlstein, D. L., Zhang, Y., Wang, T. S, Kahne, D. E., and Walker S. (2007) The direction of glycan chain elongation by peptidoglycan glycosyltransferases*, J. Am. Chem. Soc. 129*, 12674-12675.

11. Barrett, D. S., Chen, L., Litterman, N. K., and Walker, S. (2004) Expression and characterization of the isolated glycosyltransferase module of Escherichia coli PBP1b, *Biochemistry 43*, 12375-12381.

12. Schwartz, B., Markwalder, J. A., Seitz, S. P., Wang, Y., and Stein, R. L. (2002) A kinetic characterization of the glycosyltransferase activity of Escherichia coli PBP1b and development of a continuous fluorescence assay, *Biochemistry 41*, 12552-12561.

13. Zhang, Y., Fechter, E. J., Wang, T. S., Barrett, D., Walker S., and Kahne, D. E. (2007) Synthesis of heptaprenyl-lipid IV to analyze peptidoglycan glycosyltransferases*, J. Am. Chem. Soc. 129*, 3080-3081.

14. Perlstein, D. L, Wang, T. S., Doud, E. H., Kahne, D., and Walker, S. (2010) The role of the substrate lipid in processive glycan polymerization by the peptidoglycan glycosyltransferases, *J. Am. Chem. Soc. 132*, 48-49.

15. Schindler, M., Mirelman, D., and Schwarz, U. (1976) Quantitative determination of N-acetylglucosamine residues at the non-reducing ends of peptidoglycan chains by enzymic attachment of [14C]-D-galactose, *Eur. J. Biochem. 71*, 131−134.

16. Khidekel, N., Ficarro, S. B., Clark, P. M., Bryan, M. C., Swaney, D. L., Rexach, J. E., Sun, Y. E., Coon, J. J., Peters, E. C., and Hsieh-Wilson, L. C. (2007) Probing the dynamics of O-GlcNAc glycosylation in the brain using quantitative proteomics, *Nat. Chem. Biol 3*, 339−348.

17. Roquemore, E. P., Chou, T. Y., and Hart, G. W. (1994) Detection of O-linked N-acetylglucosamine (O-GlcNAc) on cytoplasmic and nuclear proteins, *Methods Enzymol. 230*, 443−460.

18. Boeggeman, E., Ramakrishnan, B., Kilgore, C., Khidekel, N., Hsieh-Wilson, L. C., Simpson, J. T., and Qasba, P. K. (2007) Direct identification of nonreducing GlcNAc residues on N-Glycans of glycoproteins using a novel chemoenzymatic method, *Bioconjug. Chem. 18*, 806−814.

19. Wang, T. S., Manning, S. A., Walker, S., and Kahne, D. E. (2008) Isolated peptidoglycan glycosyltransferases from different organisms produce different glycan chain lengths, *J. Am. Chem. Soc. 130*, 14068-14069.

20. Peng, L., Kawagoe, Y., Hogan, P., and Delmer, D. (2002) Sitosterol-beta-glycoside as primer for cellulose synthesis in plants, *Science 295*, 147-150.

21. DeAngelis, P. L. (1999) Molecular directionality of polysaccharide polymerization by the Pasteurella multocida hyaluronan synthase, *J. Biol. Chem. 274*, 26557-26 562.

22. Cartee, R. T., Foresee, W. T., and Yother, J. (2005) Initiation and synthesis of the Streptococcus pneumonia type 3 capsule on a phosphatidylglycerol membrane anchor, *J. Bacteriol. 187*, 4470-4479.

23. Tomsho, J. W., Moran, R. G., and Coward J. K. (2008) Concentration-dependent processivity of multiple glutamate ligations catalyzed by folylpolygamma-glutamate synthetase, *Biochemistry 47*, 9040-9050.

24. Jing, W., and DeAngelis P. L. (2004) Syncrhonized chemoenzymatic synthesis of monodisperse hyaluronan polymers, *J. Biol. Chem. 279*, 42345-32349.

25. Agarwal, P. K. (1985) Heterogeneous denaturation of enzymes: a distributed activation energy model with nonuniform activities, Biotech. Bioeng. 28, 1554-1563.

26. Craig, D. B., Arriaga, E. A., Wong, J. C. Y., Lu, H., and Dovichi, N. (1996) Studies on single alkaline phosphatase molecules: reaction rate and activation energy of a

reaction catalyzed by a single molecule and the effect of thermal denaturation – the death of an enzyme*, J. Am. Chem. Soc. 118*, 5245-5253.

27. Terrak, M., and Nguyen-Disteche, M. (2006) Kinetic characterization of the monofunctional glycosyltransferase from Staphylococcus aureus, *J. Bacteriol. 188*, 2528-2532.

28. Wang, Tsung-Shing (2011) Bacterial cell wall assembly: mechanism and inhibition of peptidoglycan glycosyltransferases, PhD dissertation, Harvard University (AAT #3462154)

29. Paradis-Bleau, C., Markovski, M., Uehara, T., Lupoli, T. J., Walker S., Kahne, D. E., and Bernhardt, T. G. (2010) Lipoprotein cofactors located in the outer membrane activate bacterial cell wall polymerases*, Cell 143*, 1110-1120.

30. Gampe, C., Tsukamoto H., Wang, T. S. A., Walker, S., and Kahne D. (2011) Modular synthesis of diphospholipid oligosaccharide fragments of the bacterial cell wall and their use to study the mechanism of moenomycin and other antibiotics, *Tetrahedron 67*, 9771-9778.

31. Lovering, A. L., de Castro, L. H., Lim, D., and Strynadka, N. C. J. (2007) Structural insight into the transglycosylation step of bacterial cell-wall biosynthesis, *Science 315*, 1402-1405.

32. Yuan, Y., Barrett, D., Zhang, Y., Kahne, D., Sliz, P., and Walker, S. (2007), Crystal structure of a peptidoglycan glycosyltransferase suggests a model for processive glycan chain synthesis, *Proc. Natl. Acad. Sci. U. S. A. 104*, 5348-5353.

33. Yuan, Y., Fuse, S., Ostash, B., Sliz, P., Kahne, D., and Walker, S. (2008) Structural analysis of the contacts anchoring moenomycin to peptidoglycan glycosyltransferases and implications for antibiotic design, *ACS Chem. Biol. 3*, 429-436.

34. Lovering, A.L, Gretes, M., and Stynadka, N. C. (2008) Structural details of the glycosyltransferase step of peptidoglycan assembly, *Curr. Opin. Struct. Biol. 18*, 534-543.

35. Lovering, A. L., de Castro, L., and Strynadka, N. C. (2008) Identification of dynamic structural motifs involved in peptidoglycan glycosyltransfer, *J. Mol. Biol. 383*, 167-177.

36. Ye, X.-Y., Lo, M., Brunner, L., Walker, D., Kahne, D., and Walker, S. (2001) Better substrates for bacterial transglycosylases, *J. Am. Chem. Soc. 123*, 3155-3116.

37. Adachi, M., Zhang, Y., Leimkuhler, C., Sun, B., Latour, J. V., and Kahne, D. (2006) Degradation and reconstruction of moenomycin A and derivatives: dissecting the function of the isoprenoid chain, *J. Am. Chem. Soc. 128*, 14012-14013.

1. Sauvage, E., Kerff, F., Terrak, M., Ayala, J. A., and Charlier, P. (2008) The penicillin-binding proteins: structure and role in peptidoglycan biosynthesis, FEMS Microbiol. Rev. 32, 234-258.

2. Goehring, N. W., and Beckwith, J. (2005) Diverse paths to midcell: assembly of the bacterial cell division machinery, *Curr. Biol. 15*, R514-R526.

3. Den Blaauwen, T., de Pedro, M. A., Nguyen-Disteche, M., and Ayala, J. A. (2008) Morphogenesis of rod-shaped sacculi, *FEMS Microbiol. Rev. 32*, 321-344.

4. Margolin, W. (2009) Sculpting the bacterial cell, *Curr. Biol. 19*, R812-R822.

5. Walsh, C. T., (2003) Where will new antibiotics come from?, *Nat. Rev. Microbiol. 1*, 65-70.

6. Ostash, B., and Walker, S. (2005) Bacterial transglycosylase inhibitors, *Curr. Opin. Chem. Biol. 9*, 459-466.

7. Halliday, J., McKeveney, D., Muldoon, C., Rajaratnam, P., and Meutermans, W. (2006) Targeting the forgotten transglycosylases, *Biochem. Pharmacol. 71*, 957-967.

8. Ostash, B., and Walker, S. (2010) Moenomycin family antibiotics: chemical synthesis, biosynthesis, and biological activity, Nat. Prod. Rep. 27, 1594-1617.

9. Barrett, D., Wang, T. S., Yuan, Y., Zhang, Y., Kahne, D., and Walker, S. (2007) Analysis of glycan polymers produced by peptidoglycan glycosyltransferases, *J. Biol. Chem. 282*, 31964-31971.

10. Perlstein, D. L., Zhang, Y., Wang, T. S, Kahne, D. E., and Walker S. (2007) The direction of glycan chain elongation by peptidoglycan glycosyltransferases*, J. Am. Chem. Soc. 129*, 12674-12675.

11. Barrett, D. S., Chen, L., Litterman, N. K., and Walker, S. (2004) Expression and characterization of the isolated glycosyltransferase module of Escherichia coli PBP1b, *Biochemistry 43*, 12375-12381.

12. Schwartz, B., Markwalder, J. A., Seitz, S. P., Wang, Y., and Stein, R. L. (2002) A kinetic characterization of the glycosyltransferase activity of Escherichia coli PBP1b and development of a continuous fluorescence assay, *Biochemistry 41*, 12552-12561.

13. Zhang, Y., Fechter, E. J., Wang, T. S., Barrett, D., Walker S., and Kahne, D. E. (2007) Synthesis of heptaprenyl-lipid IV to analyze peptidoglycan glycosyltransferases*, J. Am. Chem. Soc. 129*, 3080-3081.

14. Perlstein, D. L, Wang, T. S., Doud, E. H., Kahne, D., and Walker, S. (2010) The role of the substrate lipid in processive glycan polymerization by the peptidoglycan glycosyltransferases, *J. Am. Chem. Soc. 132*, 48-49.

15. Schindler, M., Mirelman, D., and Schwarz, U. (1976) Quantitative determination of N-acetylglucosamine residues at the non-reducing ends of peptidoglycan chains by enzymic attachment of [14C]-D-galactose, *Eur. J. Biochem. 71*, 131−134.

16. Khidekel, N., Ficarro, S. B., Clark, P. M., Bryan, M. C., Swaney, D. L., Rexach, J. E., Sun, Y. E., Coon, J. J., Peters, E. C., and Hsieh-Wilson, L. C. (2007) Probing the dynamics of O-GlcNAc glycosylation in the brain using quantitative proteomics, *Nat. Chem. Biol 3*, 339−348.

17. Roquemore, E. P., Chou, T. Y., and Hart, G. W. (1994) Detection of O-linked N-acetylglucosamine (O-GlcNAc) on cytoplasmic and nuclear proteins, *Methods Enzymol. 230*, 443−460.

18. Boeggeman, E., Ramakrishnan, B., Kilgore, C., Khidekel, N., Hsieh-Wilson, L. C., Simpson, J. T., and Qasba, P. K. (2007) Direct identification of nonreducing GlcNAc residues on N-Glycans of glycoproteins using a novel chemoenzymatic method, *Bioconjug. Chem. 18*, 806−814.

19. Wang, T. S., Manning, S. A., Walker, S., and Kahne, D. E. (2008) Isolated peptidoglycan glycosyltransferases from different organisms produce different glycan chain lengths, *J. Am. Chem. Soc. 130*, 14068-14069.

20. Peng, L., Kawagoe, Y., Hogan, P., and Delmer, D. (2002) Sitosterol-beta-glycoside as primer for cellulose synthesis in plants, *Science 295*, 147-150.

21. DeAngelis, P. L. (1999) Molecular directionality of polysaccharide polymerization by the Pasteurella multocida hyaluronan synthase, *J. Biol. Chem. 274*, 26557-26 562.

22. Cartee, R. T., Foresee, W. T., and Yother, J. (2005) Initiation and synthesis of the Streptococcus pneumonia type 3 capsule on a phosphatidylglycerol membrane anchor, *J. Bacteriol. 187*, 4470-4479.

23. Tomsho, J. W., Moran, R. G., and Coward J. K. (2008) Concentration-dependent processivity of multiple glutamate ligations catalyzed by folylpolygamma-glutamate synthetase, *Biochemistry 47*, 9040-9050.

24. Jing, W., and DeAngelis P. L. (2004) Syncrhonized chemoenzymatic synthesis of monodisperse hyaluronan polymers, *J. Biol. Chem. 279*, 42345-32349.

25. Agarwal, P. K. (1985) Heterogeneous denaturation of enzymes: a distributed activation energy model with nonuniform activities, Biotech. Bioeng. 28, 1554-1563.

26. Craig, D. B., Arriaga, E. A., Wong, J. C. Y., Lu, H., and Dovichi, N. (1996) Studies on single alkaline phosphatase molecules: reaction rate and activation energy of a reaction catalyzed by a single molecule and the effect of thermal denaturation – the death of an enzyme*, J. Am. Chem. Soc. 118*, 5245-5253.

27. Terrak, M., and Nguyen-Disteche, M. (2006) Kinetic characterization of the monofunctional glycosyltransferase from Staphylococcus aureus, *J. Bacteriol. 188*, 2528-2532.

[28]. Wang, Tsung-Shing (2011) Bacterial cell wall assembly: mechanism and inhibition of peptidoglycan glycosyltransferases, PhD dissertation, Harvard University (AAT #3462154)

29. Paradis-Bleau, C., Markovski, M., Uehara, T., Lupoli, T. J., Walker S., Kahne, D. E., and Bernhardt, T. G. (2010) Lipoprotein cofactors located in the outer membrane activate bacterial cell wall polymerases*, Cell 143*, 1110-1120.

30. Gampe, C., Tsukamoto H., Wang, T. S. A., Walker, S., and Kahne D. (2011) Modular synthesis of diphospholipid oligosaccharide fragments of the bacterial cell wall and their use to study the mechanism of moenomycin and other antibiotics, *Tetrahedron 67*, 9771-9778.

31. Lovering, A. L., de Castro, L. H., Lim, D., and Strynadka, N. C. J. (2007) Structural insight into the transglycosylation step of bacterial cell-wall biosynthesis, *Science 315*, 1402-1405.

32. Yuan, Y., Barrett, D., Zhang, Y., Kahne, D., Sliz, P., and Walker, S. (2007), Crystal structure of a peptidoglycan glycosyltransferase suggests a model for processive glycan chain synthesis, *Proc. Natl. Acad. Sci. U. S. A. 104*, 5348-5353.

33. Yuan, Y., Fuse, S., Ostash, B., Sliz, P., Kahne, D., and Walker, S. (2008) Structural analysis of the contacts anchoring moenomycin to peptidoglycan glycosyltransferases and implications for antibiotic design, *ACS Chem. Biol. 3*, 429-436.

34. Lovering, A.L, Gretes, M., and Stynadka, N. C. (2008) Structural details of the glycosyltransferase step of peptidoglycan assembly, *Curr. Opin. Struct. Biol. 18*, 534-543.

35. Lovering, A. L., de Castro, L., and Strynadka, N. C. (2008) Identification of dynamic structural motifs involved in peptidoglycan glycosyltransfer, *J. Mol. Biol. 383*, 167-177.

[36]. Ye, X.-Y., Lo, M., Brunner, L., Walker, D., Kahne, D., and Walker, S. (2001) Better substrates for bacterial transglycosylases, *J. Am. Chem. Soc. 123*, 3155-3116.

[37] Adachi, M., Zhang, Y., Leimkuhler, C., Sun, B., Latour, J. V., and Kahne, D. (2006) Degradation and Reconstruction of Moenomycin A and Derivatives: Dissecting the Function of the Isoprenoid Chain, *J. Am. Chem. Soc. 128*, 14012-14013.

Chapter 3: A robust, high yielding preparation of monodisperse and monomeric SgtB for solution structural studies

3.1 Introduction

Peptidoglycan glycosyltransferases (PGTs) transglycosylate Lipid II molecules to form peptidoglycan (PG).[1] The availability of well-defined substrates has enabled a series of biochemical experiments from which a working model of PGT polymerization to be proposed.[2] Briefly, the process is initiated by the uptake of two molecules of Lipid II by the PGTs to synthesize a nascent PG fragment, Lipid IV. In order for the PGT to elongate Lipid IV on its reducing end in a processive manner, the same Lipid IV molecule has to be translocated to the donor binding site so that another Lipid II molecule can bind as an acceptor. By performing multiple cycles of transglycosylation and translocation, the nascent PG is elongated in a processive manner to yield a glycan polymer of desired length before it is released. The studies presented in Chapter 2 demonstrate that the addition of Gal-Lipid IV abrogates an often observed initial lag-phase in the course of PG synthesis, providing a kinetic dimension to the model. Specifically, our evidence suggests that the synthesis of Lipid IV is the rate-limiting step, thus the addition of Gal-Lipid IV induces the enzyme to take on an "activated" elongation-competent state. Additionally, a recent study by Paradis-Bleau, Markovski, Uehara, and coworkers identified an accessory protein LpoB from Escherichia coli that produces a similar "activation" effect with Escherichia coli PBP1B, providing further evidence that the PGTs can take on a distinct "activated" elongation-competent state.[3] Structural studies of PGTs (apo and Moenomycin A bound) have suggested that the lower lobe is floppy and some of these conformational dynamics may be important in performing its catalytic function.[4,5,6,7,8] To date, there is no structural data that depicts how PG fragments interact with the PGT. A structure of a Gal-Lipid IV bound PGT would enable

one to compare and contrast the differences in conformation, as well as changes in structural mobility between the apo and substrate-bound enzyme.

Nuclear Magnetic Resonance (NMR) spectroscopy is the only structural technique that enables one to obtain a three-dimensional structure of a protein and quantitatively probe the conformational dynamics of the protein at an atomic-level without introducing additional structural perturbations.[9,10] However, this structural technique requires an abundance of well-behaved monodisperse protein that is stable at room temperature for a few weeks.[11]

Assuming the target protein has a mass of 25 kDa, a typical 500 μL protein NMR sample at a concentration of 500 μM would require 6-7 mg of pure, isotopically labeled, monodisperse and monomeric protein. Assuming that we are able to recover 90% of the target protein at each processing step, a sample preparation methodology involving 5 processing steps – immobilized affinity chromatography (IMAC), buffer exchange by dialysis, purification tag removal, size-exclusion chromatography, and final sample buffer exchange – would required the ability to obtain at least 10 mg of IMAC purified soluble protein. The material requirements are further elevated since proteins are often recombinantly expressed as a mixture of oligomers and well-behaved monomers, thus the practical implementation of a solution structural project would require access to at least 20 mgs of IMAC purified protein.[12] Furthermore, large quantities of protein will be required for screening optimal buffer conditions that maximize protein stability and spectral resolution. The incorporation of isotopic labels (^{2}H, ^{15}N, ^{13}C) can be prohibitively expensive and every effort has to be made to streamline processing and minimize waste.

Chapter 3 presents the development of an efficient preparative method for obtaining sufficient quantities of our target PGT, the monofunctional glycosyltransferase SgtB from

Staphylococcus aureus. We are able to obtain upwards of 7 mg of monodisperse and monomeric SgtB protein with this preparation from one liter of LB culture, and 5 mg of monodisperse and monomeric SgtB protein from one liter of M9 minimal media culture. The method presented maximizes the protein throughput and recovery with each processing step and minimizes sample volume manipulation by centrifugal diafiltration. Because the method can be completed within a single day, it is possible to obtain 100 mg of well-behaved SgtB in a single week using common laboratory equipment.

3.2 Results and Discussion

3.2.1 Challenges of preparing large quantities of monodisperse and monomeric PGTs

PGTs are membrane-associated enzymes which are difficult to prepare and handle because they are extremely prone to aggregation. Protein sequence hydrophobicity analysis suggested this might from two potential sites for nonspecific interaction: an N-terminal transmembrane anchoring helix and a second potential membrane association face.[13,14] As a result, recombinantly expressed PGTs often form inclusion bodies or soluble aggregates even in the presence of detergent.[15] Early strategies for isolating involved removing the N-terminal transmembrane helix anchor and attaching a GST solubility tag in its place.[16,17,18] Unfortunately, the isolated monomeric and monodisperse protein can quickly become polydisperse, forming soluble oligomers at higher concentrations, eventually resulting in precipitation even when stored at 4 ^{o}C.[15] Despite these challenges, the first two crystal structures of PGT were presented in 2007, with another two published in 2009, including one presenting the transmembrane helix anchor.[4,5,6,19,20] The structural data presented confirms the existence of a large hydrophobic surface that is situated at the base of the lower lobe of

the PGTs which presumably enables the enzyme to interact with the surface of the cytoplasmic phospholipid membrane bilayer. Additionally, the perceived structural flexibility of the PGTs may expose interaction sites or result in partially unfolded conformations that promote aggregation.

3.2.2 Maximizing protein yield: lessons from the purification of *Aquifex aeolicus* PBP1A PGT

We picked the *Aquifex aeolicus* PBP1A PGT ΔTM construct, aaPGT(51-243) as a starting point for developing a method for obtaining pure, monodisperse PGT protein. This was because prior research done by a former member of the group, Dr. Yanqiu Yuan on a series of aaPGT constructs put in place a protocol that gave pure, monodisperse, dimeric protein that was suitable for crystallographic analysis, albeit at low yields.[21]

Dr. Yuan's preparation of aaPGT(51-243) was an extension of Novagen's cell lysis and protein extraction methodology, with the insertion of an additional extraction step in a buffer containing 1% (w/v) CHAPS detergent (3-[(3-Cholamidopropyl)dimethylammonio]-1-propanesulfonate) based buffer before the crude soluble protein extracts were loaded onto an Ni-NTA immobilized metal affinity chromatography (IMAC) column for a first-pass crude purification.[22] This additional extraction step with the 1% (w/v) CHAPS buffer improved the yield of soluble protein that can be obtained from an overexpression culture by up to 2-fold. In my discussions with Dr. Yuan, while the existing process enabled her to produce pure, monodisperse protein for crystallographic work, the yield of protein per liter culture was low because a lot of protein was lost through the multiple centrifugal diafiltration process used to concentrate proteins throughout the preparation.

Our first objective was to minimize the loss of protein through centrifugal concentration because it is important to be able to manipulate the volume and concentration of a protein sample throughout its polishing process without suffering from a severe loss of material. Higher recoveries of protein from centrifugal concentration would dramatically boost yields from this process and enable the preparation of highly concentrated samples of isotopically labeled protein with minimal wastage.

Previous research has shown that proteins can adhere non-specifically to the surface of ultrafiltration membranes resulting in reduced recovery yields. At high g-forces, the centrifugal force and flow of solvent packs a very dense layer of protein against the ultrafiltration membrane, giving rise to an environment that promotes protein aggregation, unfolding and precipitation, resulting in fouling of the fine meshwork of the ultrafiltration membrane and low protein recovery.[23] For proteins such as the PGTs which are inherently prone to aggregation, concentrating proteins by centrifugal diafiltration can result in protein aggregation and denaturation that depress recovery yields.

A technique commonly used by bioprocessing community is to passivate the diafiltration membrane surface of the Amicon Ultra-15 centricon units by incubating it with a 1% BSA solution or a dilute solution of detergent.[24,25] Indeed, a combination of pre-treating the centricons with 1%(w/v) BSA solution, using a low centrifugal speed (max 1500×g) with frequent resuspensions to prevent the build up of protein material at the membrane interface between spins (every 20 minutes) allowed us to boost protein recoveries from 20% to 85-90%.

Our second objective was to obtain a concentrated stock of protein coming off the IMAC column by minimizing the volume of eluant required for releasing all the bound

protein. This will minimize the need to manipulate large volumes of dilute protein solution which is cumbersome to handle, and will require long downstream concentration times that inevitably will lead to protein loss from non-specific absorption when it comes in contact with large surfaces. We decided to optimize this process on two fronts – (1) minimize the amount of IMAC-resin used to pull-down and isolate the 6XHis-tagged protein, and (2) improve the efficiency of protein elution from the Ni-NTA resin by using a higher concentration of imidazole coupled with a very slow elution flow rate that allows the Imidazole to completely exchange with the 6XHis-tagged protein. Following the published protocol, the complete elution of aaPGT(51-243) requires 11 or more column volumes (CV) of elution buffer, yielding a dilute protein solution.[5] By increasing the Imidazole concentration in the elution buffer from 200 mM to 500 mM, and allowing a 5 minute equilibration time before collection of each elution fraction, we were able to completely elute our protein using 3 CV.

The downstream payoffs from utilizing this column concentration effect are numerous: (1) the removal of Imidazole by dialysis is more efficient because smaller dialysis cassettes can be used, minimizing material losses from non-specific absorption onto the membranes, (2) proteolytic cleavage of the solubility/purification tags will not require additional concentration steps to increase the protein substrate to protease ratio, and (3) both the number of Amicon Ultra-15 concentrators required for concentrating the protein for injection onto a size-exclusion chromatographic system as well as the amount of time in which the protein is exposed to centrifugal diafiltration are reduced. In all, minimizing the number of handling steps enabled us to maximize our protein yield from processing. Taken together, our improvements in the preparatory process of aaPGT(51-243) resulted in a 4-fold

improvement in the yield of monodisperse aaPGT(51-243) protein (3-4 mg/L from <1 mg/L) at existing protein expression levels. In the following section, we apply these strategies to optimizing the preparation of SgtB for solution structural work.

3.2.3 SgtB as a candidate for solution structural studies

In 2009, researchers at Pfizer published a high resolution crystal structure of *Staphylococcus aureus* monofunctional glycosyltransferase, SgtB bound to its natural inhibitor, Moenomycin A.[20] We are interested in SgtB because it is one of the three PGTs present in the clinically relevant pathogen, *Staphylococcus aureus*.[26] SgtB is a good model system for characterizing the PGT domain because it is a fully functional PGT that lacks a transpeptidase domain, and its small size (26.2 kDa) makes it amenable for NMR spectroscopy.[27] In Chapter 2, we have also observed that SgtB displayed the largest rate-enhancement effect when preincubated with Gal-Lipid IV, suggesting that we might be able to observe clear changes in its conformational state and dynamics when it binds Gal-Lipid IV. Because the PGTs are highly conserved across bacterial species, findings from the SgtB model system will bring insight into how the PGTs work as a class of enzymes.[28] Additionally, previous reports have suggested that SgtB can be isolated as a monomer in the presence of 0.7% (w/v) CHAPS detergent.[27] Given that Pfizer had successfully obtained a crystal structure with an SgtB construct, we believed that obtaining sufficient quantities of well-behaved SgtB protein was within reach.

Through a material transfer agreement with Pfizer, we were able to obtain the exact construct used for crystallographic studies by Pfizer: His_6-TEV_{pc}-SgtB(68-269). This was a ΔTM(1-67) SgtB construct that was cloned into a pET15b equivalent vector, incorporating an

N-terminal Tobacco-etch virus (TEV) protease cleavage sequence (TEV_{pc}) that allowed the swift removal of 6XHis purification tag. It is highly similar to previous SgtB constructs used for recombinant overexpression, differing only in the type of N-terminal protease cleavage sequence that facilitated the removal of the 6XHis tag (**Figure 3.1**).

Reference	Expression Host	Vector	Protein Construct			Overexpression
SgtB for Protein NMR Spectroscopic Analysis	BL-21(DE3) (Novagen)	pET-15b Derivative	6X His	TEV Cut Site	SgtB(68-269) E100Q	"Marley"-M9, OD600 ~ 5.0 0.1 mM IPTG, 6 hrs at 37 °C
H. Heaslet et. al. Pfizer R&D (2009) *J. Struct. Biol.*, 167, 129-135	BL-21(DE3)tolC-	pET-15b Derivative	6X His	TEV Cut Site	SgtB(68-269) E100Q	2xYT media OD600 ~ unknown 0.5 mM IPTG 3 hrs at 37 °C
Wang, Q.M., et. al. Eli Lilly R&D (2001) *J. Bacteriol.*, 183, 4779-4785	BL-21(DE3) pLysS (Novagen)	pET-16b (Novagen)	6X His	Factor Xa Cut Site	SgtB(68-269)	TY media OD600 ~ unkonwn 1.0 mM IPTG 4-5 hrs at 30 °C
Terrak, M. and Ngyuen-Disteche, M. (2006) *J. Bacteriol.*, 188, 2528-2532	C41(DE3)	pET-28b (Novagen)	6X His	Thrombin Cut Site	SgtB(68-268)	LB media OD600 ~ 0.6 1.0 mM IPTG 3 hrs at 37 °C

Figure 3.1 Various published SgtB overexpression constructs

Unfortunately, despite our best efforts, we were unable to obtain large quantities of well-behaved SgtB using published protocols (**Figure 3.2**). In our personal communication with the Pfizer research team that crystallized SgtB, we learned that they minimized, and at times omitted the use of CHAPS detergent from their processing of the protein for crystallization. Our experience with SgtB suggested that the level of salts and CHAPS detergent used during processing by the Pfizer team would cause the protein to form soluble aggregates that cannot be disrupted by dilution (see Chapter 4, Figure 4.18). Our experience with aaPGT taught us that the use of CHAPS detergent was crucial to extracting and stabilizing the PGT during biomass processing and protein purification. We decided to apply

the same highly tuned process for preparing SgtB. We briefly delineate our optimized process for preparing sgtB in the section that follows.

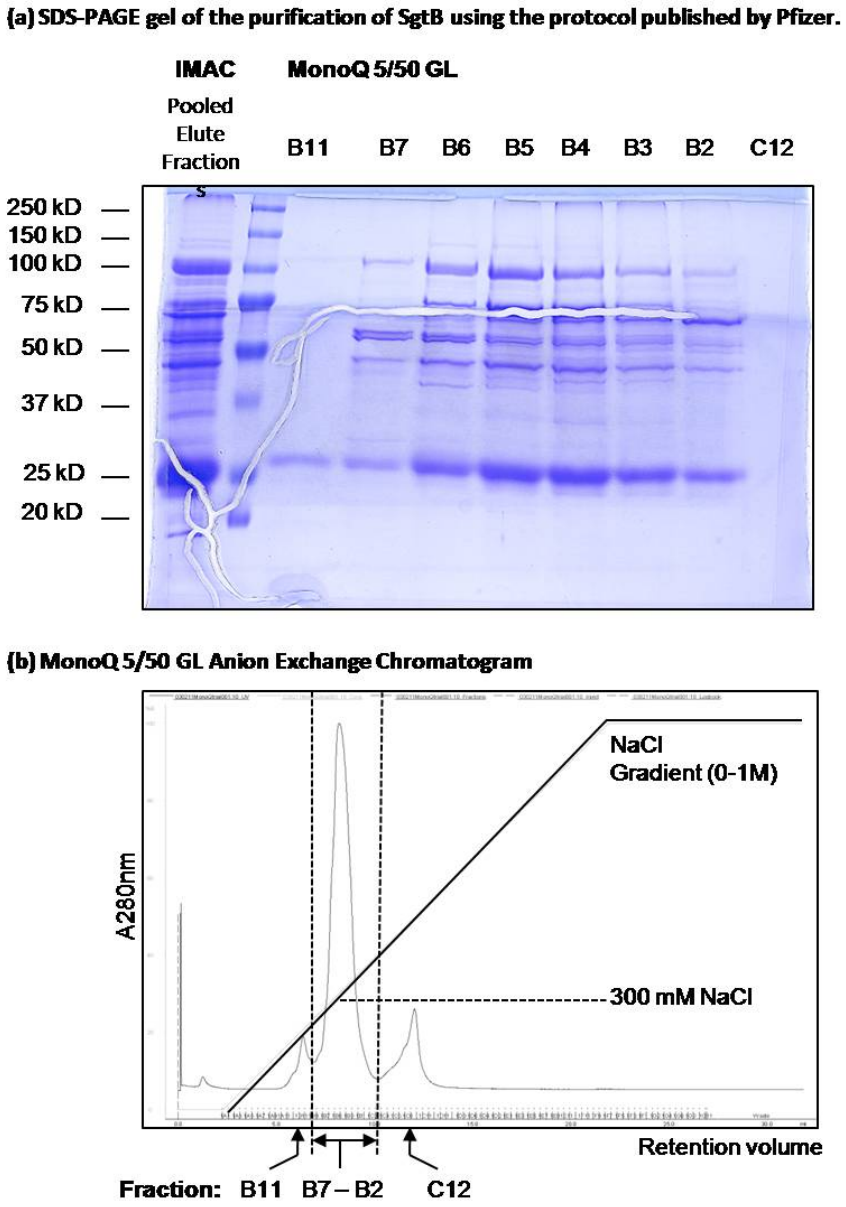

Figure 3.2 Purification of His_6-TEV_{pc}-SgtB(68-269) following Pfizer's published protocol. Briefly, the protein is first purified by IMAC and subsequently by anion exchange chromatography. (a) SDS-PAGE gel of preparatory process. (b) Anion Exchange Chromatography, gradient elution of the protein by NaCl.

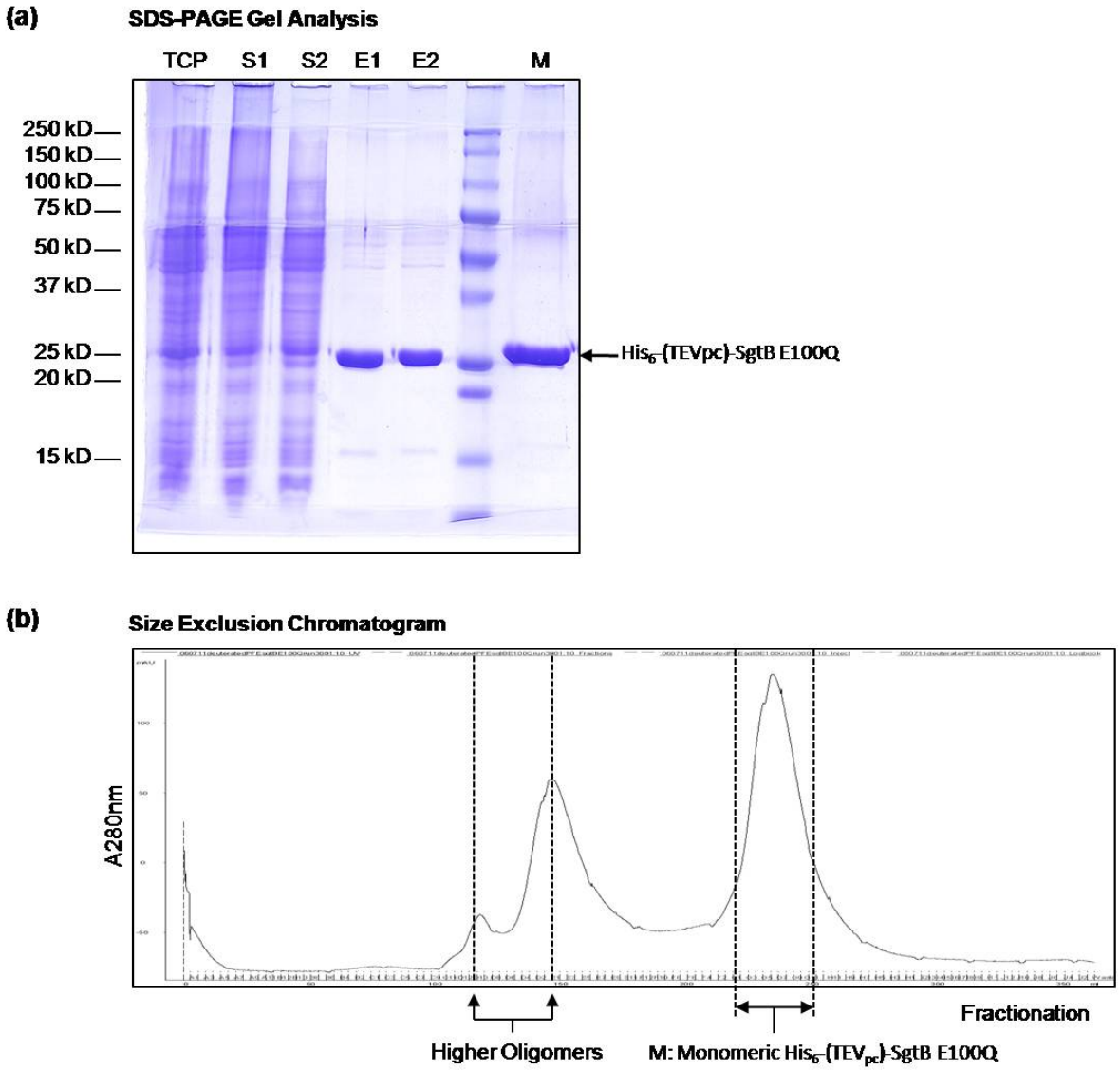

Figure 3.3 Purification of His_6-TEV_{pc}-SgtB(68-269) expressed in unlabeled M9 minimal media. following the methodology described in Section 3.2.4. (a) SDS-PAGE gel of the purification process. TCP: Total cell protein. S1: Novagen Bugbuster soluble extracts. S2: 1% CHAPS buffer soluble extracts. E1: Ni-NTA IMAC purified His_6-TEV_{pc}-SgtB(68-269). E2: Ni-NTA IMAC purified His_6-TEV_{pc}-SgtB(68-269) from a different purification batch, showing consistency. M: Size-exclusion (Superdex 200) purified monomeric His_6-TEV_{pc}-SgtB(68-269). (b) Preparatory size-exclusion profile of His_6-TEV_{pc}-SgtB(68-269).

3.2.4 A robust method for preparing large quantities of monodisperse and monomeric SgtB

Upon lysis, SgtB rapidly degrades even in the presence of a large amount of broad-spectrum protease inhibitors. We minimized lysis times which were important in preventing proteolytic degradation of the protein. We found that 10 mL of Bugbuster suspension is required for every 2 grams of biomass to enable efficient lysis within 15 minutes at 4^{o}C. The supernatant is rapidly passed through a Ni-NTA column 3 times to saturate the resin with 6XHis-tagged bound SgtB to minimize loading times and contact with proteases. Re-extraction of the pellet with 1% CHAPS qualitatively allowed us to improve our yields by almost 2-fold. We optimized the biomass:Ni-NTA resin mass ratio which allowed us to minimize the number of wash steps during IMAC since a lower amount of resin would result in smaller amounts of impurities that are non-specifically bound to the resin. Once again, by using a small amount of resin with high concentration of Imidazole (500 mM), we were able to utilize the column concentration effect in IMAC to minimize the volume of the eluted SgtB protein sample. The immediate addition of CHAPS to a final concentration of 8 mM (~0.5% w/v) when the protein is eluted off IMAC retarded the spontaneous aggregation and precipitation of the protein prior to processing by size-exclusion chromatography (**Figure 3.3 and 3.4**). In order to maximize the fraction of monomeric protein present in the protein sample that is loaded onto size-exclusion chromatographic system, we investigated the possibility of omitting the lengthy step of removing Imidazole by dialysis. Surprising, we found that high concentrations of Imidazole is crucial for slowing the formation of aggregates (**Figure 3.5a and 3.5b**).

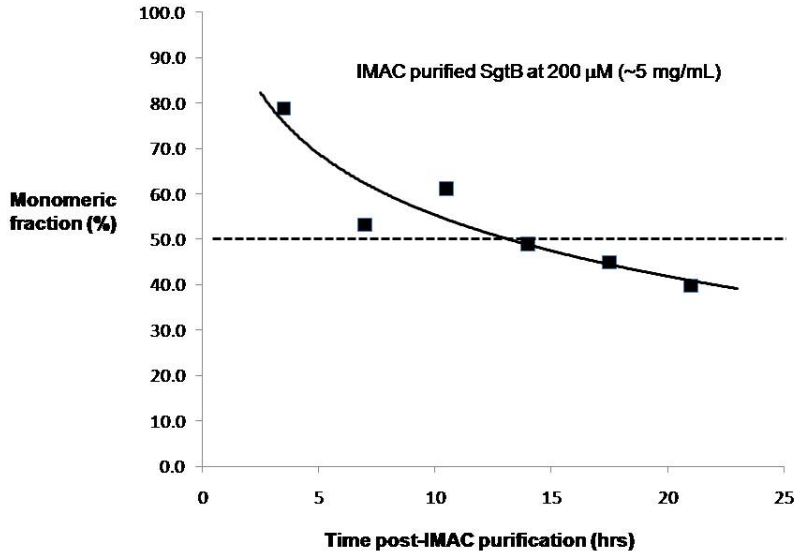

Figure 3.4 Decrease in the relative abundance of monomeric His_6-TEV_{pc}-SgtB(68-269) after IMAC purification over time despite the addition of CHAPS detergent. Relative abundance of monomeric protein versus higher oligomers as measured by area under Abs(280nm) peaks from analytical size-exclusion profiles.

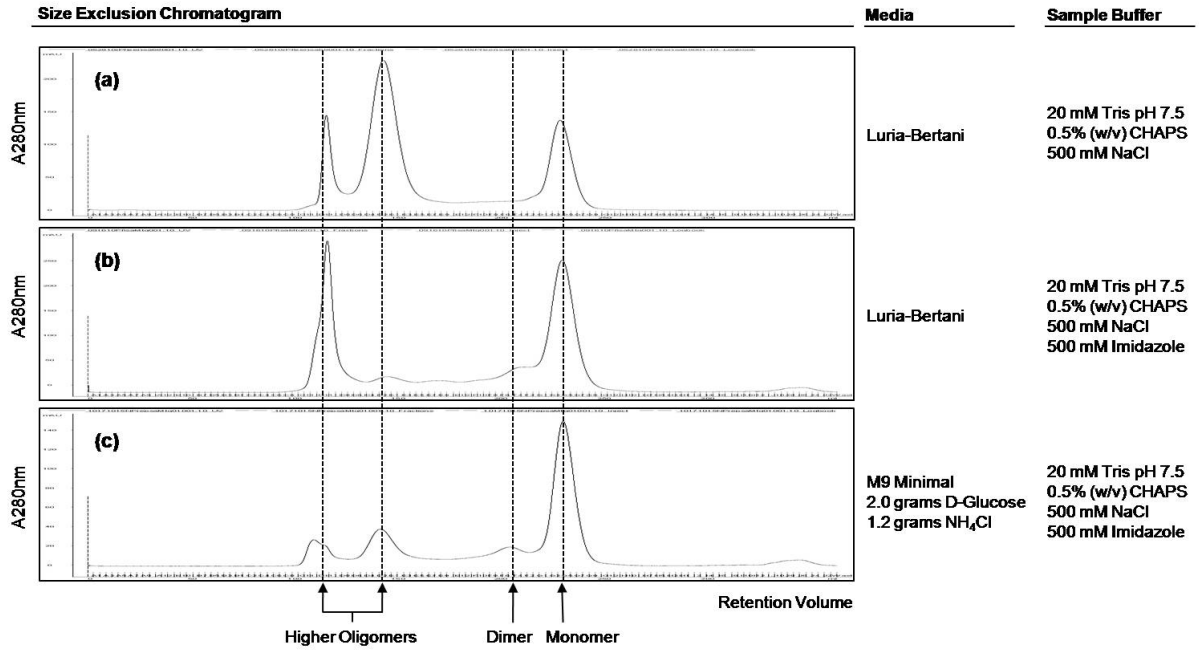

Figure 3.5 Size-exclusion profiles of IMAC purified His_6-TEV_{pc}-SgtB(68-269). (a) Size-exclusion profile of IMAC purified His_6-TEV_{pc}-SgtB(68-269) that was dialyzed overnight to remove imidazole. (b) Size-exclusion profile of IMAC purified His_6-TEV_{pc}-SgtB(68-269) that is immediately chromatographed. (c) Size-exclusion profile of IMAC purified His_6-TEV_{pc}-SgtB(68-269) grown in unlabeled M9 minimal media.

In order to maximize the throughput on a 300 mL HiLoad 26/60 Superdex 200 size-exclusion chromatographic system, we had to determine the total amount of protein we could load onto a 2 mL sample loop (largest sample loop available from the GE Healthcare AKTA FPLC series). We found that concentrating our IMAC purified SgtB beyond 15 mg/mL (~ 570 μM) would decrease the chromatographic yield of monomeric protein because these high concentrations push the equilibrium towards the formation of soluble aggregates and precipitates. As a result, we have a maximum throughput of 30 mg (2 mL X 15 mg/mL) of IMAC purified SgtB for each chromatographic run which takes 4 hours to complete at a flow rate of 1.8 mL/min. Because 1 liter of LB culture yields 15 mg of IMAC purified SgtB, this implies 2 liters of LB culture (approximately 7 g wet biomass)

Earlier on, our observation that the combination of 500 mM imidazole and 8 mM CHAPS retards but does not abrogate SgtB aggregation meant that the maximal amount of biomass that can be processed per day is limited at ~ 7g+ (2L of LB culture, 1L of M9/H_2O culture, 0.5L of M9/D_2O). Allowing IMAC-purified protein stock to stand in line for 4 hours for a subsequent chromatographic run would drastically decrease the yield of monomeric SgtB (**Figure 3.4**).

In order to prepare isotopically labeled His_6-TEV_{pc}-SgtB(68-269), we applied the Marley method to expressing SgtB in M9 minimal media because it was a time and cost efficient way of producing isotopically labeled proteins for protein sample optimization.[29] We observed that the size-exclusion profile of the IMAC purified His_6-TEV_{pc}-SgtB(68-269) obtained from M9 minimal media expression as markedly different from that obtained from expression in LB media (**Figure 3.5c**). There was a greater proportion of protein that is monomeric – suggesting that the reduced growth and expression process in minimal media

may be better suited to producing His_6-TEV_{pc}-SgtB(68-269) that is correctly folded. This is in line with previous observations that expression yields of PBPs and PGTs are improved with late induction (OD600: 0.85-1.20) where cell growth rates are very slow.[30]

In sum, expressing His_6-TEV_{pc}-SgtB in M9 minimal media, spiking the IMAC elution fractions with CHAPS and rapid processing with passivated centricons for size-exclusion chromatography allowed us to access large amounts of monomeric His_6-TEV_{pc}-SgtB(68-269). A summary of all published methods for preparing SgtB is provided in the following page (**Figure 3.6**).

Figure 3.6 Summary of all published preparations of SgtB

3.3 Selected Methods and Materials

3.3.1 Components of M9 minimal media (adapted from formulation courtesy of Dr. Alexander Koglin)

All chemicals are purchased from Mallinckrodt Chemicals unless otherwise noted. 1.0 mL of 1M $MgSO_4$, 0.2 mL of 1M $CaCl_2$, 0.2 mL of 1M $FeCl_3$, 0.2 mL of Vitamin mix described below) and 80 μL of autoclaved glycerol are added to 500 mL of H_2O and stirred vigorously. 2.0 g of D(+)Glucose anhydrous (CalBioChem), 1.2 g of NH_4Cl are added to the solution. 200 mL of 5X M9 salt solution (described below) is added and stirred vigorously. The pH of the media is adjusted to 7.5, topped up with H_2O to make 1000 mL and passed through a 0.2micron filter. The media is made fresh and used immediately. Vitamin mix is prepared by mixing the following compounds purchased from Sigma-Aldrich in 15 mL of H_2O: 0.4 g Choline Chloride (2-hydroxyethyl)trimethylammonium chloride), 0.5 g Folic acid ((2S)-2-[(4-{[(2-amino-4-hydroxypteridin-6-yl)methyl]amino}phenyl)formamido]pentanedioic acid), 0.5 g Pantothenic acid (3-[(2,4-Dihydroxy-3,3-dimethylbutanoyl)amino]propanoic acid), 0.5 g Nicotinamide (pyridine-3-carboxamide) , 1 g Myo-inositol ((1R,2R,3S,4S,5R,6S)-cyclohexane-1,2,3,4,5,6-hexol), 0.5 g Pyridoxal HCl (3-hydroxy-5-(hydroxymethyl)-2-methylpyridine-4-carbaldehyde), 0.5 g Thiamin HCl (2-[3-[(4-Amino-2-methyl-pyrimidin-5-yl)methyl]-4-methyl-thiazol-5-yl] ethanol), 0.05 g Riboflavin (7,8-Dimethyl-10-[(2S,3S,4R)-2,3,4,5-tetrahydroxypentyl]benzo[g]pteridine-2,4-dione), 0.1g Adenosine ((2R,3R,4S,5R)-2-(6-amino-9H-purin-9-yl)-5-(hydroxymethyl)oxolane-3,4-diol) and 0.1g Biotin (5-[(3aS,4S,6aR)-2-oxohexahydro-1H-thieno[3,4-d]imidazol-4-yl]pentanoic acid). The vitamin mix is stored at -20 ^oC and away from light. The 5X M9 salt solution consist of 33.9 g Na_2HPO_4, 15.0 g KH_2PO_4 and 2.5 g NaCl in 1000 mL of H_2O which is then passed through a 0.2 micron filter.

3.3.2 Overexpression of His_6-TEV_{pc}-SgtB(68-269) in unlabeled M9 minimal media

20 mL from a 50 mL Luria-Bertani (LB) with Ampicillin (10 μg/mL) overnight culture of BL(21)DE3 host cells carrying pET24b vector encoding His_6-TEV_{pc}-SgtB(68-269) is used to innoculate 2L LB with Ampicillin (10 μg/mL) culture. The 2L culture is grown at 37 ^oC for exactly 4.5 hours and harvested by centrifugation at 22 ^oC. The cell pellet is resuspended in 200 mL of M9 salt buffer and centrifuged at 22 ^oC to remove the M9 salt wash buffer. The cell pellet is then resuspended in 1L of M9 media, with glucose as the carbon source and ammonium chloride as the nitrogen source. The M9 culture is then grown for 1.5 hours at 37 ^oC before induction with 0.1 mM IPTG and allowed to grow at 37 ^oC for 6 hours. The culture is harvested by centrifugation at 4 ^oC to obtain 8 grams of wet biomass which is then stored as two 4 gram pellets at -80 ^oC.

3.3.3 Purification of His_6-TEV_{pc}-SgtB(68-269)

Each 4 gram pellet of wet biomass is thawed on ice for 2 hours and thoroughly resuspended in a mixture of 20 mL of Bugbuster (Novagen) lysis buffer and 1 mL of EDTA-free Protease Inhibitor Cocktail III (Novagen) over a course of 15 minutes on ice. 10 μL of Benzonase (Novagen) and 10 μL of rLysozyme (Novagen) is added to the resuspended biomass and the mixture is stirred at 4 ^oC for 20 minutes. The cell lysate is then centrifuged at 16000 × g, 4 ^oC for 35 minutes to obtain a clarified supernatant crude protein extract S1, taking care not to disturb the viscous emulsion that lies on the interface of supernatant and the pellet. 20 mL of pre-chilled 1% CHAPS (Anatrace) extraction buffer (20 mM Tris pH 7.5, 500 mM NaCL, 16 mM CHAPS, 5 μL of Benzonase, 5 μL of rLysozyme) is used to resuspend the pellet along

with the viscous emulsion for 20 minutes. In the meantime, S1 is passed through an IMAC column (charged with 2 mL settled bed volume of Ni-NTA resin and pre-equilibrated with 10 mM Imidazole IMAC Buffer) 3 times at a flow rate of 1 mL/min. The pellet emulsion extract is centrifuged for 35 minutes at 16000 × g, 4 ^{o}C to obtain a clarified supernant S2. S2 is immediately loaded onto the IMAC column charged with Ni-NTA resin at a flow rate of 0.3 mL/min. The IMAC column is washed with 12 mL of 10 mM Imidazole IMAC buffer, allowing the buffer to run to the top of the resin before washing with 24 mL of 10 mM Imidazole IMAC buffer. Subsequently, the IMAC column is washed with 12 mL of 60 mM Imidazole IMAC buffer, allowing the buffer to run to the top of the resin before washing with 48 mL of 60 mM Imidazole IMAC buffer. 315 μL of 10% CHAPS (w/v) solution is added to a 50 mL Falcon tube to be used a collection receptacle for the IMAC-purified SgtB protein. 2 mL of 500 mM Imidazole IMAC buffer is added to the IMAC column and collected immediately as the first elution fraction. Another 2 mL of 500 mM Imidazole IMAC buffer is added the IMAC column and incubated with the resin for 5 minutes before collecting the elution at a flow rate of 0.3 mL/min to give the second elution fraction. This incubation-elution process is repeated once more to yield the third elution fraction. All three elution fractions are combined and concentrated immediately in a passivated Centricon (Amicon MWCO 10K) at 1500 × g, 4 ^{o}C for approximately 15 minutes to give a 2 mL protein stock (~15 mg/mL) that is loaded onto a HiLoad 26/60 Superdex 200 size-exclusion column without delay. The protein is chromatographed at a flow rate of 1.8 mL/min to yield 14 mg of pure, monodisperse, and monomeric His_6-TEV_{pc}-SgtB(68-269). IMAC buffer is defined as 20 mM Tris, 500 mM NaCl, with the specified concentration of Imidazole. This entire purification process can be easily accomplished within 10 hours/1 workday.

3.4 References

1. Sauvage, E., Kerff, F., Terrak, M., Ayala, J. A., and Charlier, P. (2008) The penicillin-binding proteins: structure and role in peptidoglycan biosynthesis, FEMS Microbiol. Rev. 32, 234-258.
2. Wang, T.S.; Lupoli, T. J., Sumida, Y., Tsukamoto, H., Wu, Y., Rebets, Y., Kahne, D.E., and Walker S. (2011) Primer preactivation of peptidoglycan polymerases, *J. Am. Chem. Soc.* 133, 8528-8530.
3. Paradis-Bleau, C., Markovski, M., Uehara, T., Lupoli, T. J., Walker S., Kahne, D. E., and Bernhardt, T. G. (2010) Lipoprotein cofactors located in the outer membrane activate bacterial cell wall polymerases*, Cell 143*, 1110-1120.
4. Lovering, A. L., de Castro, L. H., Lim, D., and Strynadka, N. C. J. (2007) Structural insight into the transglycosylation step of bacterial cell-wall biosynthesis, *Science 315*, 1402-1405.
5. Yuan, Y., Barrett, D., Zhang, Y., Kahne, D., Sliz, P., and Walker, S. (2007), Crystal structure of a peptidoglycan glycosyltransferase suggests a model for processive glycan chain synthesis, *Proc. Natl. Acad. Sci. U. S. A. 104*, 5348-5353.
6. Yuan, Y., Fuse, S., Ostash, B., Sliz, P., Kahne, D., and Walker, S. (2008) Structural analysis of the contacts anchoring moenomycin to peptidoglycan glycosyltransferases and implications for antibiotic design, *ACS Chem. Biol. 3*, 429-436.
7. Lovering, A.L, Gretes, M., and Stynadka, N. C. (2008) Structural details of the glycosyltransferase step of peptidoglycan assembly, *Curr. Opin. Struct. Biol. 18*, 534-543.

8. Lovering, A. L., de Castro, L., and Strynadka, N. C. (2008) Identification of dynamic structural motifs involved in peptidoglycan glycosyltransfer, *J. Mol. Biol. 383*, 167-177.

9. Boehr, D. D., Dyson, J., and Wright, P. E. (2006) An NMR perspective on enzyme dynamics, Chem. Rev. 106, 3055-3079.

10. Marintchev, A., Frueh, D., and Wagner, G. (2007) NMR methods for studying protein-protein interactions involved in translation initiation, *Method Enzymol. 430*, 283-331.

11. Bagby, S., Tong, K. Il, and Ikura, M. (2001) Optimization of protein solubility and stability for protein nuclear magnetic resonance, Method Enzymol. 339, 20-41.

12. Hewitt, L., and McDonnell, J. M. (2004) Screening and optimizing protein production in E. coli, *Methods Mol. Biol. 278*, 1-16.

13. Nicholas, R. A., Lamson, D. R., and Schultz, D. E. (1993) Penicillin-binding protein 1B from Escherichia coli contains a membrane association site in addition to its transmembrane anchor, J. Biol. Chem. 268, 5632-5641.

14. Wang, C. C., Schultz, D. E., and Nicholas R. A., (1996) Localization of a putative second membrane association site in penicillin-binding protein 1B of Escherichia coli, *Biochem. J. 316*, 149-156.

15. Offant, J., Michoux, F., Dermiaux, A., Biton, J., and Bourne, Y. (2006) Functional characterization of the glycosyltranferase domain of penicillin binding protein 1a from Thermotoga maritima, *Biochim. Biophys. Acta 1764*, 1036-1042.

16. Di Guilmi, A. M., Dessen, A., Dideberg, O., and Vernet T. (2003) The glycosyltransferase domain of penicillin-binding protein 2a from Streptococcus

pneumonia catalyzes the polymerization of murein glycan chains, *J. Bacteriol. 185*, 4418-4423.

17. Di. Guilmi, A. M., Mouz, N., Andrieu, J. P., Hoskins, J., Jaskunas, S. R., Gagnon, J., Dideberg, O., and Vernet, T. (1998) Identification, purification, and chacterization of transpeptidase and glycosyltransferase domains of Streptococcus pneumonia penicillin-binding protein 1a, *J. Bacteriol. 180*, 5652-5659.

18. Di. Guilmi, A. M., Dessen, A., Dideberg, O., and Vernet, T. (2003) Functional characaterization of penicillin-binding protein 1b from Streptococcus pneumonia, *J. Bacteriol. 185*, 1650-1658.

19. Sung, M. T., Lai, Y. T., Huang, C. Y., Chou, L. Y., Shih, H. W., Cheng, W. C., Wong, C. H., and Ma, C. (2009) Crystal structure of the membrane-bound bifunctional transglycosylase PBP1b from Escherichia coli, *Proc. Natl. Acad. Sci. U. S. A. 106*, 8824-8829.

20. Heaslet, H., Shaw, B., Bistry, A., and Miller, A. A. (2009) Characterization of the active site of S. aureus monofunctional glycosyltransferase (Mtg) by site-directed mutation and structural analysis of the protein complexed with moenomycin, *J. Struct. Biol. 167*, 129-135.

21. Yuan, Y. (2008) Targeting bacterial cell wall – structural insight into peptidoglycan glycosyltransferases and moenomycin inhibition, *PhD Dissertation*, Harvard University (Publication: 3312581).

22. pET system manual, 11th edition, Novagen.

23. Meireles, M., Aimar, P., and Sanchez, V. (2004) Albumin denaturation during ultrafiltration: effects of operating conditions and consequences on membrane fouling, *Biotech. Bioeng. 38*, 528-534.

24. Schratter, P., (2004) Purification and concentration by ultrafiltration, *Meth. Mol. Biol.: Protein Purification Protocols 244*, 101-116

25. Sweryda-Krawiec, B., Devaraj, H., Jacob, G., and Hickman, J. J. (2004) A new interpretation of serum albumin surface passivation, *Langmuir 20*, 2054-2056.

26. Reed, P., Veiga, H., Jorge, A. M., Terrak, M., and Pinho, M. G. (2011) Monofunctional transglycosylases are not essential for Staphylococcus aurues cell wall synthesis, *J. Bacteriol. 193*, 2539-2556.

27. Terrak, M., and Nguyen-Disteche, M. (2006) Kinetic characterization of the monofunctional transglycosylase from Staphylococcus aureus, *J. Bacteriol. 188*, 2528-2532.

28. Goffin, C., and Ghuysen, J. M. (1998) Multimodular penicillin-binding proteins: an enigmatic family of orthologs and paralogs, *Microbiol. Mol. Biol. Rev. 62*, 1079-1093.

29. Marley, J., Lu, M., and Bracken, C. (2001) A method for efficient isotope labeling of recombinant proteins, *J. Biomol. NMR 20*, 71-75.

30. Wang, T. S. A., Manning, S. A., Walker, S., and Kahne, D. (2008) Isolated peptidoglycan glycosyltransferases from different organisms produce different glycan chain lengths, *J. Am. Chem. Soc. 130*, 14068-9.

Chapter Four: Development of an SgtB sample for NMR spectroscopy

The work presented in this chapter is a result of a collaboration between the Kahne, Walker and Wagner research groups at Harvard Medical School. Protein biochemistry was performed by Yihui Wu (Kahne). Spectroscopic data acquisition was performed by Dr. Ricard Rodriguez-Mias (Wagner) and Dr. Haribabu Arthanari (Wagner).

4.1 Introduction

In 2007, Strynadka et. al. solved both the ligand-free and Moenomycin A-bound crystal structure of the *Staphylococcus aureus* PBP2 (saPBP2).[1] Their efforts provided the first structural insight to the conformational changes that may occur when the only known natural inhibitor of the peptidoglycan glycosyltransferases (PGT), Moenomycin A (MmA) forms a tight non-covalent interaction with the enzyme. MmA has been proposed to be a competitive inhibitor of the polymeric product of the PGT (Lipid IV and longer peptidoglycan fragments) because of the similarities in chemical structure between MmA and Lipid IV.[2] Recent kinetic data supports this view that MmA binds to the donor-site of the PGT as preincubation with Gal-Lipid IV, a known donor-site specific binder increases the IC_{50} of MmA by 5 fold in Escherichia coli PBP1a.[3] The enzymological studies detailed in Chapter 2 show that Gal-Lipid IV is able to enhance the initial rate of PG synthesis, possibly by inducing a conformational change on the PGT.[4] As a result, we were intrigued by the large conformational difference between the apo and the MmA-bound structure of saPBP2 in the lower lobe region (also called "jaw" region) because it may suggest a structural mechanism of how the PGT is activated for peptidoglycan (PG) biosynthesis.[5,6,7,8,9]

Given this backdrop, we were motivated to obtain a Nuclear Magnetic Resonance (NMR) solution structure of a PGT with Gal-Lipid IV from *Staphylococcus aureus* for several reasons: (1) it would enable us to visualize the structure and analyze the conformational dynamics that are involved in the activation of the PGT enzyme derived from the clinically relevant Staphylococcus aureus pathogen, (2) comparing the structure of Gal-Lipid IV bound PGT with a the existing MmA bound PGT structures would bring mechanistic insight on how MmA inhibits the function of the PGT, and (3) structural

information on how various ligands, such as Lipid II or a new inhibitor/probe interact with the PGT can be quickly deciphered by titrating the NMR protein sample with the ligand of interest, without having to redevelop crystallization conditions for each protein:ligand complex.

PGTs are a challenging class of proteins to work with because of their conformational flexibility and its amphiphilic structural properties that come with being a membrane-associated protein.[10] Successful overexpression and purification of soluble PGTs often require the removal of the hydrophobic transmembrane helix anchor (ΔTM).[11,12,13,14,15] However, the PGTs still possess a large hydrophobic surface situated at the base of its lower lobe that allows the protein to interact with the cytoplasmic membrane (**Figure 4.1**) that causes it to form soluble aggregates that are difficult to disperse.[16,17] As a result, a small monofunctional PGT such as the 26.2 kDa ΔTM SgtB can form dimers and higher oligomers with a molecular mass upwards of 52 kD (not including the mass of the bound detergent micelle which can contribute significantly to the final mass) that would make the protein intractable for solution structural work by NMR.

In Chapter 3, we developed a robust method for obtaining multi-milligram quantities of SgtB that is monodisperse and monomeric. In Chapter 4, we observed that the SgtB construct, His_6-TEV_{pc}-SgtB(68-269) becomes polydisperse and aggregates at concentrations relevant for solution NMR work (250 μM and up). To improve the stability of the protein construct at high concentrations, further investigations into buffer conditions, construct redesign and the addition of solubility-enhancement tags are needed. This chapter presents the systematic development of an SgtB protein sample that is amenable for solution structural work by NMR.

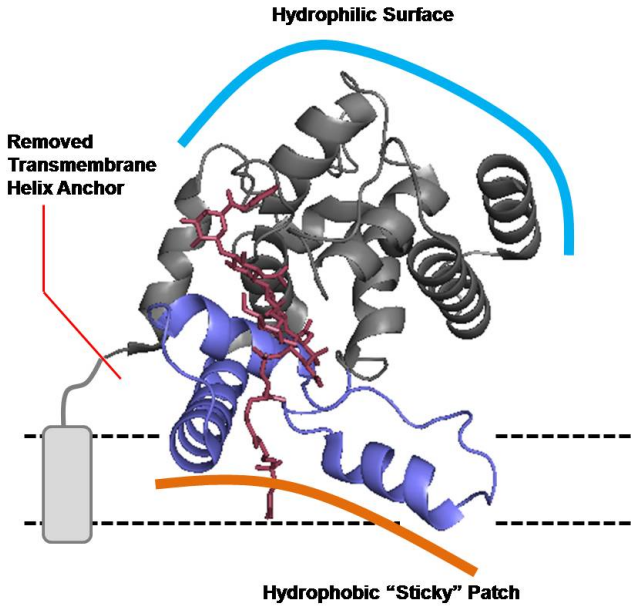

Figure 4.1 Amphiphilic structural properties of the PGTs. The upper lobe (grey) is displays a mostly hydrophilic surface whereas the lower lobe (blue) has a sticky hydrophobic patch that contacts the cytoplasmic membrane.

4.2 Results and Discussion

4.2.1 Initial foray with SgtB construct: His_6-TEV_{pc}-SgtB(68-269)

The overarching goal of this exercise is to develop a ligand-free sample of SgtB that is well-behaved and stable at the high concentrations and the extensive room temperature exposure required for solution structural studies. Any ligand of interest, e.g. Gal-Lipid IV can be added to this stabilized SgtB protein sample to produce a protein-ligand complex for spectroscopic analysis. The ligand-free SgtB can then serve as a standard for comparing the perturbations caused by the ligand of interest.

We began our journey by investigating the feasibility of solution structure work on the His_6-TEV_{pc}-SgtB(68-269) construct. We chose His_6-TEV_{pc}-SgtB(68-269) construct as our starting point because we were able to prepare multimilligram quantities of SgtB using

this construct through an efficient, high yielding protocol which has the added benefit of being able to incorporate NMR-active isotopic labels through a minimal media expression system.[18] Our preparation method gives us access to at least 7 milligrams of isotopically-labeled (^{15}N) His_6-TEV_{pc}-SgtB(68-269) protein that is required for preparing a fresh 500 µL protein sample at concentration of 500 µM in a single operation for spectroscopic measurements: 7-8 g wet biomass from 1 liter of ^{15}N-M9 minimal media culture yields approximately 10 mg of monodisperse and monomeric His_6-TEVpc-SgtB(68-269).

Protein fingerprinting by recording [^{1}H,^{15}N]-HSQC spectra is the gold-standard test on the feasibility of pursuing solution structure work because having sufficient spectral dispersion and peak count suggests that (1) the individual amide peaks are assignable, and (2) the protein was well-behaved at high concentrations - the protein is folded and does not form large soluble aggregates with extensive exposure at room temperature.[19] Our first objective was to obtain a [^{1}H,^{15}N]-HSQC spectra of His_6-TEV_{pc}-SgtB(68-269) so that we can map out possible improvements and changes that can be made with the sample going forward.

The protein sample for NMR spectroscopy is ideally buffered by agents that are transparent to the spectrometer - free of carbon and nitrogen atoms, and be at an acidic pH (<7.0) so as to minimize the exchange of the amide backbone hydrogen with the bulk water solvent which reduces the number of visible peaks.[20] The His_6-TEV_{pc}-SgtB(68-269) protein sample prepared using our protocol is not appropriately buffered for spectroscopic measurements. Our sample buffer contained a basic carbon-based buffer (20 mM Tris buffered at pH 7.5), a high concentration of CHAPS detergent (8 mM) that will contribute a strong N-H signal right in the middle of fingerprint spectral window and plenty of salt (500

mM NaCl) that will lead to longer 90°-pulse lengths, sample heating and poorer signal-to-noise ratios, especially with modern cryogenic probes.[21]

In order to prepare our sample for this initial fingerprinting, we chose to focus on finding an optimal acidic pH that would confer reasonable stability to the protein for the duration of a 2-3 hour HSQC experiment (inclusive of time required for pulse sequence and water signal suppression optimization). We were less concerned with the amount of salt in the sample because the recent development of a salt-tolerant cold-probe as well as specially configured sample tubes presented an effective solution towards improving spectral resolution on a lossy sample.[22,23,24] The CHAPS detergent did not present a serious impediment to obtaining solution structures of Calcineurin B and eFI4E through the application of isotope-edited pulse sequences minimized the interfering detergent signals.[25,26,27]

We tried to identify the optimal acidic pH that stability as judged by the amount of precipitated protein formed from dialysing a 300 μM sample of His_6-TEV_{pc}-SgtB(68-269) into a series phosphate buffers with a pH ranging from 5.0 to 7.2 at room temperature. We were hoping to identify a pH and a buffering agent which would result in no precipitation of the protein. The predicted pI of His_6-TEV_{pc}-SgtB(68-269) is 6.87 (ProtParam, ExPASY Server) which suggests that a pH lower than the pI, i.e. one or two units less than 6.87 might result in greater stability due to greater solubility from an increased net charge.[28] Unfortunately, all our samples contained precipitates - albeit to different extents. In fact, samples dialyzed into buffers at a lower pH resulted in more precipitation than those at a higher pH. We singled out a buffer containing 20 mM NaPi pH 6.8 because it was the most acidic buffer that had the least amount of precipitate as judged by eye. Analytical size-

exclusion analysis of the soluble fraction in our most acidic sample (NaPi pH 6.8) showed that the majority of soluble protein (>70%) exists as a monomer, with a small fraction forming small oligomers. We reasoned that the amount of monomeric protein present in this sample might yield sufficient signal to give us an initial [^{1}H,^{15}N]-HSQC fingerprint of the protein that can guide construct and buffer optimization going forward.

We managed to prepare 1000 μL of a 300 μM sample of His_6-TEV_{pc}-SgtB(68-269) - 8 mg of isotopically labeled protein in all - using our existing protocol which had the added step of a final buffer exchange facilitated by a PD-Minitrap G25 Sephacryl column (GE Healthcare) that acidified the pH from 7.5 to 6.8 while introducing D_2O into the sample as a lock component (5% v/v). The PD-Minitrap G25 Sephacryl column was pre-equilibrated with the final NMR buffer of 20 mM Sodium Phosphate (NaPi), 500 mM NaCl, 8 mM CHAPS and 5% (v/v) D_2O before use. We split the sample in two: one half was used to obtain a [^{1}H,^{15}N]-HSQC spectra, and the other half was used to obtain a size-exclusion profile of the sample to determine the aggregation state of the sample being measured over time.

The [^{1}H,^{15}N]-HSQC spectra was acquired using the fastHSQC (fHSQC) pulse sequence: a flip-back WATERGATE-HSQC sequence that does not require extensive calibration, minimizing the time between sample loading and spectral acquisition.[29] As a result, we were able to rapidly obtain a spectra of His_6-TEV_{pc}-SgtB(68-269) with minimal exposure time to room temperature conditions in the spectrometer. However it displayed poorly resolved, poorly dispersed, and broadened peaks (**Figure 4.2**). These features are characteristic of protein sample that might be either partially unfolded, are undergoing an aggregation process of forming larger oligomers, or both. Subsequently, using the same

sample, we acquired a [^{1}H, ^{15}N]-HSQC spectra using the TROSY pulse sequence which is designed to improve spectral resolution and sensitivity with larger protein masses.[30,31] The TROSY-HSQC spectra showed a slight improvement in dispersion, but was nonetheless poorly resolved and poorly dispersed, an indication that our protein was forming an aggregate. The analytical size-exclusion profile of the sample over the course of the HSQC measurement indicated that the protein was steadily accumulating higher oligomers that cannot be broken down through the dilution effect of the size-exclusion chromatography (**Figure 4.3**). A possible explanation for this observation might be that the flexible end regions of the protein such as the N-terminal His_6-TEV_{pc} appendage (21 amino acids long) drive a nonspecific interaction that results in the formation of aggregates. If this were true, clipping off the His_6-TEV_{pc} appendage might separate the individual monomers within the aggregate and prevent the formation of oligomers at high concentrations.

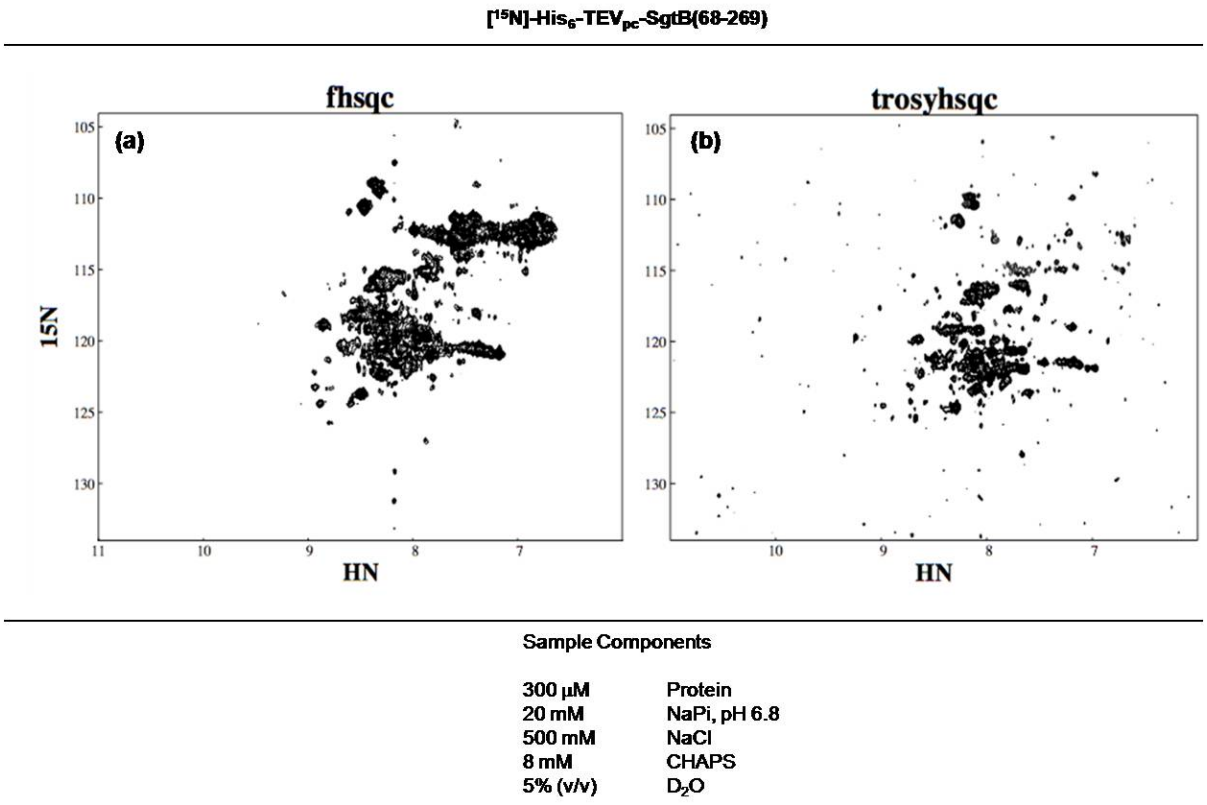

Figure 4.2 Initial [^{1}H,^{15}N]-HSQC spectra of His$_6$-TEV$_{pc}$-SgtB(68-269). (a) Spectra acquired with fHSQC pulse sequence. (b) Spectra acquired with TROSY pulse sequence.

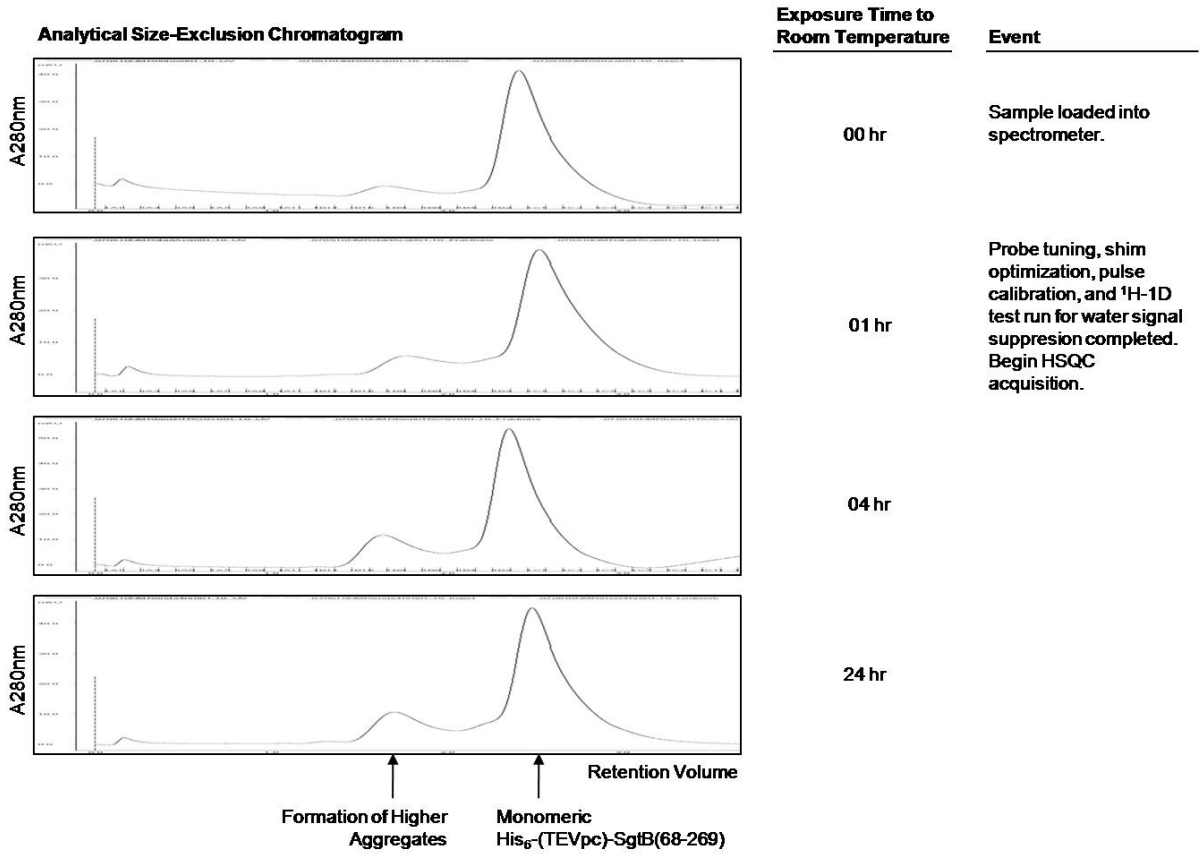

Figure 4.3 Analytical size-exclusion profile of the NMR sample of His_6-TEV_{pc}-SgtB(68-269) at a concentration 300 μM, in the presence of 20 mM NaPi, 500 mM NaCl, 8 mM CHAPS, 5% (v/v) D_2O.

4.2.2 SgtB(68-269), sans His_6-TEV_{pc} appendage

To test our hypothesis, we took the existing aggregated His6-TEVpc-sgtB(68-269) NMR sample and digested it with a 6XHis-tagged TEV pretease which clipped off the His_6-TEV_{pc} appendage.[32] The TEV protease and His_6-TEV_{pc} appendage were removed by repeated passage (3X) of the digestion reaction mixture through a Ni-NTA based immobilized metal affinity chromatography (IMAC) column to yield pure SgtB(68-269) (**Figure 4.4**). The size-exclusion profile indicated that we manage to recover most of our protein as free monomers, firming up our suspicion that the His_6-TEV_{pc} appendage was indeed contributing to the aggregation behavior of our protein. However, when we concentrated up the digested SgtB(68-269) sample which was diluted by size-exclusion chromatography, we obtained a poorly dispersed [^{1}H,^{15}N]-TROSY HSQC spectrum indicating the protein sample at high concentrations was either partially unfolded or aggregated (**Figure 4.5**). Although the His_6-TEV_{pc} appendage contributed aggregation behavior, there were probably other sites that can form nonspecific interactions.

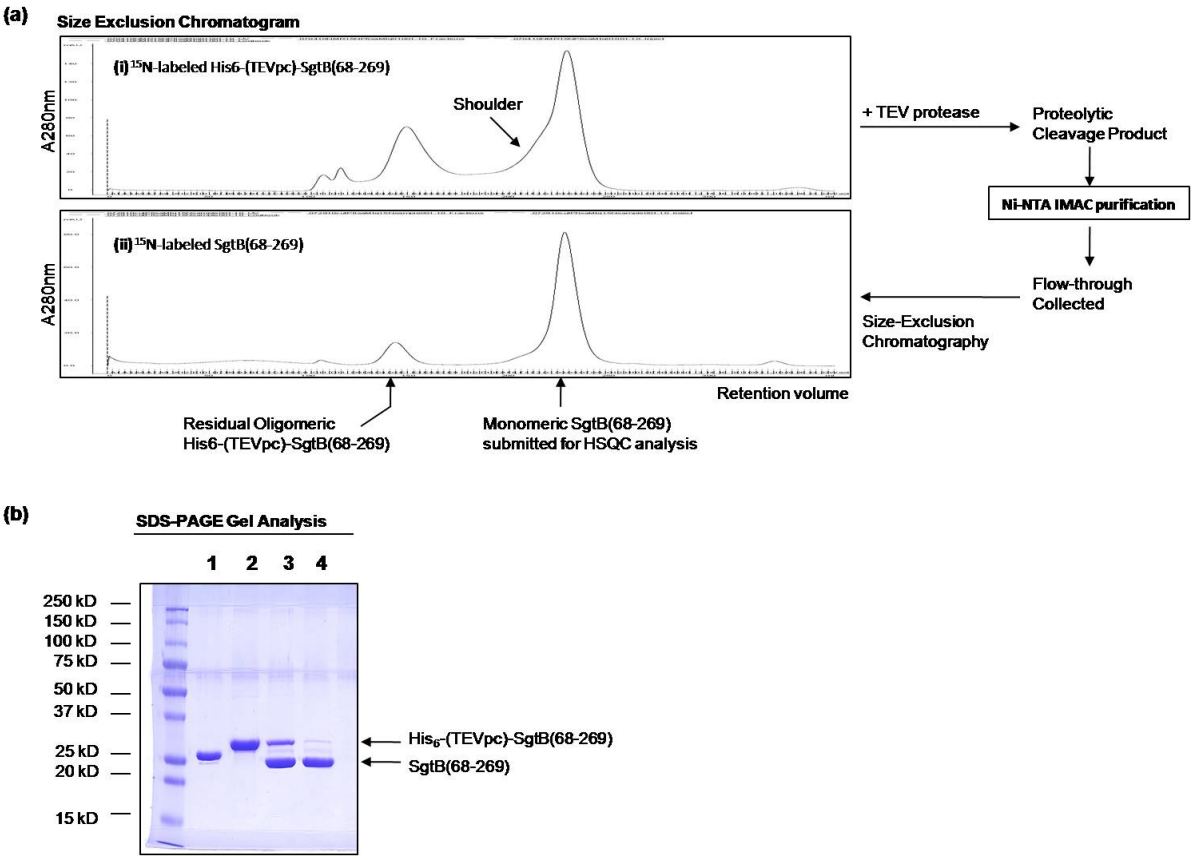

Figure 4.4 Removal of His_6-TEV_{pc} appendage from His_6-TEV_{pc}-SgtB(68-269). (a)(i) Size-exclusion profile of His_6-TEV_{pc}-SgtB(68-269) after 1 day of NMR measurements is digested with TEV protease and purified by Ni-NTA IMAC chromatography. The product, SgtB(68-269) is polished by size-exclusion chromatography (ii) to remove traces of His_6-TEV_{pc}-SgtB(68-269) aggregates. (b) Lane 1: TEV protease, Lane 2: His_6-TEV_{pc}-SgtB(68-269) after NMR measurements, Lane 3:TEV protease digestion product of His_6-TEV_{pc}-SgtB(68-269) = SgtB(68-269), and Lane 4: Purified SgtB(68-269).

[^{15}N]-SgtB(68-269)

TROSY HSQC Spectra

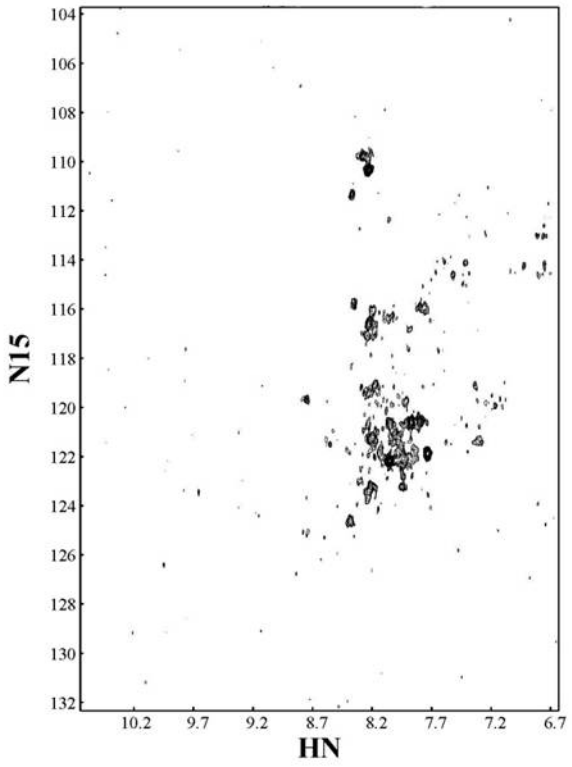

Sample Components

250 µM	**Protein**
20 mM	**NaPi, pH 6.8**
500 mM	**NaCl**
8 mM	**CHAPS**
5% (v/v)	**D_2O**

Figure 4.5 [^{1}H,^{15}N]-TROSY HSQC spectrum of SgtB(68-269) after removal of the His_6-TEV_{pc} appendage.

4.2.3 Introducing a high affinity ligand: Moenomycin A bound His_6-TEV_{pc}-SgtB(68-269)

We had several options ahead of us to prevent aggregation in the sample: (1) identify a buffer composition that would stabilize interactions within the protein that keep it well-folded while destabilizing unfavorable protein-protein interactions, and (2) adding solubility-enhancement tags that can act as a shield against unfavorable protein-protein interactions while modulating the electrostatic and hydration properties of SgtB. Alternatively, we could use a high affinity ligand that possibly locks the protein into one conformational state and prevents it from sampling states that are aggregation-prone. Although we would not be able to obtain solution structural information on the apo-state of SgtB, we could still obtain solution structural information on a broad variety of tight binding ligands of interest e.g. new PGT inhibitors, PG fragments.

We opined that the addition of a high affinity ligand would enable us to make the biggest advance in terms of structural stability because locking the protein into one conformational state would prevent it from sampling states which lead to aggregation. Two candidates immediately stand out: Gal-Lipid IV and MmA. Previous work within the Kahne research group has suggest that Lipid IV binds tightly to the PGTs.[33] Additionally, in Chapter 2, we have shown that Gal-Lipid IV possibly induces a conformational change in the PGT that enhances the initial rate of PG synthesis. Introducing Gal-Lipid IV at this point would expedite the development of a Gal-Lipid IV bound SgtB sample for solution structural studies. However, this is not a viable solution because we did not have access to the approximately 1-3 mg of Gal-Lipid IV needed to test this strategy (a new robust synthetic route towards Lipid IV is being developed within the Kahne research group). We decided to

test this strategy with MmA, since we worked out a well-honed protocol access to hundreds of milligrams of pure MmA. MmA derivatives with shorter lipid moieties (C_{10}, C_{15}) can also be prepared in multimilligram quantities.[34,35]

In contrast, the addition of a solubility-enhancement tag would require the construction of new expression vectors, possibly with new methods of overexpression and purification. Exhaustive buffer screening, while immediately feasible, will be laborious with no obvious starting point given the infinite combinations of detergent, salts and buffers.

We prepared a 1.0 mL partially deuterated (to take advantage of the TROSY effect), ^{15}N-labeled sample of His_6-TEV_{pc}-SgtB(68-269) at 350 μM.[36] We then split the sample in two and added an excess amount (~5 equivalents) of C_{15}-(Z,E)-Farnesyl-MmA to one half of it. We used C_{15}-(Z,E)-Farnesyl-MmA because its shortened lipid tail gave it better solubility properties in aqueous media than Moenomycin A (**Figure 4.6**).

The difference between the [^{1}H,^{15}N]-TROSY HSQC spectra obtained from the liganded versus ligand-free protein samples showed that the addition of C_{15}-(Z,E)-Farnesyl-MmA resulted in a vast improvement in spectral dispersion and peak count (**Figure 4.7**). Improved sample stability due to the addition of C_{15}-(Z,E)-Farnesyl-MmA was also observed from the greatly reduced amount of precipitated protein in the NMR sample with C_{15}-(Z,E)-Farnesyl-MmA in contrast to the ligand-free sample. However, although the peak dispersion observed in the spectra was encouraging, there were insufficient peaks in the spectra for us to proceed with investingating the feasibility of obtaining a full spectrum assignment. The amount of precipitated protein was still significant and more had to be done to improve the stability of the protein sample.

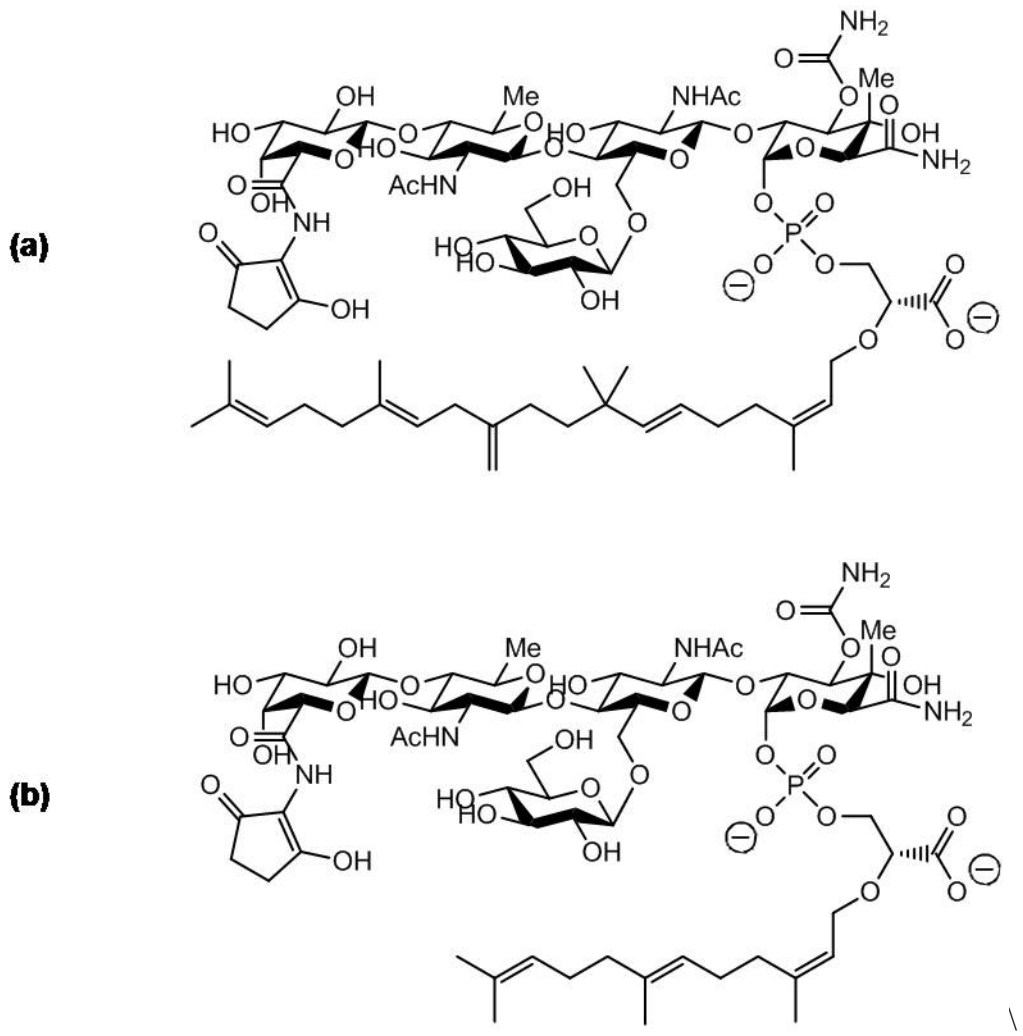

Figure 4.6 Moenomycin A and its derivatives. (a) Moenomycin A**.** (b) Moenomycin A derivative with a shortened lipid tail: C_{15}-(Z,E)-farnesyl-Moenomycin A. Shortened lipid derivatives of Moenomycin A possess an IC_{50} on the PGTs that is similar to Moenomycin A.[38]

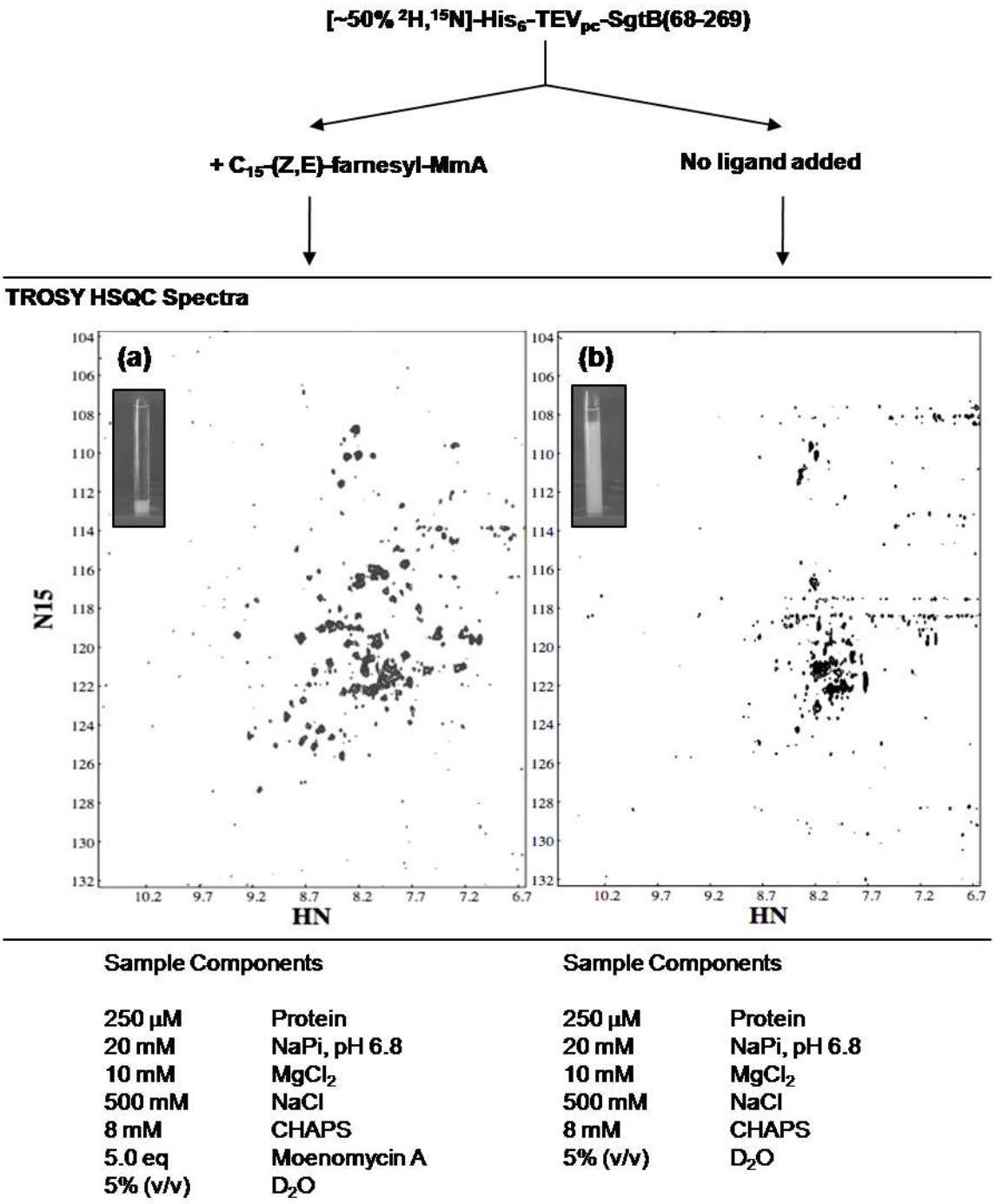

Figure 4.7 [^{1}H,^{15}N]-TROSY HSQC spectra of partially deuterated ^{15}N-labeled His$_6$-TEV$_{pc}$-SgtB(68-269) with and without the Moenomycin A derivative, C$_{15}$-(Z,E)-farnesyl-Moenomycin A. (a) [^{1}H,^{15}N]-TROSY HSQC spectrum of His$_6$-TEV$_{pc}$-SgtB(68-269) with C$_{15}$-(Z,E)-farnesyl-Moenomycin A added, and image of protein sample after measurement. (b) [^{1}H,^{15}N]-TROSY HSQC spectrum of ligand free His$_6$-TEV$_{pc}$-SgtB(68-269), and image of protein sample after measurement. Note the copious amounts of precipitated protein.

4.2.4 Incorporation of the solubility-enhancement tags, GB1

The use of Streptococcal protein G domain 1 (GB1) solubility enhancement tags has been used by numerous research groups to improve the stability and solubility protein samples that were otherwise intractable for solution structural work.[37] The GB1 solubility enhancement tag's key advantage over other solubility enhancement tags such as Thioredoxin protein (Trx), Maltose-binding protein (MBP), and Glutathion S-transferase (GST) commonly available in overexpression vectors is its small mass: one can incorporate 2 GB1-tags to solubilize a passenger protein, adding only a modest 12.4 kDa to the overall mass of the fusion protein.[38] Furthermore, the GB1 tags are available in an acidic (GB1A, pI = 4.6) and basic form (GB1B, pI = 8.0) that can be appropriately matched to the pI of the protein to maintain the optimal charged state for solubility. Based on the crystal structure of SgtB (PDB: 3HZS), the protein has a hydrophobic, membrane-interacting surface that is located near the N-terminus, which is in close proximity to the site where the transmembrane helix anchor would be connected. In an aqueous environment, these hydrophobic surfaces might have a high tendency to form nonspecific interactions, giving rise to large oligomeric complexes that eventually precipitate from solution. The addition of a GB1-solubility enhancement tag on the N-terminus of SgtB could mitigate this problem by shielding this hydrophobic surface.

We screened a series of SgtB constructs incorporating acidic and basic variants of the GB1-tag on the N-terminus of the protein and identified a construct, His_6-GB1A-SgtB(64-269), an N-terminal 6XHis acidic GB1-SgtB fusion that produced the highest amount of soluble protein in M9 minimal media. Subsequently, we prepared a partially deuterated, ^{15}N-labeled sample of this construct at a concentration of 250 μM and supplemented it with 1.3

equivalents of MmA. The [^{1}H,^{15}N]-TROSY HSQC spectra presented the characteristic fingerprint of the GB1-tag, and there was no dispersion of the SgtB amide backbone hydrogen peaks (**Figure 4.7a and 4.8**). We were surprised that we did not even observe the same levels of dispersion despite the addition of MmA which we had previously observed to provide structural order to the protein. The only improvement we observed was the vast improvement in the solubility of the sample. After 12 hours of exposure at room temperature and in the presence of 1.3 equivalents of MmA, the His_6-GB1A-SgtB(64-269) construct produced far lesser amounts of precipitated protein compared with His_6-TEV_{pc}-SgtB(68-269). This suggests that the GB1 tag improved the overall solubility of the sample. We performed an enzyme activity test on His_6-GB1-sgtB(64-269) and determined that the enzymatic domain of the fusion protein is active, hence the tag did not result in misfolding of SgtB.

One possible explanation for the sum of these observations is the SgtB passenger protein aggregated whereas the GB1-tag remained dynamically free since it is attached to the flexible N-terminal segment of the protein. The observed peak broadening of the GB1 associated peaks in the HSQC spectra might result from being attached to the large aggregated mass of SgtB influencing the overall tumbling of the fusion protein. Given that SgtB might interact with other cell-wall remodeling proteins present in the periplasm, the C-terminal face of SgtB may have surfaces that facilitate protein-protein interaction. The addition of a second GB1-tag on to the C-terminus might shield these sticky surfaces and prevent the formation of aggregates.

We identified a construct, His_6-GB1A-SgtB(64-269)-gly-GB1A that incorporates a glycine spacer between the C-terminus of the SgtB protein and the acidic GB1 solubility tag

that produced soluble protein in M9 minimal media. We were able to prepare a partially deuterated, ^{15}N-labeled sample of it at 250 μM for spectroscopic characterization in the presence of MmA. Again, we did not observe good dispersion of the amide backbone hydrogen peaks from SgtB in the HSQC spectra of this 38.6 kD fusion protein construct (**Figure 4.7b**). Similar to the single N-terminally GB1-tagged SgtB construct, the protein sample remained soluble as there were only minute amounts of precipitate. Given that the use of GB1-solubility enhancement tags together with the addition of MmA did not improve the peak count and peak dispersion in the [^{1}H, ^{15}N]-TROSY HSQC spectrum, we decided to forgo the use of solubility enhancement tags to improve protein stability at high concentrations.

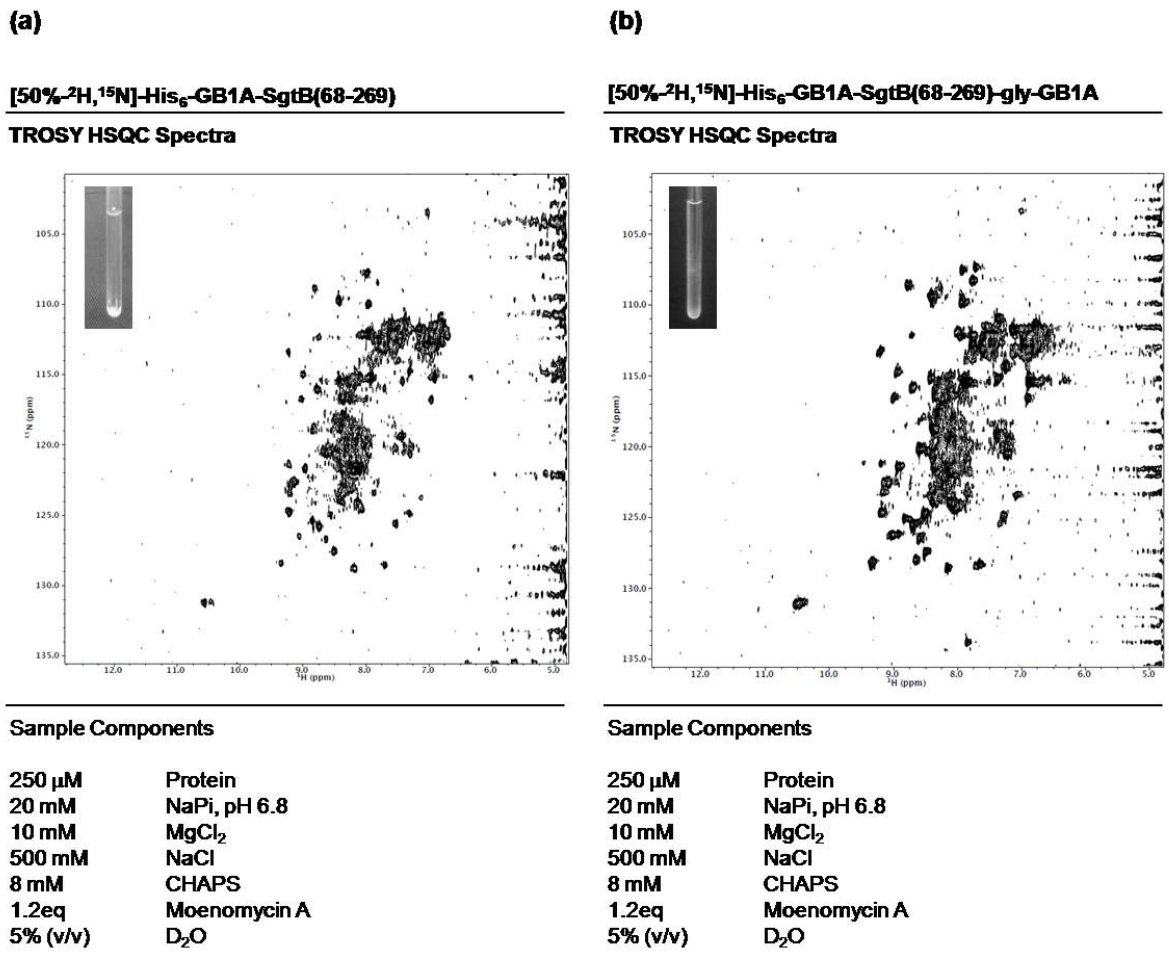

Figure 4.8 [^{1}H,^{15}N]-TROSY HSQC spectra of GB1-tagged SgtB. (a) [^{1}H,^{15}N]-TROSY HSQC spectrum of partially deuterated, ^{15}N-labeled His$_6$-GB1A-SgtB(64-269) with 1.2 equivalents of Moenomycin A added, and image of protein sample after measurement. (b) [^{1}H,^{15}N]-TROSY HSQC spectrum of partially deuterated, ^{15}N-labeled His$_6$-GB1A-SgtB(64-269)-gly-GB1A with 1.2 equivalents of Moenomycin A added, and image of protein sample after measurement.

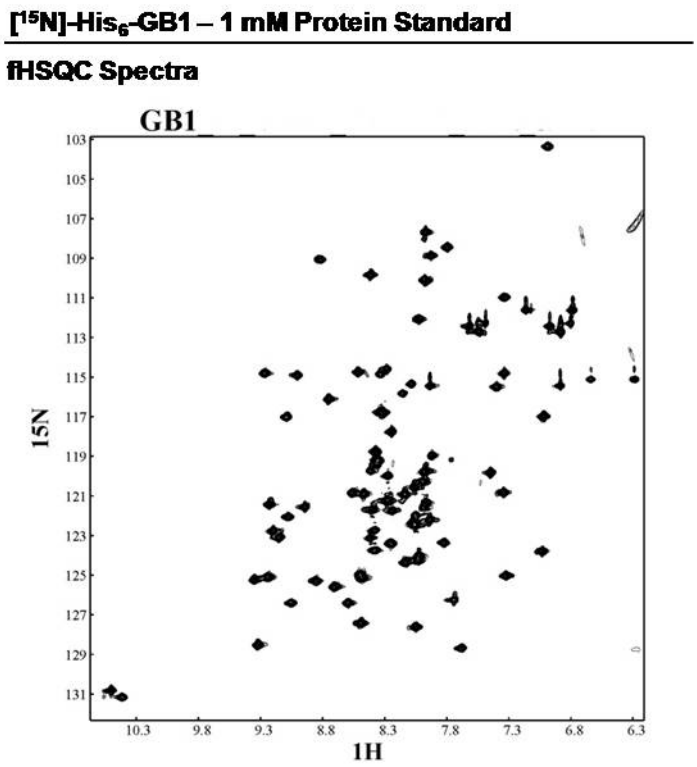

Figure 4.9 Characteristic [^{1}H,^{15}N]-HSQC spectra of 1 mM His$_6$-GB1A (prepared by Dr. Ricard Rodriguez-Mias, Wagner group).

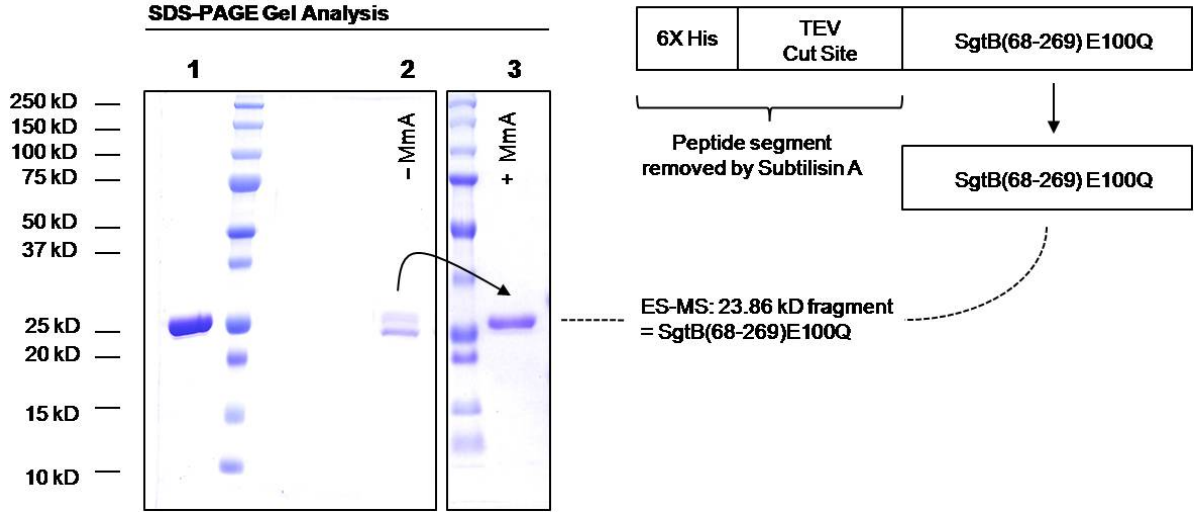

Figure 4.10 Limited proteolysis of His$_6$-TEV$_{pc}$-SgtB(68-269) in the presence and absence of Moenomycin A by Subtilisin A. Lane 1: His$_6$-TEV$_{pc}$-SgtB(68-269) standard before Subtilisin A digestion, Lane 2: 1 hour digestion product of His$_6$-TEV$_{pc}$-SgtB(68-269) without Moenomycin A added, and Lane 3: 1 hour digestion product of His$_6$-TEV$_{pc}$-SgtB(68-269) with Moenomycin A added.

4.2.5 Optimizing the MmA bound His_6-TEV_{pc}-SgtB(68-269) sample: Limited proteolytic analysis with Subtilisin A

We redoubled our efforts on the His_6-TEV_{pc}-SgtB(68-269) construct because it gave us our most promising [^1H,^{15}N]-TROSY HSQC spectrum thus far. We prepared the inactivated mutant His_6-TEV_{pc}-SgtB(68-269) E100Q because we were interested in optimizing a construct would enable us to analyze reactive PGT substrates in a static enzyme system. We knew that the addition of a high affinity ligand Moenomycin A improved the peak dispersion of the sample by bringing more structural order to the protein as seen from the improved chemical shift dispersion of the spectrum. We wanted to see if it was possible to remove segments of the protein that remain disordered in the presence of Moenomycin A that may promote aggregation by limited proteolytic analysis.[39,40]

Proteolytic digestion of His_6-TEV_{pc}-SgtB(68-269) E100Q with the nonspecific protease Subtilisin A in the presence of 1 equivalent of MmA at a protein concentration of 40 μM yielded a stable protease-resistant fragment at 23-24 kDa (**Figure 4.10**). We analyzed this fragment by N-terminal Edman sequencing and ESI-MS and determined it to be SgtB(68-269) E100Q: it turns out that it is the very same fragment that would have been obtained from the removal of the His_6-TEV_{pc} appendage from His_6-TEV_{pc}-SgtB(68-269) E100Q by the TEV protease. In the absence of MmA, we did not obtain a protease resistant fragment when His_6-TEV_{pc}-SgtB(68-269) E100Q was digested with Subtilisin A. Taken together, MmA appears to tighten the fold of the protein such that a non-specific protease such as Subtilisin A is unable to efficiently digest the protein by acting on a segment of the protein that is poorly structured.

4.2.6 Preserving the monomeric state by adding MmA at low protein concentrations

The fact that SgtB(68-269) E100Q turns out to be the stable core fragment surprised us because our earlier [^{1}H,^{15}N]-TROSY HSQC spectra of SgtB(68-269) suggested that the protein was aggregated at high concentrations (300 μM). We wondered whether the simple addition of MmA to the 300 μM sample of SgtB(68-269) E100Q would inhibit aggregation. Tracing the steps involved in preparing the 300 μM sample of SgtB(68-269) mentioned in section 4.2.2, we observed that SgtB(68-269) protein used to prepare the highly concentrated sample was monomeric and monodisperse as seen from its size-exclusion profile. The protein concentration after size-exclusion chromatography was 10-20 μM. This suggests that the formation of aggregates must occur at some point between the pooling and concentrating of fractions after size-exclusion chromatography to the act of acquiring the [^{1}H,^{15}N]-TROSY HSQC spectrum. To investigate this, we prepared two identical samples of SgtB(68-269) E100Q at a protein concentration of 550 μM from freshly prepared 20 μM monomeric stock of SgtB(68-269) E100Q (**Figure 4.11**). The first sample was immediately loaded onto a size-exclusion column for profiling, while the second sample was stored at 4 ^{o}C for one hour before analytical profiling on a size-exclusion column. In the first sample, we observed the formation of small amounts of high molecular weight aggregates that cannot be broken apart by the dilution process of size-exclusion chromatography.[41] In the second sample, we observed that these high molecular weight aggregates have increased proportion over the monomeric population. Taken together, these results show that the aggregates form as soon as the SgtB(68-269) E100Q protein is concentrated up from the pooled monomeric fractions.

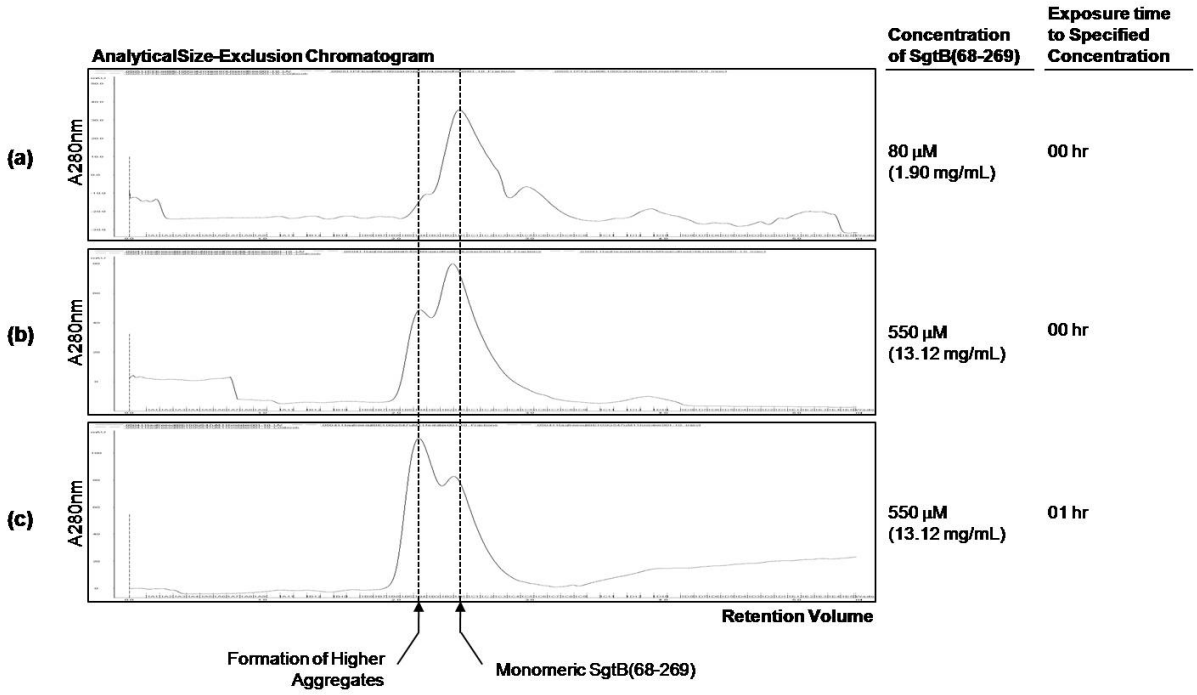

Figure 4.11 Analytical size-exclusion profile of SgtB(68-269) at prepared at various protein concentrations. (a) SgtB(68-269) at 80 µM, (b) SgtB(68-269) concentrated from 80 µM to 550 µM and profiled immediately, and (c) SgtB(68-269) concentrated from 80 µM to 550 µM, incubated at 4 ^{o}C for 1 hour before profiling.

In order to prepare a monomeric, monodisperse sample of SgtB(68-269) E100Q at high concentrations, one must find an additive that preserves the monomeric state of the protein at a dilute concentration immediately after the removal of the His_6-TEV_{pc} appendage before proceeding with the sample concentration step. Thus far, we have learned that MmA is able to (1) enforce structural order on SgtB that resulted in a dispersed [^{1}H,^{15}N]-TROSY HSQC spectra and the identification of a protease resistant core and (2) improve the solubility of the protein by preventing precipitation from aggregation. We hypothesized that if we add MmA to SgtB(68-269) E100Q immediately after the removal of the His_6-TEV_{pc} appendage while the protein sample is still dilute and monomeric, we can lock the enzyme in a conformation that does not aggregate. The MmA bound SgtB(68-269) E100Q protein can

then be concentrated to the desired level required for NMR analysis, preserving the monomeric state throughout the final processing steps.

In our collective experience of preparing various samples of SgtB, we observed that the protein remained monodisperse and monomeric at concentrations below 80 μM. Specifically, our proteolytic digestion analysis of His_6-TEV_{pc}-SgtB(68-269) E100Q in the presence of MmA was performed at 40 μM. We decided to prepare a solution of SgtB(68-269) E100Q at 80 μM that would be mixed with an equal volume of buffer containing 1.3 equivalents of MmA, bringing the final concentration of the protein species in the mixture to 40 μM. The mixture is incubated at 4^{o}C with gentle rocking for 3 hours. The entire operation is carried out at a buffered pH of 7.5 because the enzymatic function of SgtB has been previously found to be optimal in a slightly basic medium. We were able to concentrate our sample at 4^{o}C to a final concentration at 600 μM without any protein material precipitating.

4.2.7 Heat as a polishing step: exposing the protein sample to ambient room temperature

We tested the heat susceptibility of our sample by incubating for 24 hours at ambient room temperature (22 ^{o}C). After 12 hours of exposure at room temperature, we observed that some of the protein was beginning to precipitate from solution. We monitored the protein concentration remaining in solution over several days and observed that the protein concentration had stabilized at approximately 450 μM after 72 hours of exposure at room temperature (**Figure 4.12a**). Analytical size-exclusion analysis of the protein fraction that remained solvent showed that the soluble protein was monodisperse and appeared to be monomeric. We tracked the soluble protein concentration and size-exclusion profile for a

period of 25 days. There were no further changes to the size-exclusion profile and soluble protein concentration after the 3rd day, remarkably, the size-exclusion profile on the 25th day indicated the protein was still monomeric: the observed peak retention volume was under 43 kDa that comes matches up with the expected mass 32.5 kDa (23.9 kDa SgtB(68-269) E100Q + 1.6 kDa MmA + ~7.0 kDa CHAPS micelle) (**Figure 4.13**). We lost approximately 25% of our original sample to precipitation, presumably because there is always some proportion of overexpressed SgtB protein that cannot bind MmA well because it is not optimally folded. Fortunately, the remaining 75% of the protein remained soluble, monodisperse and monomeric. We recovered this well-behaved protein that is thermally stable at room temperature by low g-force centrifugation to remove the precipitates. In summary, exposing the sample to ambient room temperature is an excellent way of removing heterogeneity in the protein sample: poorly behaved proteins are precipitated by this gentle "heat" treatment, leaving behind a pristine solution of monomeric and monodisperse MmA bound SgtB(68-269) E100Q.

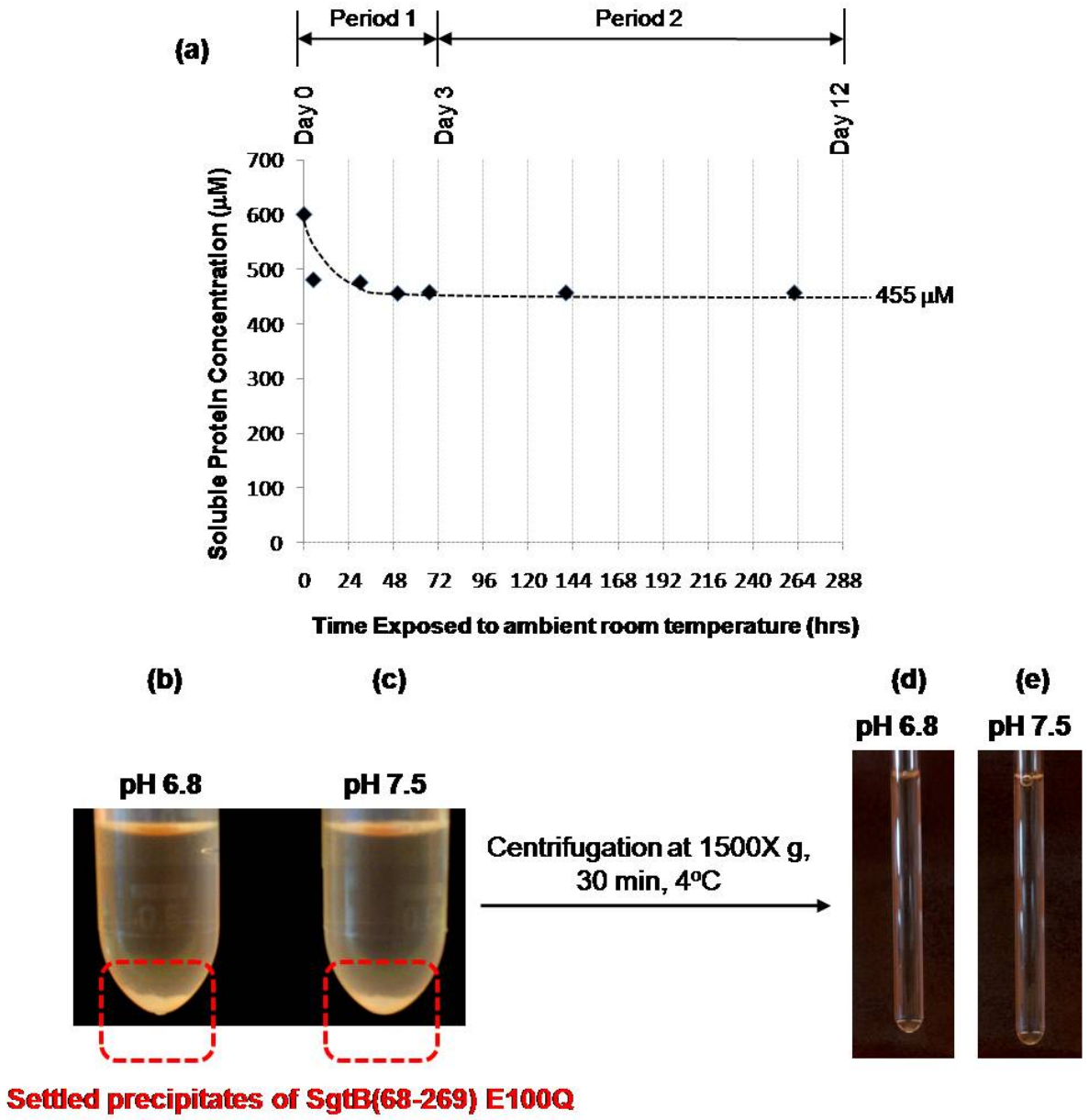

Figure 4.12 Heat polishing the Moenomycin A bound SgtB(68-269) protein complex sample. (a) During Period 1, soluble protein concentration drops sharply from 600 μM to 480 μM in the first 24 hours of exposure to ambient room temperature. The soluble protein concentration stabilizes at ~ 455 μM after 72 hours and remains at approximately the same level thereafter in period 2. (b) Moenomycin A bound SgtB(68-269) sample buffered at pH 6.8 after 72 hours of exposure to ambient room temperature. (c) Moenomycin A bound SgtB(68-269) protein complex sample buffered at pH 7.5 after 72 hours of exposure to ambient room temperature. (d) and (e) Well-behaved Moenomycin A bound SgtB(68-269) protein complex sample buffered at pH 6.8 and 7.5 respectively.

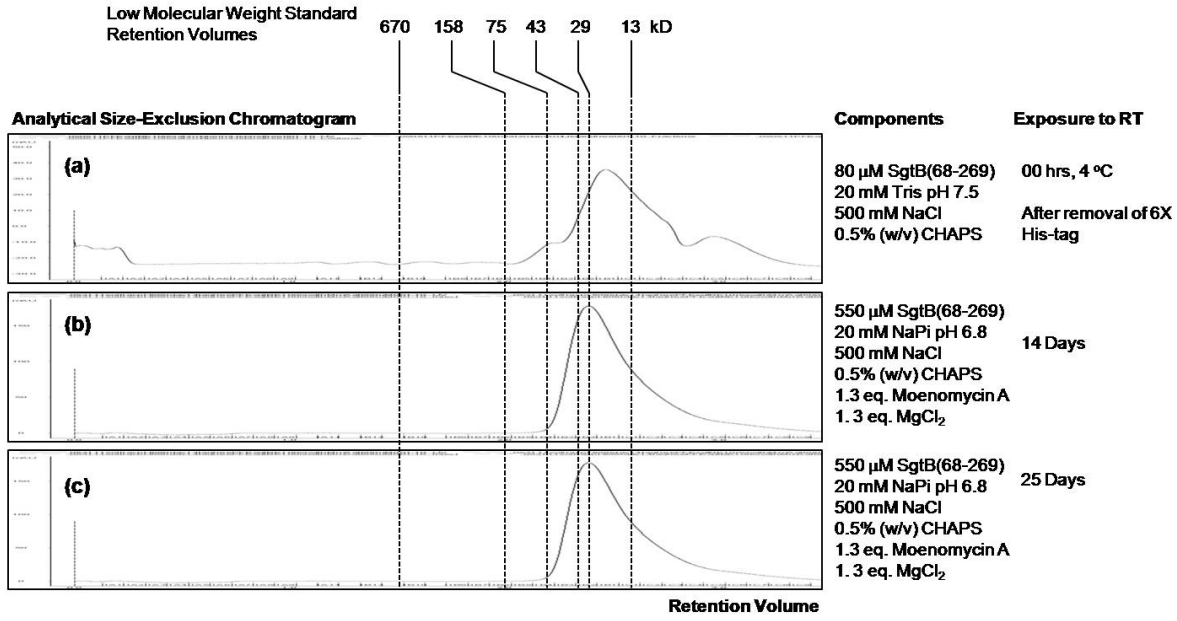

Figure 4.13 Size-exclusion profiles of Moenomycin A bound SgtB(68-269) sample prepared using the methodology described in section 4.2.8. (a) Monomeric SgtB(68-269) protein stock prior to sample preparation, (b) Moenomycin A bound SgtB(68-269) sample at 550 µM after 14 days exposure to ambient room temperature. (c) Moenomycin A bound SgtB(68-269) sample at 550 µM after 25 days exposure to ambient room temperature.

4.2.8 Preparation of a stable, well-behaved MmA bound SgtB NMR sample at a final concentration of 550 µM.

Thus far, our protein sample has been buffered with Tris base at a pH 7.5. Sample pH values greater than 7.5 can be problematic for NMR because spectral quality is impaired from the exchange of labile backbone and side chain amide protons with solvent protons. We lowered the pH of our sample by exchanging the basic Tris buffer to Sodium Phosphate buffer at a pH 6.8 while simultaneously introducing 5% (v/v) D_2O required for deuterium field-frequency lock. This was accomplished using a PD-Minitrap G25 Sephadex cartridge

(GE Healthcare) that was pre-equilibrated in our final sample buffer containing 20 mM Sodium Phosphate at pH 6.8, 5% (v/v) D_2O in addition to 500 mM NaCl and 8 mM CHAPS.

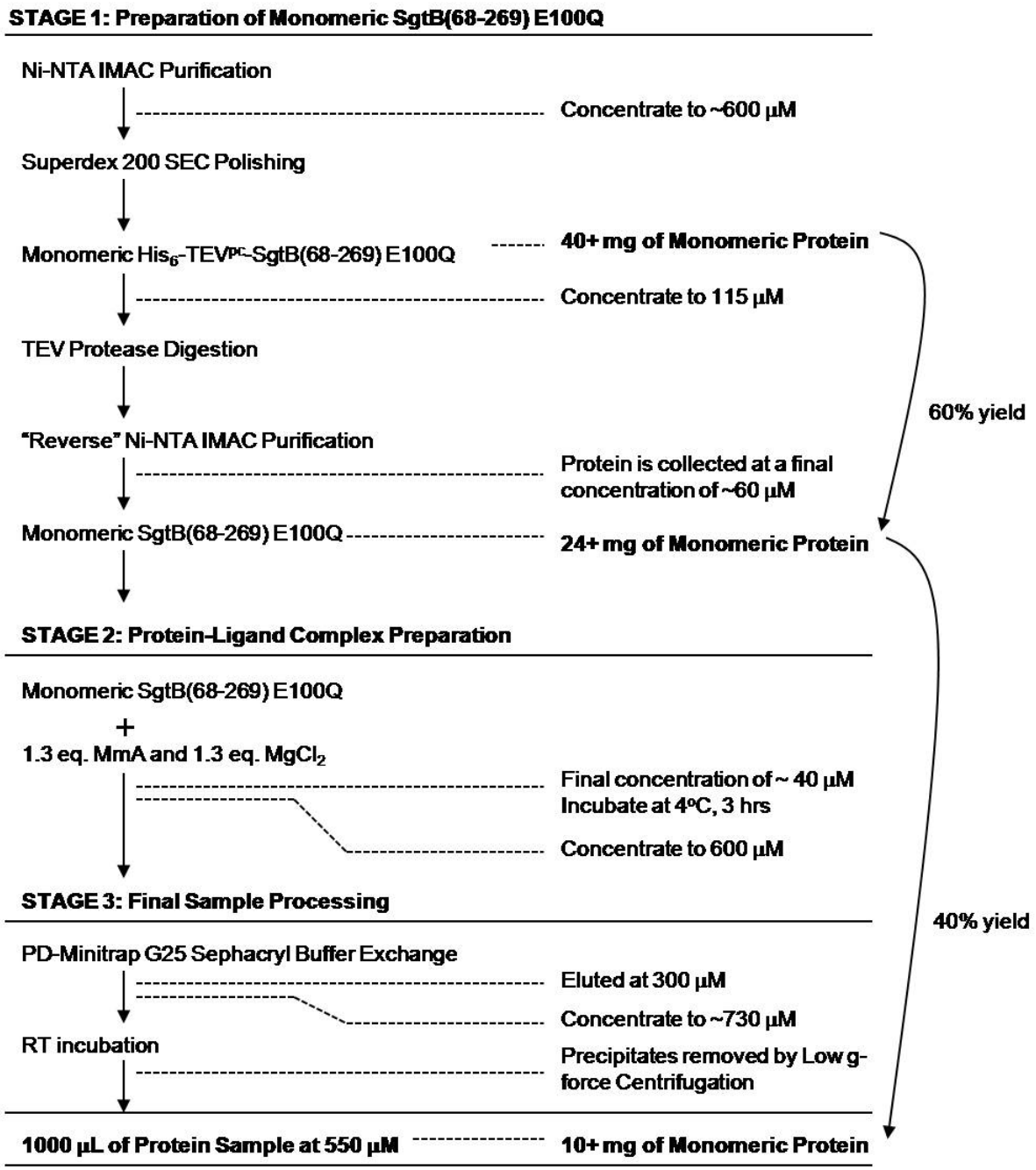

Figure 4.14 Summary of the preparation methodology for a well-behaved Moenomycin A bound SgtB(68-269) at 550 µM.

A graphic summary of our sample preparation methodology is presented in **Figure 4.14**. We prepared two 550 μM partially deuterated, ^{15}N-labeled samples of MmA bound SgtB(68-269) E100Q, buffered at pH 6.8 and 7.5 for [^{1}H,^{15}N]-TROSY HSQC characterization. Briefly, His_6-TEV_{pc}-SgtB(68-269) E100Q was overexpressed and purified in D_2O/^{15}N-labeled M9 minimal media expression system developed in Chapter 3. Approximately 40 mg of His_6-TEV_{pc}-SgtB(68-269) E100Q was accumulated using this process, storing the monomeric fractions of the protein at ~20 μM (0.5 mg/mL) concentration to retard aggregation. The monomeric His_6-TEV_{pc}-SgtB(68-269) E100Q stock is then concentrated to 115 μM and digested with TEV protease. The digestion product, SgtB(68-269) E100Q is then cleaned up by passage through a Ni-NTA IMAC column and immediately incubated with 1.3 equivalents of MmA at a final concentration of 40 μM for 3 hours at 4 ^{o}C. The protein sample is then concentrated to 600 μM for buffer exchange. Finally, the sample is concentrated up to ~730 μM and incubated at 22 ^{o}C for 3 days. The precipitates are removed by low g-force centrifugation to obtain a highly concentrated well-behaved, monomeric and monodisperse MmA bound SgtB(68-269) E100Q sample at 550 μM.

The [^{1}H,^{15}N]-TROSY HSQC spectra acquired on a 500MHz instrument equipped with a room temperature triple resonance probe was well-dispersed for both samples (**Figure 4.15 and 4.16**). Not surprisingly, the spectrum acquired from the sample buffered at pH 6.8 reveals additional amide proton peaks compared with the sample at pH 7.5 (**Figure 4.17**). Closer examination of the spectra revealed that 60-70% of the 286 expected peaks amide peaks are visible. Because Asparagine and Glutamine make up more than 17% of our SgtB(68-269) E100Q construct, the extensive overlap by their side chain amide protons alone

may account for half of these missing peaks (**Figure 4.18**). Additionally, SgtB contains a large number of alpha-helices which may result in extensive peak overlaps because the amide backbones sample a less diverse chemical environment.[42] Peaks may be also be broadened in regions undergoing μs-ms conformational dynamics.[43]

At this stage, we were ready to optimize the sample buffer by reducing the salt and detergent concentrations. A stable well behaved sample of Moenomycin A bound SgtB(68-269) at 600 μM was prepared and exchanged into various buffers using PD-minitrap G25 sephacryl column. Reducing the NaCl salt and CHAPS detergent concentrations resulted in the formation of soluble aggregates in 12 hours (**Figure 4.19**). This series of experiments show that the addition of Moenomycin A alone cannot prevent the formation of aggregates. The high salt and detergent levels were equally crucial in stabilizing the protein.

Currently, we are pursuing triple resonance experiments on a 800 MHz instrument equipped with a HCN salt-tolerant cryoprobe that will determine the feasibility of obtaining a full spectral assignment of our protein with a high-salt tolerant cryoprobe that also promises greater signal sensitivity.

Sample Components

550 µM	Protein
20 mM	NaPi, pH 6.8
500 mM	NaCl
8 mM	CHAPS
1.2 eq	Moenomycin A
1.2 eq	$MgCl_2$
5% (v/v)	D_2O

TROSY HSQC Spectra, [50%-^{2}H, ^{15}N] SgtB(68-269) E100Q

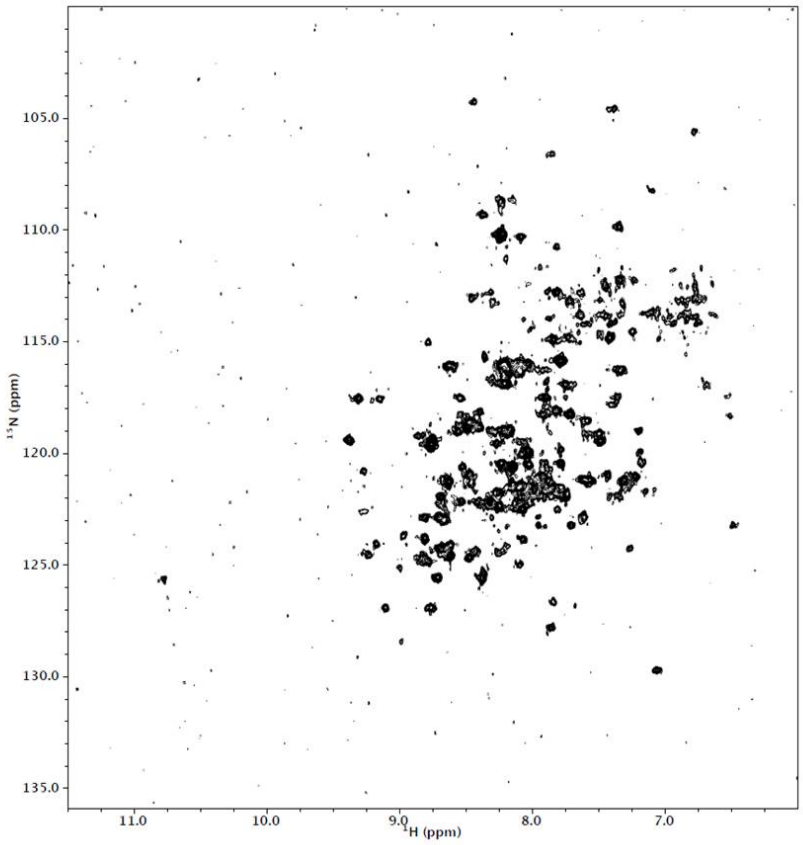

Figure 4.15 [^{1}H,^{15}N]-TROSY HSQC of partially deuterated ^{15}N-labeled Moenomycin A bound SgtB(68-269) sample at pH 6.8, prepared using the methodology described in Section 4.2.8.

Sample Components

550 µM	Protein
20 mM	NaPi, pH 7.5
500 mM	NaCl
8 mM	CHAPS
1.2 eq	Moenomycin A
1.2 eq	$MgCl_2$
5% (v/v)	D_2O

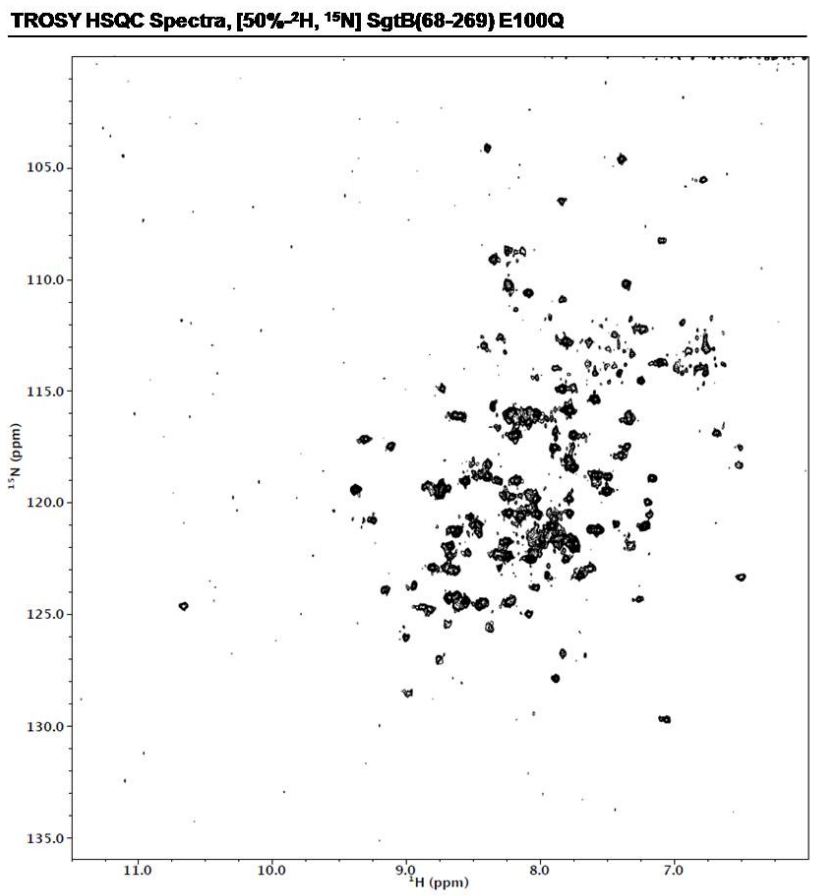

Figure 4.16 [^{1}H,^{15}N]-TROSY HSQC of partially deuterated ^{15}N-labeled Moenomycin A bound SgtB(68-269) sample at pH 7.5, prepared using the methodology described in Section 4.2.8.

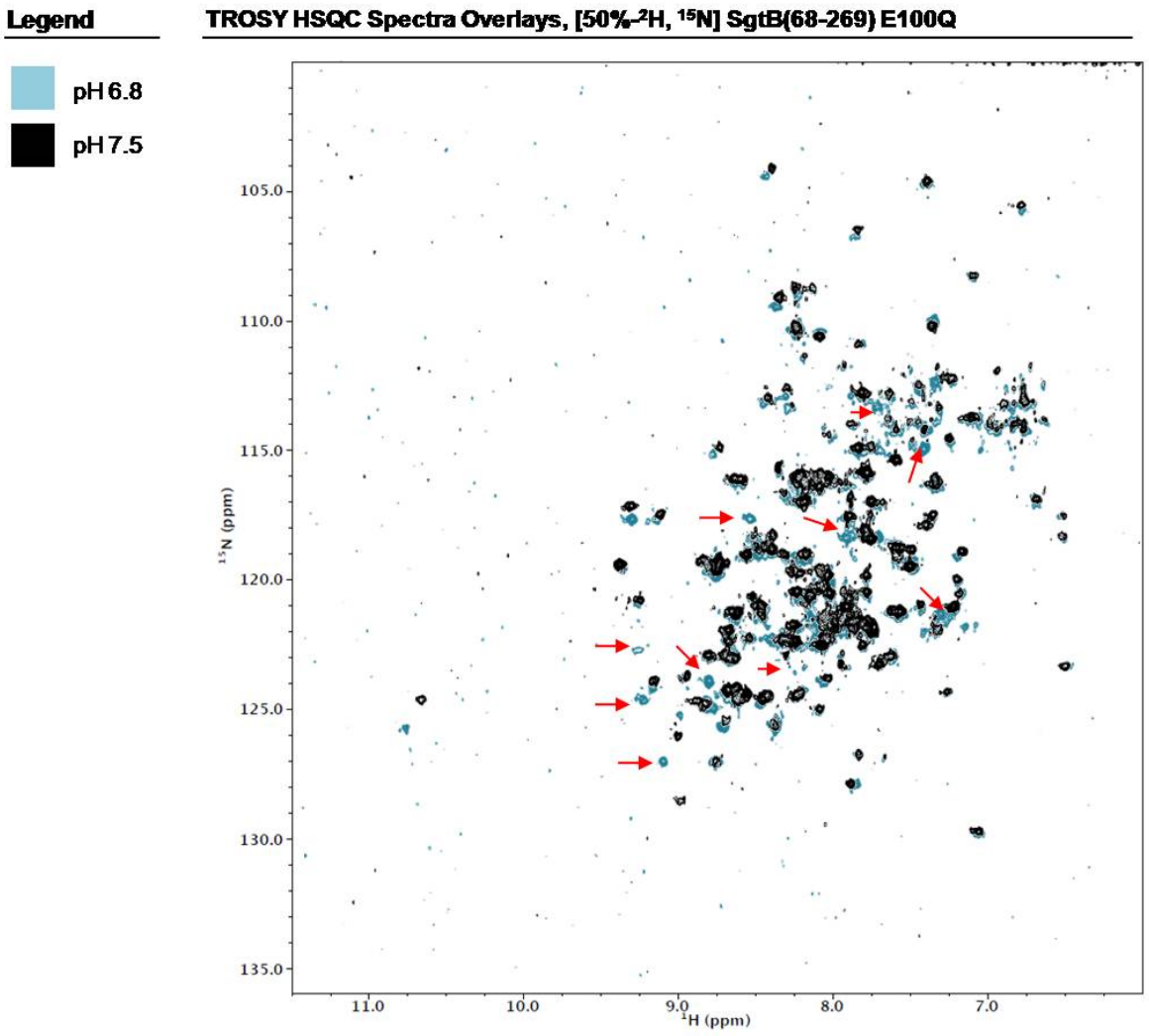

Figure 4.17 Overlay of [^{1}H,^{15}N]-TROSY HSQC spectra of pH 6.8 versus pH 7.5 Moenomycin A bound SgtB(68-269) samples. Indicated with red arrows are examples of additional peaks observed in the sample buffered at pH 6.8.

(a)

	207	Amino Acids
–	2	Proline
+	0	Tryptophan Nε-Hε
+	26	Glutamine Nε-$Hε_2$ ← 9% of expected peaks
+	46	Asparagine Nδ-$Hδ_2$ ← 16% of expected peaks
+	9	Arginine Nε-Hε
	286	**Expected N-H peaks**

(b)

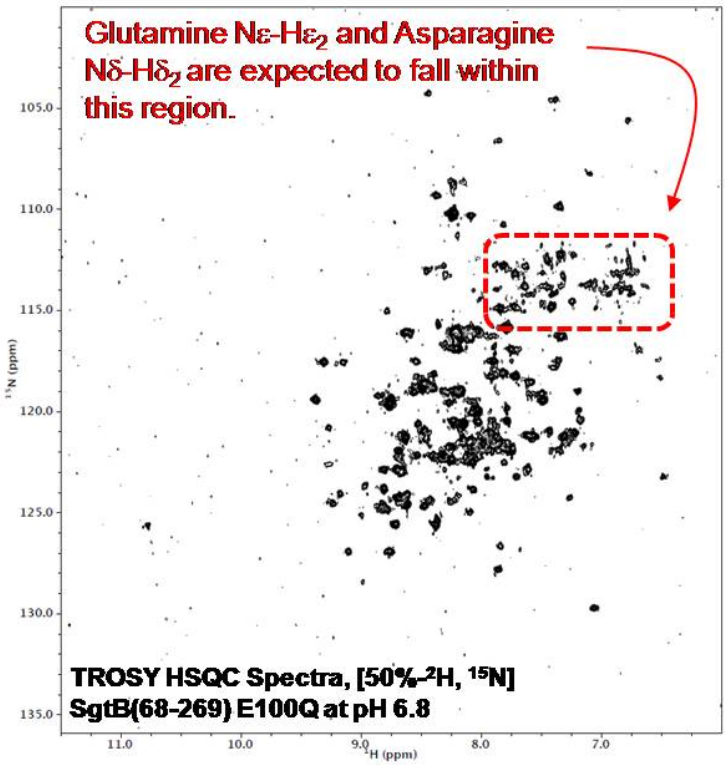

Figure 4.18 Accounting for the expected number of observed N-H peaks in the [^{1}H,^{15}N]-TROSY HSQC spectrum of SgtB(68-269). (a) Expected number of N-H peaks in the spectrum. (b) Notably, 25% of the expected N-H peaks originate from glutamate and asparagines side chains N-H that tend to be crowded in a typical HSQC spectrum.

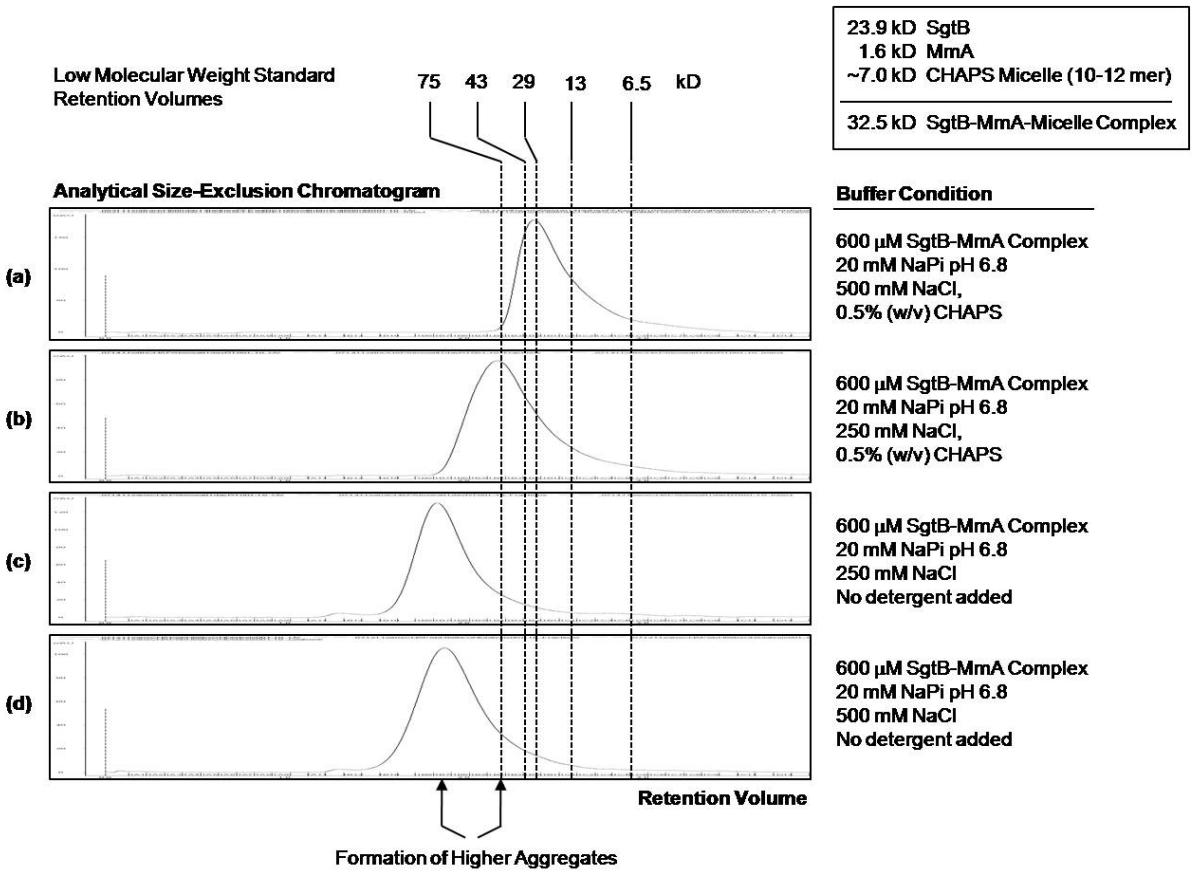

Figure 4.19 Optimizing the sample salt and detergent concentrations. (a) 600 µM sample of Moenomycin A bound SgtB(68-269) prepared using the methodology decribed in section 4.2.8. (b) 600 µM sample of Moenomycin A bound SgtB(68-269) prepared using the methodology decribed in section 4.2.8. that has been exchanged into a buffer with a reduced salt concentration. (c) 600 µM sample of Moenomycin A bound SgtB(68-269) prepared using the methodology decribed in section 4.2.8. that has been exchanged into a buffer with a reduced salt concentration and no detergent. (d) 600 µM sample of Moenomycin A bound SgtB(68-269) prepared using the methodology decribed in section 4.2.8. that has been exchanged into a buffer with 500 mM NaCl and no detergent.

4.2.9 Insights into the structure of Moenomycin A bound SgtB

In our quest to prepare a long-lived, monodisperse and monomeric sample of SgtB for protein NMR characterization, we have observed that ligand-free SgtB(68-269) has a strong tendency to aggregate at high concentrations even at temperatures as low as 4 ^{o}C. Studies have shown that proteins aggregate when natively folded monomeric proteins are able to sample a series of expanded conformations that are aggregation-competent. We believe that ligand-free SgtB(68-269) aggregates mainly because of conformational flexibility. Aggregation-prone surfaces are exposed in the due course of sampling many distinct conformations. The fact that monomeric MmA bound SgtB(68-269) does not form aggregates even after extensive exposure to ambient room temperature suggests that the aggregation-prone surfaces that exposed in the MmA bound SgtB(68-269) complex must be greatly reduced, and the large exposed hydrophobic surface on the base of the lower lobe does not have sufficient pliability to form moulded non-specific interaction interface with other protein partners. If this was not the case, then one should observe the aggregation and precipitation of the MmA bound SgtB(68-269) complex.

As a result, we believe that the ensemble of structures presented by MmA bound SgtB(68-269) must be structurally and dynamically distinct from its ligand-free form. Additionally, our [^{1}H,^{15}N]-TROSY HSQC data suggests that the MmA bound SgtB(68-269) complex retains some level of floppiness. Given that size-exclusion analysis of our protein sample suggests that the MmA bound SgtB(68-269) complex exists as a monomeric complex, we postulate that a number of missing amide backbone proton peaks in the spectrum may arise from flexible regions in the protein that are undergoing μs-ms conformational exchange that broadens out their signal. Because this SgtB construct was

identified by trimming disordered regions at the termini of the protein with a non-specific protease, Subtilisin A, we think that the majority of these pockets of flexibility originate from internal structures within the protein and not flexible termini. The lack of electron density in segments of the lower lobe region in the crystal structures of PGT domain from *S. aureus* PBP2, *A. aeolicus* PBP1A and *E. coli* PBP1B suggests this helix-loop region near the catalytic domain to be one obvious candidate. There may be other regions of flexibility that are critical for catalytic function/impairment of the enzyme that are not readily apparent from the crystal structures. A detailed comparison of the conformational dynamics between a MmA bound SgtB(68-269) complex with a Gal-Lipid IV bound SgtB(68-269) complex by NMR will shed light on this issue.

Chapter 4.3 Selected Materials and Methods

S. aureus SgtB (D68-R269), overexpression plasmid was obtained from Dr. Alita Miller (Pfizer Global Research and Development, MTA:A12545). The pET30a plasmid containing 6XHis-GB1A (pET30a:6XHis-GB1A) was obtained from Dr. Ricard Rodriguez-Mias, (Wagner group). Moenomycin A was prepared by Dr. Hirokazu Tsukamoto (Kahne group) and Yihui Wu (Kahne group). C_{15}-(Z,E)-Farnesyl-MmA was synthesized by Dr. Hirokazu Tsukamoto (Kahne group). Protein biochemistry was performed by Yihui Wu (Kahne group). NMR spectra acquisition was performed by Dr. Ricard Rodriguez-Mias (Wagner group) and Dr. Haribabu Arthanari (Wagner group) on a Varian or Bruker spectrometer equipped with room temperature probe operating at 500 MHz field strength. Recycled D_2O used for culture growth was purified and distilled by Dr. Tsyr-Yan Yu (Wagner group). TEV protease was prepared by Dr. Jiaoyang Jiang (Walker group).

4.3.1 Cloning of His_6-GB1A-SgtB(64-269) and His_6-GB1A-SgtB(64-269)-gly GB1A

sgtB gene containing SgtB(60-269) was PCR amplified from Staphylococcus aureus COL genomic DNA with KOD hotstart polymerase (Novagen) with BamHI and EcoRI restriction sites and subcloned into pET30a:6XHis-GB1A to give pET30a:6XHis-GB1A-SgtB(60-269). sgtB gene containing SgtB(64-269) was PCR amplified from pET30a:6XHis-GB1A-SgtB(60-269) using KOD hotstart polymerase (Novagen) with BamHI and EcoRI restriction sites subcloned into pET30a vector containing 6XHis-GB1A to give the expression vector pET30a:6XHis-GB1A-SgtB(64-269) for the protein His_6-GB1A-SgtB(64-269).

GB1A was PCR amplified from pET30a:6XHis-GB1A using the forward primer 5'-AAA-AAG-AAT-TCA-TGC-AGT-ACA-AAC-TGA-TCC-TGA-ACG-G-3' and reverse

primer 5'-AAA-AAC-TCG-AGT-TAT-TCG-GTA-ACG-GTG-AAG-GTT-TTG-3', incorporating EcoRI and XhoI restriction sites and inserted into pET30a:6XHis-GB1A-SgtB(64-269) to give pET30a:6XHis-GB1A-SgtB(64-269)-GB1A. C-terminal GB1A glycine linker vector pET30a:6XHis-GB1A-SgtB(64-269)-gly-GB1A was made using site-directed mutagenesis kit Quikchange II (Agilent/Stratagene), in the presence of 5% DMSO (v/v) (Sigma Aldrich), with the following modified PCR program: (1) 95 ^{o}C – 2 min, (2) 95 ^{o}C – 1 min, (3) 55 ^{o}C – 1 min, (4) 68 ^{o}C – 10 min, (5) 68 ^{o}C – 7 min, and (6) 4 ^{o}C, looping steps (2) to (4) 18 times over. The forward primer used to create this insertion is 5'-TCA-ACA-GGC-TAT-GTC-ACA-ATT-AAA-TCG-TGG-AGA-ATT-CAT-GCA-GTA-CAA-ACT-G-3' and the reverse primer is 5'-CAG-TTT-GTA-CTG-CAT-GAA-TTC-TCC-ACG-ATT-TAA-TTG-TGA-CAT-AGC-CTG-TTG-A-3' that were designed using Agilent/Strategene's proprietary primer design software available online at http://www.genomics.agilent.com. The integrity of both vectors pET30a:6XHis-GB1A-SgtB(64-269) and pET30a:6XHis-GB1A-SgtB(64-269)-gly-GB1A were confirmed by DNA sequencing.

4.3.2 Detailed preparation of Moenomycin A bound SgtB(68-269) NMR sample

M9 minimal media for overexpressing partially deuterated ^{15}N-labeled His$_6$-TEV$_{pc}$-SgtB(68-269) was prepared using the formulation presented in Chapter 3, incorporating 1.2 g of $^{15}NH_4Cl$ (Cambridge Isotopes) in place of unlabeled ammonium chloride, and recycled D_2O (originally purchased from Cambridge Isotopes) in place of H_2O. His$_6$-TEV$_{pc}$-SgtB(68-269) is overexpressed and purified as described in Chapter 3. Only the most concentrated fractions (~ 20 μM, 0.5 mg/mL) coming off the FPLC near the maximum 280nm absorbance are pooled. A total of ~40 mg of partially deuterated, ^{15}N-labeled His$_6$-TEV$_{pc}$-SgtB(68-269)

is stockpiled from 4 successive rounds of preparation. The entire stockpile of partially deuterated, ^{15}N-labeled His_6-TEV_{pc}-SgtB(68-269) is concentrated using an angled rotor benchtop centrifuge (Eppendorf) to 115 μM using 1% BSA (w/v) passivated Amicon Ultra concentrators (10K MWCO) at 4 ^{o}C, 1500Xg. TEV protease at 0.5 mg/mL is added to the protein stock and the digestion reaction is incubated at 4 ^{o}C for 24 hours to yield SgtB(68-269). SgtB(68-269) is purified by repeated passage (3X) through Ni-NTA affinity column which is then washed with 1 column volume of buffer (20 mM Tris pH 7.5, 500 mM NaCl, 8 mM CHAPS) to give a protein stock at ~ 60-80 μM. The protein is immediately added to a buffer containing 1.3 equivalents of Moenomycin A, 1.3 equivalents of $MgCl_2$, 20 mM Tris pH 7.5, 500 mM NaCl, and 8 mM CHAPS at 4 ^{o}C for 3 hours, giving a final protein concentration of 40 μM. Moenomycin A bound SgtB(68-269) complex is concentrated to 600 μM using 1% BSA (w/v) passivated Amicon Ultra concentrators (10K MWCO) at 4 ^{o}C, 1500Xg.

A Sephacryl PD-minitrap G25 (GE Healthcare) column prepared for buffer exchange by washing with 3 column volumes of H_2O, followed by 6 column volumes of Buffer A containing 5% D_2O (v/v), 20 mM sodium phosphate pH 6.8, 500 mM NaCl, and 8 mM CHAPS at room temperature. The Moenomycin A bound SgtB(68-269) complex is loaded onto the Sephacryl PD-minitrap G25 column at room temperature, and eluted with Buffer A per the manufacturer's instructions to yield a final protein complex concentration of ~ 300 μM. Moenomycin A bound SgtB(68-269) is concentrated with 1% BSA (w/v) passivated Amicon Ultra concentrators (10K MWCO) at 4 ^{o}C, 1500Xg to the target concentration e.g. 600 μM and incubated at ambient room temperature (22 ^{o}C) for 3 days. The precipitated

protein in the sample is removed by centrifugation at 1500Xg for 30 min at 4 ^{o}C, soluble fraction is retained as the protein sample for NMR spectroscopy.

4.4 References

1. Lovering, A. L, de Castro, L. H., Lim, D., and Strynadka, N. C. J. (2007) Structural insight into the transglycosylation step of bacterial cell-wall biosynthesis, *Science 315*, 1402-1405.
2. Welzel, P. (2005) Syntheses around the transglycosylation step in peptidoglycan biosynthesis, *Chem. Rev. 105*, 4610-4660.
3. Gampe, C. M., Tsukamoto, H., Wang, T.-S. A., Walker, S., and Kahne, D. (2011) Modular synthesis of diphospholipid oligosaccharide fragments of the bacterial cell wall and their use to study the mechanism of moenomycin and other antibiotics, *Tetrahedron 67*, 9771-9778.
4. Wang, T. S., Lupoli, T. J., Sumida, Y., Tsukamoto, H., Wu, Y., Rebets, Y., Kahne, D. E., and Walker, S. (2011) Primer preactivation of peptidoglycan polymerases, *J. Am. Chem. Soc. 133*, 8528-8530.
5. Yuan, Y. Q., Barrett, D., Zhang, Y., Kahne, D., Sliz, P., and Walker, S., (2007) Crystal structure of a peptidoglycan glycosyltransferase suggests a model for processive glycan chain synthesis, Proc.. Natl. Acad. Sci. U. S. A. 103, 5348-5353.
6. Yuan, Y., Fuse, S., Ostash, B., Sliz, P., Kahne, D., and Walker, S. (2008) Structural analysis of the contacts anchoring moenomycin to peptidoglycan glycosyltransferases and implications for antibiotic design, *ACS Chem. Biol. 3*, 429-436.
7. Lovering, A. L, Gretes, M., and Strynadka, N. C. (2008) Structural details of the glycosyltransferase step of peptidoglycan assembly, *Curr. Opin. Struct. Biol. 18*, 534-543.
8. Heaslet, H., Shaw, B., Bistry, A., and Miller, A. A. (2009) Characterization of the active site of S. aureus monofunctional glycosyltransferase (Mtg) by site-directed

mutation and structural analysis of the protein complexed with moenomycin, *J. Struct. Biol. 167*, 129-135.

9. Sung, M. T., Lai, Y. T., Huang, C. Y., Chou, L. Y., Shih, H. W., Cheng, W. C., Wong, C. H., and Ma, C. (2009) Crystal structure of the membrane-bound bifunctional transglycosylase PBP1b from Escherichia coli, *Proc. Natl. Acad. Sci. U. S. A. 106*, 8824-8829.

10. Sanders, C. R., and Sönnichsen, F. (2006) Solution NMR of membrane proteins: practice and challenges, Magn. Reson. Chem. 44, S24-S40.

11. Wang, T. S., Manning, S. A., Walker, S., and Kahne, D. (2008) Isolated peptidoglycan glycosyltransferases from different organisms produce different glycan chain lengths, *J. Am. Chem. Soc. 130*, 14068-14069.

12. Offant, J., Michoux, F., Dermiaux, A., Biton, J., and Bourne, Y. (2006) Functional characterization of the glycosyltranferase domain of penicillin binding protein 1a from Thermotoga maritima, *Biochim. Biophys. Acta 1764*, 1036-1042.

13. Di Guilmi, A. M., Dessen, A., Dideberg, O., and Vernet T. (2003) The glycosyltransferase domain of penicillin-binding protein 2a from Streptococcus pneumonia catalyzes the polymerization of murein glycan chains, *J. Bacteriol. 185*, 4418-4423.

14. Di. Guilmi, A. M., Dessen, A., Dideberg, O., and Vernet, T. (2003) Functional characaterization of penicillin-binding protein 1b from Streptococcus pneumonia, *J. Bacteriol. 185*, 1650-1658.

15. Di. Guilmi, A. M., Mouz, N., Andrieu, J. P., Hoskins, J., Jaskunas, S. R., Gagnon, J., Dideberg, O., and Vernet, T. (1998) Identification, purification, and chacterization of

transpeptidase and glycosyltransferase domains of Streptococcus pneumonia penicillin-binding protein 1a, *J. Bacteriol. 180*, 5652-5659.

16. Nicholas, R. A., Lamson, D. R., and Schultz, D. E. (1993) Penicillin-binding protein 1B from Escherichia coli contains a membrane association site in addition to its transmembrane anchor, J. Biol. Chem. 268, 5632-5641.

17. Wang, C. C., Schultz, D. E., and Nicholas R. A., (1996) Localization of a putative second membrane association site in penicillin-binding protein 1B of Escherichia coli, *Biochem. J. 316*, 149-156.

18. Marley, J., Lu, M., Bracken, C. (2001) A method for efficient isotopic labeling of recombinant proteins, J. Biomol. NMR 20, 71-75.

19. Kwan, A. H., Mobli, M., Gooley, P. R., King, G. F., and Mackay, J. P. (2011) Macromolecular NMR spectroscopy for the non-spectroscopist, *FEBS J. 278*, 687-703

20. Bagby, S., Tong, K. I., and Ikura, M. (2001) Optimization of protein solubility and stability for protein nuclear magnetic resonance, *Methods Enzymol. 339*, 20-41.

21. Kovacs, H., Moskau, D., and Spraul, M. (2005) Cryogenically cooled probes - a leap in NMR technology, *Prog. Nucl. Magn. Reson. Spectrosc. 46*, 131-155.

22. Voehler, M. W., Collier, G., Young, J. K., Stone, M. P., Germann, M. W. (2006) Performance of cryogenic probes as a function of ionic strength and sample tube geometry, *J. Magn. Reson. 183*,102-109.

23. Binbuga, B., Boroujerdi, A. F. B., and Young, J. K. (2007) Structure in an extreme environment: NMR at high salt, *Protein Sci. 16*, 1783-1787.

24. Robosky, L. C., Reily, M. D., and Avizonis, D. (2007) Improving NMR sensitivity by use of salt-tolerant cryogenically cooled probes, *Anal. Bioanal. Chem. 387*, 529-532.

25. Anglister, J., Grzesiek, S., Ren, H., Klee, C. B., and Bax, A. (1993) Isotope-edited multidimensional NMR of calcineurin B in the presence of non-deuterated detergent CHAPS, *J. Biomol. NMR 3*, 121-126.

26. McGuire, A. M., Matsuo, H., and Wagner, G. (1998) Internal and overall motions of the translation factor eIF4E: cap binding and insertion in a CHAPS detergent micelle, *J. Biomol. NMR 12*, 73-88.

27. Matsuo, H., Li, H., McGuire, A. M., Fletcher, C. M., Gingras, A. C., Sonenberg, N., and Wagner, G. (1997) Structure of translation factor eIF4E bound to m7GDP and interaction with 4E-binding protein, *Nat. Struct. Biol. 4*, 717-724.

28. Chi, E. Y., Krishnan, S., Randolph, T. W., and Carpenter, J. F. (2003) Physical stability of proteins in aqueous solution: mechanism and driving forces in nonnative protein aggregation, *Pharm. Res. 20*, 1325-1336.

29. Mori, S., Abeygunawardana, C., Johnson, M. O., and van Zijl, P. C. (1995) Improved sensitivity of HSQC spectra of exchanging protons at short interscan delays using a new fast HSQC (FHSQC) detection scheme that avoids water saturation, *J. Magn. Reson. B 108*, 94-8.

30. Riek, R., Pervushin, K., and Wüthrich, K. (2000) TROSY and CRIEPT: NMR with large molecular and supramolecular structures in solution, *Trends Biochem. Sci. 25*, 462-468.

31. Pervushin, K., Riek, R., Wider, G., and Wüthrich, K. (1997) Attenuated T2 relaxation by mutual cancellation of dipole-dipole coupling and chemical shift anisotropy

indicates an avenue to NMR structures of very large biological macromolecules in solution, Proc. Natl. Acad. Sci. U. S. A. 94, 12366-12371.

32. Kapust, R. B., Tözēr, J., Copeland, T. D., and Waugh, D. S. (2002) The P1' specificity of tobacco etch virus protease, *Biochem. Biophys. Res. Commun. 294*, 949-955.

33. Wang, T. S. A., (2011) Bacterial cell wall assembly: mechanism and inhibition of peptidoglycan glycosyltransferases, *PhD Dissertation, Harvard University*, (Publication nbr: 3462154)

34. Adachi, M., Zhang, Y., Leimkuhler, C., Sun, B., Latour, J. V., and Kahne D. (2006) Degradation and reconstruction of Moenomycin A and derivatives: dissecting the function of the isoprenoid chain, *J. Am. Chem. Soc. 128*, 14012-14013.

35. Fuse, S., Tsukamoto, H., Yuan, Y., Wang, T. S., Zhang, Y., Bolla, M., Walker, S., Sliz, P. and Kahne, D. (2010) Functional and structural analysis of a key region of the cell wall inhibitor moenomycin, *ACS Chem. Biol. 5*, 701-711.

36. Eletsky, A., Kienhöfer, A., and Pervushin, K. (2001) TROSY NMR with partially deuterated proteins, *J. Biomol. NMR 20*, 177-180.

37. Zhou, P., and Wagner, G. (2010) Overcoming the solubility limit with solubility-enhancement tags: successful applications in biomolecular NMR studies, *J. Biomol. NMR 46*, 23-31.

38. Esposito, D., and Chatterjee, D. K. (2006) Enhancement of soluble protein expression through the use of fusion tags, *Curr. Opin. Biotechnol. 17*, 353-358.

39. Fontana, A., de Laureto, P. P., Spolaore, B., Frare, E., Picotti, P., and Zambonin, M. (2004) Probing protein structure by limited proteolysis, *Acta Biochim. Pol. 51*, 299-321.

40. Wernimont, A., and Edwards, A. (2009) In situ proteolysis to generate crystals for structure determination: an update, *PLOS One 4*, e5094.

41. Mahler, H.-C., Friess, W., Grauschopf, U., and Kiese, S. (2009) Protein aggregation: pathways, induction factors and analysis, *J. Pharm. Sci. 98*, 2909-2934.

42. Trbovic, N., Klammt, C., Koglin, A., Löhr, F., Bernhard, F., and Dötsch, V. (2005) Efficient strategy for the rapid backbone assignment of membrane proteins, *J. Am. Chem. Soc. 127*, 13504-13505.

43. Boehr, D. D., Dyson, J., and Wright, P. E. (2006) An NMR perspective on enzyme dynamics, *Chem. Rev. 106*, 3055-3079.

Chapter Five: Prospective studies on SgtB

The work presented in this chapter is a result of a collaboration between the Kahne, Walker and Wagner research groups at Harvard Medical School. The data acquisition for the [^{15}N,^{1}H]-TRACT experiment mentioned in the text was performed by Dr. Tsyr-Yan Yu (Wagner).

5.1. Opportunities with a Lipid IV bound SgtB sample.

The observation of SgtB transglycosylation rate-enhancement by Gal-Lipid IV prompted us to pursue an NMR structure-based strategy that can give insight into the conformational dynamics that accompany the initiation of glycan synthesis. Ideally, this can be accomplished if we can produce an NMR-amenable ligand-free SgtB sample. Based on our results in Chapter 4, we believe that it will be difficult to obtain monodisperse and monomeric ligand-free SgtB at concentrations amenable for structural characterization, either by X-ray crystallography or NMR because the protein aggregates at high concentrations required for structural characterization. The hydrophobic amino acids on the exposed surface of SgtB can be mutated to more polar variants to minimize non-specific adhesion between proteins - even then, it may prevent protein aggregation.[1] The conformational flexibility of the protein might reveal internal sites that can promote non-specific association.

On the upside, it may be possible to obtain a stable, well-behaved sample of Lipid IV bound SgtB(68-269) E100Q complex in the near future for X-ray crystallography or solution structure by NMR using the sample preparation methodology presented in section 4.2.8 of this thesis. We have established that SgtB(68-269) E100Q can be stabilized for NMR solution structural studies by Moenomycin A (MmA), possibly by locking it in a conformational state that minimizes the exposure of aggregation-prone surfaces and preventing the protein from sampling aggregation-competent conformations. Because Lipid IV is able to induce conformational changes in SgtB such that it takes on a distinct "activated" rate-enhanced state, we believe that Lipid IV will most likely be able to provide a similar stabilizing effect to SgtB. Although the affinity of Lipid IV for SgtB has never been

directly measured, studies have shown that it because SgtB has to bind Lipid IV tightly in order to synthesize a long glycan strand in a processive fashion.[2]

In order to test this possibility, milligram quantities of Gal-Lipid IV will be required. As mentioned in Chapter 4, it is a non-trivial task to obtain Gal-Lipid IV in such quantities.[3],[4] An improved synthesis of Lipid IV which is more robust and scalable is being developed within our research group. Efforts to scale up the synthesis are ongoing. The structural characterization of the Lipid IV bound SgtB complex will provide insight into the "activated"-state of the enzyme. Specifically, the SgtB:Lipid IV complex sample presents a unique opportunity to study the conformational dynamics that accompany downstream events stemming from the uptake of Lipid II in the acceptor site such as the translocation of newly synthesized glycan strand from the acceptor site to the donor site. For instance, the uptake of Lipid II by SgtB may trigger off conformational rearrangements that remodel the active site for translocation by unfolding of the alpha-helix that physically separates the donor and acceptor site.[5] By comparing the change in conformational dynamics before and after the incorporation of Lipid II, and mapping these “hotspots” of activity to the structure of the Lipid IV bound SgtB complex, one can uncover key amino acid residues that enable the physical communication and coordination between different moving parts in the protein. Extending our analysis to the conformational dynamics of MmA bound SgtB complex may reveal entropy related subtleties that make MmA potent inhibitor of the PGTs.

5.2. Path towards Lipid IV bound and MmA bound SgtB solution structures.

In Chapter 4, we have established a preparation method that yields a SgtB sample that is sufficiently long-lived and well-behaved for the collection of higher-order triple resonance

correlational data sets required for the assignment of the individual H, C, and N atom resonances. Subsequently, throughspace conformational restraints can be measured via NOESY-based experiments. Additionally, atomic and bond torsional restraints are collected by residual dipolar coupling experiments. However, the road towards a solution structure of SgtB is far from paved.[6]

While the computation of an ensemble of solution structures from geometrical restraints has become routine in the recent years with the advent of powerful computational software, the task of peak identification and assignment is still largely a manual, time consuming art in itself.[7] Theoretically, the redundent, overlapping nature of triple resonance correlational data sets enable a spectroscopist to assign peaks by moving sequentially from the N to C terminus along the protein polypeptide chain.[8] However, unresolved and missing peaks often derail such efforts. We expect the peak assignment exercise for the MmA bound SgtB complex to be challenging because our [^{1}H,^{15}N]-TROSY HSQC spectrum only displays approximately 60-70% expected peaks. This is not surprising because SgtB, as seen from its crystal structure, comprises of 10 alpha-helices which translates into a high degree of peak overlap due to inherently narrower chemical shift dispersion of alpha-helical structures.[9]

There are no easy tricks to increase peak count of a sample. The most direct way is to improve the signal intensity by increasing protein concentration of the NMR sample. We prepared a 1 mM sample of partially deuterated ^{15}N-labeled MmA bound SgtB(68-269) E100Q and we observed that the peaks from the HSQC fingerprint were qualitatively broader than that of a 550 μM sample. [^{15}N,^{1}H]-TRACT experiments (with Dr. Tsyr-Yan Yu) suggest a molecular weight of approximately 60 kD, suggesting dimerization at high protein

concentrations (>550 μM).[10] More investigations will have to be done in terms of finding the optimal concentration for making sophisticated NMR measurements.

Increasing the level of deuteration of our sample can also minimize signal losses due to spin relaxation.[11] Additionally, this will also enable one to take full advantage of the TROSY effect. This is especially crucial for triple resonance NMR experiments which have many coherence transfer steps.[12] Ultimately, the most efficacious way to obtain a complete assignment of the protein may be to isotopically label a select number of amino acids in a combinatorial fashion in order to identify a greater number of amino acids resonances on the HSQC spectra that can be used as anchor points for sequential assignment.[13] Successful implementation of this assignment strategy will hinge on our ability to develop a cell-free expression system that will allow the efficient incorporation of select isotopically labeled amino acids into SgtB.[14]

5.3. Prospective for a High-Throughput Screen for New Inhibitors of PGTs

The synthesis of peptidoglycan is necessary for bacterial growth and survival.[15] The PGTs are the only known, highly conserved enzymes that can assemble the polysaccharide backbone of peptidoglycan, hence they are a validated target for development of new antibacterials.[16] The Moenomycin family of antibiotics are the only known class of molecules that inhibit the transglycosylase function of the PGTs.[17] In particular, Moenomycin A has potent antibacterial activity against Gram-positive pathogens. Unfortunately, its clinical development has been hampered by its non-specific interaction with serum albumin, resulting in an unfavorable pharmacokinetic profile (a long half-life and low oral bioavailability) for the molecule. Various attempts to remove or shorten the

offending appendages on Moenomycin A such as its C_{25}-lipid moiety resulted in a dramatic decrease in its potency.[18,19] Attempts to reduce the size of the molecule in order to improve its potency against Gram-negative pathogens have been unsuccessful thus far.[20] The challenges encountered in optimizing the complex pharmacophore of Moenomycin A create an impetus to discover new chemical structures that inhibit the PGTs in the same manner as Moenomycin A.[21]

In principle, new inhibitors of PGT transglycolase activity can be identified by a high-throughput screen that employs a fluorescent-polarization probe displacement format (**Figure 5.1**). Such screens are relatively easy to scale and implement because they are formatted for a simple mix-and-measure protocol that does not require additional downstream processing of the microplate well contents.[22] Because Moenomycin A is a known inhibitor of the PGTs, one can design a fluorescent-polarization probe by attaching of a fluorescent moiety as an appendage to Moenomycin A. Such a probe would enable the screen to identify compounds that bind to the PGTs at the same site as Moenomycin A.

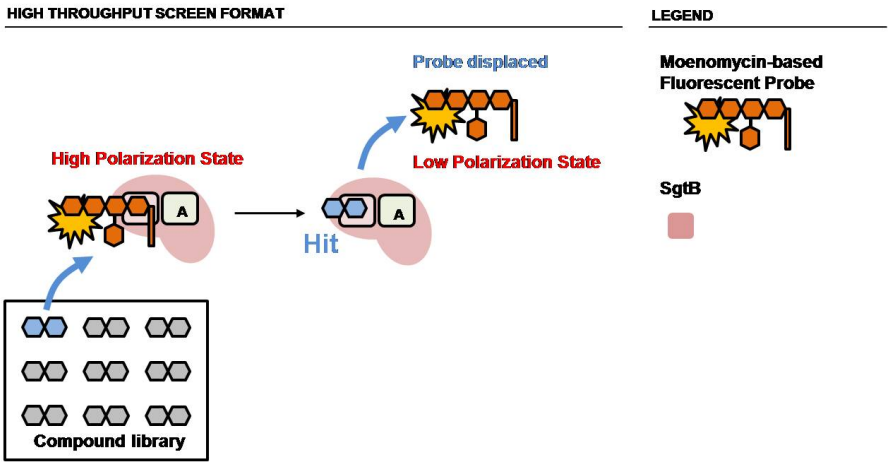

Figure 5.1 High throughput screen for PGT inhibitors using a fluorescent polarization probe displacement format.

In practice, it is difficult to implement a high-throughput screen of the aforesaid format because of several factors: (1) Enzyme-based high-throughput screens require large multimilligram (>20 mg) quantities of protein material at high levels of purity so that assay readouts can be directly attributed to the enzyme target of interest. As mentioned in earlier chapters, it is hard to obtain large quantities of pure, well-behaved PGT enzyme. Previous attempts at developing high-throughput screens for transglycosylase inhibitors circumvented this problem by using crude bacterial cell-membrane extracts as a source for PGT enzymes.[23] The use of impure sources of enzyme requires the use of a probe that binds specifically to the target enzyme of interest. It is not known whether Moenomycin A is able to form some level of interaction with other enzymes that are present in the bacterial cell-membrane extract. This may result in the accumulation of off-target hits, increase the burden of hit validation and thus decrease the efficiency of the screen. (2) The synthetic chemistry used to manipulate and modify the Moenomycins is complex.[24] Although the first total synthesis of Moenomycin A has been reported in 2006, the development of chemically-modified probes has been slow to come forth. The challenges encountered in handling lipid-glycerate moieties that are prone to acid-catalyzed rearrangements and oxidation processes as well as the difficulties in glycosylating a lipid-glycerate moiety hamper the range and physical quantity of probes that can be produced for tuning the binding affinity towards the PGTs – a crucial parameter in a competitive displacement screen.[25,26,27]

The work in this thesis has enabled the rapid preparation of large quantities of monodisperse and monomeric SgtB – 7 mg from 1 liter of Luria-Bertani media. Assuming that 0.1 μg of SgtB is required per compound well, one week of preparative purification of SgtB can accumulate 100 mg of SgtB that can enable a screen against 1 million compound

library. Moreover, using SgtB as a screening target carries the benefit that the hits identified will bind to SgtB, PGT from the clinically relevant pathogen S. aureus that may play a critical role in salvaging peptidoglycan biosynthesis under stressful conditions.[28] As more robust methods for synthesizing fragments of Moenomycin A come online, we are confident that a well-tuned fluorescent probe can be designed and synthesized, finally enabling us to carry out a well-defined high-throughput screen for transglycosylase inhibitors.

5.4 References

1. Ito, T., and Wagner, G. (2003) Using codon optimization, chaperone-coexpression, and rational mutagenesis for production and NMR assignments of human eIF2α, *J. Biomol. NMR 28*, 357-367.
2. Wang, T. S. A., (2011) Bacterial cell wall assembly: mechanism and inhibition of peptidoglycan glycosyltransferases, *PhD Dissertation, Harvard University*, (Publication nbr: 3462154)
3. Zhang, Y., Fechter, E. J., Wang, T. S., Barrett, D., Walker, S., and Kahne, D. E. (2007) Synthesis of heptaprenyl-lipid IV to analyze peptidoglycan glycosyltransferases, *J. Am. Chem. Soc. 129*, 3080-3081.
4. Gampe, C. M., Tsukamoto, H., Wang, T.-S. A., Walker, S., and Kahne, D. (2011) Modular synthesis of diphospholipid oligosaccharide fragments of the bacterial cell wall and their use to study the mechanism of moenomycin and other antibiotics, Tetrahedron 67, 9771-9778.
5. Lovering, A. L., de Castro, L., Strynadka, N. C. (2008) Identification of dynamic structural motifs involved in peptidoglycan glycosyltransfer, *J. Mol. Biol. 383*, 167-177.
6. Nietlispach, D., Mott, H. R., Stott, K. M., Nielsen, P. R., and Thiru, A. (2004) Structure determination of protein complexes by NMR, *Methods Mol. Biol. 278*, 255-288.
7. Billeter, M., Wagner, G., and Wüthrich K. (2008) NMR structure determination of proteins revisited, *J. Biomol. NMR 42*, 155-158.

8. Whitehead, B., Craven, C J., and Waltho, J. P. (1997) Double and triple resonance NMR methods for protein assignment, Methods Mol. Biol. 60, 29-52.

9. Trbovic, N., Klammt, C., Koglin, A., Löhr, F., Bernhard, F., and Dötsch, V. (2005) Efficient strategy for the rapid backbone assignment of membrane proteins, *J. Am. Chem. Soc. 127*, 13504-13505.

10. Lee, D., Hilty, C., Wider, G., and Wüthrich, K. (2006) Effective rotational correlation times of proteins from NMR relaxation interference , J. Magn. Reson. 178, 72-76.

11. Matthews, S., (2004) Perdeuteration/Site-specific protonation approaches for high-molecular weight proteins, Methods Mol. Biol. 278, 35-45.

12. Liu, Y., Prestegard, J. H. (2011) Multi-dimensional NMR without coherence transfer: minimizing losses in large systems, J. Magn. Reson. 212, 289-298.

13. Hefke, F., Bagaria, A., Reckel, S., Ullrich, S. J., Dötsch, V., Glaubitz, C., Güntert, P. (2011) Optimization of amino acid type-specific 13C and 15N labeling for the backbone assignment of membrane proteins by solution- and solid-state NMR with the UPLABEL algorithm, J. Biomol. NMR 49, 75-84.

14. Junge F., Haberstock, S., Roos, C., Stefer, S., Proverbio, D., Dötsch, V., Bernhard, F., Advances in cell-free protein synthesis for the functional and structural analysis of membrane proteins, New Biotech. 28, 262-271.

15. Holtje, J. V. (1998) Growth of the stress-bearing and shape-maintaining murein sacculus of Escherichia coli, *Microbiol. Mol. BIol. Rev. 62*, 181-203.

16. Koch, A. L. (2003) Bacterial wall as target for attack: Past, present, and future research, *Clin. Microbiol. Rev 16*, 673-687.

17. Kahne, D., Leimkuhler, C., Lu, W., and Walsh, C. (2005) Glycopeptide and lipoglycopeptide antibiotics, *Chem. Rev. 105*, 425-448.

18. Adachi, M., Zhang, Y., Leimkuhler, C., Sun, B., Latour, J. V., and Kahne D. (2006) Degradation and reconstruction of Moenomycin A and derivatives: dissecting the function of the isoprenoid chain, *J. Am. Chem. Soc. 128*, 14012-14013.

19. Fuse, S., Tsukamoto, H., Yuan, Y., Wang, T. S., Zhang, Y., Bolla, M., Walker, S., Sliz, P. and Kahne, D. (2010) Functional and structural analysis of a key region of the cell wall inhibitor moenomycin, *ACS Chem. Biol. 5*, 701-711.

20. Welzel, P. (2005) Syntheses around the transglycosylation step in peptidoglycan biosynthesis, *Chem. Rev. 105*, 4610-4660.

21. Ostash, B., and Walker, S. (2010) Moenomycin family antibiotics: chemical synthesis, biosynthesis, and biological activity, Nat. Prod. Rep. 27, 1594-1617.

22. Huang, X., and Aulabaugh, A. (2009) Application of Fluorescence Polarization in HTS Assay*, High Throughput Screening 565*, 127-143.

23. Ostash, B., and Walker, S. (2005) Bacterial transglycosylase inhibitors, *Curr. Opin. Chem. Biol. 9*, 459-466.

24. Taylor, J. G., Li, X., Oberthur, M., Zhu, W., and Kahne, D. E. (2006) The total synthesis of moenomycin A, J. Am. Chem. Soc. 128, 15084-15085.

25. Vogel, S., Buchynskyy, A., Stembera, K., Richter, K., Hennig, L., Muller, D., Welzel, P., Maquin, F., Bonhomme, C., and Lampilas, M. (2000) Some selective reactions of moenomycin A, *Bioorg. Med. Chem. Lett. 10*, 1963-1965.

26. Vogel, S., Stembera, K., Hennig, L., Findeisen, M., Giesa, S., Welzel, P., Tillier, C., Bonhomme, C., and Lampilas, M. (2001) Moenomycin analogues with long-chain amine lipid parts from reductive aminations, Tetrahedron 57, 4147-4160.

27. Hu, Y., Helm, J. S., Chen, L., Ginsberg, C., Gross, B., Kraybill, B., Tiyanont, K., Fang, X., Wu, T., and Walker, S. (2004) Identification of selective inhibitors for the glycosyltransferase MurG via high-throughput screening, *Chem. Biol. 11*, 703-711.

28. Yuriy Rebets, *Manuscript in preparation.*